I. NON-LINEAR EFFECTS IN A SELF-CONSISTENT CALCULATION OF SU_3

SYMMETRY BREAKING IN STRONG INTERACTION COUPLING CONSTANTS

II. DIRECT-CHANNEL REGGEIZATION OF STRONG INTERACTION

SCATTERING AMPLITUDES

Thesis by

Stephen Paul Creekmore

In Partial Fulfillment of the Requirements

For the Degree of

Doctor of Philosophy

California Institute of Technology

Pasadena, California

1969

(Submitted April 4, 1969)

ACKNOWLEDGMENTS

The author is indebted to Professor Steven Frautschi for suggesting the problems treated in this thesis, and for providing guidance throughout the performance of the research. Many useful and informative discussions were had with Professors Fredrik Zachariasen and Peter Kaus, as well as with Dr. Lorella Jones.

The author would also like to commend Mrs. Bette Brent for her excellent job in typing this manuscript, as well as Ken Heitner for assistance in the preparation of the illustrations.

ABSTRACT

The thesis is divided into two parts. Part I generalizes
a self-consistent calculation of residue shifts from SU_3 symmetry,
originally performed by Dashen, Dothan, Frautschi, and Sharp, to in-
clude the effects of non-linear terms. Residue factorizability is
used to transform an overdetermined set of equations into a variational
problem, which is designed to take advantage of the redundancy of the
mathematical system. The solution of this problem automatically
satisfies the requirement of factorizability and comes close to
satisfying all the original equations.

Part II investigates some consequences of direct channel
Regge poles and treats the problem of relating Reggeized partial wave
expansions made in different reaction channels. An analytic method
is introduced which can be used to determine the crossed-channel
discontinuity for a large class of direct-channel Regge representations,
and this method is applied to some specific representations.

It is demonstrated that the multi-sheeted analytic structure
of the Regge trajectory function can be used to resolve apparent
difficulties arising from infinitely rising Regge trajectories. Also
discussed are the implications of large collections of "daughter
trajectories."

Two things are of particular interest: first, the threshold
behavior in direct and crossed channels; second, the potentialities of
Reggeized representations for us in self-consistent calculations. A
new representation is introduced which surpasses previous formulations

in these two areas, automatically satisfying direct-channel threshold constraints while being capable of reproducing a reasonable crossed-channel discontinuity. A scalar model is investigated for low energies, and a relation is obtained between the mass of the lowest bound state and the slope of the Regge trajectory.

TABLE OF CONTENTS

INTRODUCTION

In the following pages, we will discuss several mathematical techniques which have applications to problems in the theory of strong interactions. To illustrate these techniques, we will investigate specific cases in which our methods are useful. The thesis is divided into two parts: Part I generalizes a self-consistent calculation of strong interaction couplings, originally performed by Dashen, Dothan, Frautschi and Sharp (1); Part II investigates some consequences of Regge poles and treats the problem of relating Regge trajectories in different reaction channels.

Part I begins with a formulation of the problem of self-consistent calculations of residue shifts. These calculations derive from a general property of strong interaction theory: corresponding to each single-particle intermediate state, the scattering amplitude will have a pole as a function of energy. The residue of this pole is the product of the coupling constants between the intermediate state and the initial and final states. Denoting the initial and final configurations by the numbers 1 and 2, respectively, the specified single particle intermediate state by the letter $\underline{i}$, and all other intermediate states by $\underline{j}$, we can represent A, the scattering amplitude for the reaction, schematically as follows:

$$A\left\{1 \to 2\right\} = A\left\{1 \to i \to 2\right\} + \sum_{j \neq i} A\left\{1 \to j \to 2\right\}$$

For values of the energy variable near the rest energy of the intermediate state, we can write

$$A\{1 \to 2\} \approx A\{1 \to i \to 2\} \approx \frac{R_{12}^i}{W-W^i}$$

and

$$R_{12}^i = -g_1^i \cdot g_2^i$$

where R_{12}^i is the residue and g_1^i and g_2^i are the coupling constants of the intermediate state to the initial and final states, respectively.

In Section I of Part I, we show that the factorizability of the residue is a powerful constraint on the nature of possible solutions of the strong interaction problem. Typically, a calculation of the properties of an N-channel scattering system with an intermediate state $\underline{i}$ will yield separate estimates for each of the N^2 elements of the N x N residue matrix. If no errors are present in the treatment of this system, the set of elements obtained will be consistent with the requirement of factorizability, that there are only N independent quantities and $N^2 - N$ of the residue equations are redundant. In general, however, errors will be present which make the problem seriously over-determined. As a consequence, some way must be found to extract information from the N^2 inconsistent residue equations. Intuitively, we might feel that, especially in the presence of errors, two equations are in some sense better than one, or that it should be possible to take advantage of the redundancy of the mathematical system.

Two general procedures are fruitful in such cases. First,

some knowledge about the nature of the approximations may allow us to reformulate our set of equations in such a way as to minimize the effect of the errors. In the broken SU_3 mass shift and residue shift calculations of DDFS, "enhancement" plays the role of such a reformulation, although the approximations made by DDFS require the restriction of their method to the case of infinitesimal shifts. Of special interest is the problem of finite shifts, and in Section III of Part I, we generalize the enhancement mechanism of DDFS to allow for higher-order terms in the calculation of spontaneously broken SU_3 symmetry.

The second procedure we will discuss involves the application of prior knowledge of the properties of the "solution" to our overdetermined set of equations. In Section III of Part I, we use the factorizability property of residue matrices to transform the inconsistent set of residue equations into a variational problem, whose solution automatically satisfies the requirement of factorizability and comes close to satisfying all the original equations.

Calculations of the type discussed in Part I are ultimately limited by the underlying strong interaction model, which in Part I is an SU_3 generalization of the static model for pion-nucleon scattering. In Part II, we investigate some models which may have a greater validity. In principle, the methods discussed in Part I could be applied to the model developed in Part II; this step, however, was considered to be beyond the scope of this work.

Part II begins with a review of the basic principles underlying the Reggeization of scattering amplitudes. Direct-channel resonances and bound states can be described in terms of the

relatively simple behavior of Regge trajectories in the direct channel.
The introduction of crossed-channel Regge trajectories can remove
difficulties arising from the high-energy behavior of high-spin ex-
changes. The relation of the direct-channel and crossed-channel
Regge trajectories, however, is not as simple as the relation, in the
static model, of direct-channel and crossed-channel fixed-spin inter-
mediate states. In fact, many Reggeized "models" fail even the simple
test of reducing to fixed-spin resonance models in the appropriate
kinematic region. Outside this region, one expects a crossed-channel
Reggeized model, for example, to be useful for describing processes at
high energies near the forward direction; the behavior at intermediate
energies and angles, however, is not easily treated in terms of Regge
trajectories: naive application of some of the standard formulations
of Regge pole theory can lead to impossibly difficult calculations.

If a scattering amplitude can be represented by an analytic
function, then the amplitude should be determined, in all channels, by
sufficiently precise specifications of its properties in only one
channel. For example, it should be possible to express the partial
wave amplitudes in one channel in terms of the set of partial wave
amplitudes in another channel. The problem of the analytic continu-
ation of partial wave expansions is intimately connected with the
relation of Regge trajectories in two channels, since Regge poles arise
in a technique for the summation of these partial wave expansions.
In a practical implementation of any such continuation scheme, the
essential difficulties are associated with the fact that the physical
region for scattering on one channel lies on a cut in the analytic

continuation of the partial wave expansion in any other channel, and
the discontinuity across this cut is of fundamental physical interest.
In other words, we are interested in determining the discontinuity of
a function defined in terms of a (divergent) infinite series. In
Section I of Part II, we introduce an analytic method which can be
used to determine this discontinuity for a large class of Regge
representations, and in Sections II and III of Part II, we apply this
method to some specific representations, for which we determine a
segment of the crossed-channel cut in terms of the distribution of
Regge poles in the direct channel. Also discussed in Section I is a
numerical method for the continuation of divergent partial wave sums.

In the phenomenology of strong interaction scattering, the
observed sequence of bound states and resonances seems to indicate
the indefinite rise of Regge trajectories with rising energy. By way
of contrast, Regge trajectories in non-relativistic potential scatter-
ing always turn around for high enough energy. In fact, some authors
have supposed there to be difficulties in the phase shifts or analytic
structure of scattering amplitudes, necessarily associated with
infinitely rising Regge trajectories. In Section I of Part II we
show how the multi-sheeted analytic structure of the Regge trajectory
function can be used to resolve these apparent paradoxes; added
consequences of this picture are new insights into the interpretation
of the behavior of phase shifts in terms of rising trajectories. Also
discussed in Section I is the relation of crossed-channel Regge trajec-
tories to the requirement that there be large collections of "daughter
trajectories" associated with any observed Regge trajectory, a

possibility which has been suggested by other arguments.

Section II of Part II is devoted to the application of the mathematical apparatus developed in Section I to some Regge representations introduced by other investigators. Specific strengths and shortcomings of these formulations are examined. Two things are of particular interest: first, the threshold behavior in direct and crossed channels; second, the potentialities of these representations for use in self-consistent or "bootstrap" calculations.

Finally, in Section III of Part II, a new representation is introduced which surpasses the capabilities of the previous formulations in these two areas. Just as in Section II, the mathematical devices developed in Section I are applied to demonstrate their usefulness in practical analysis. We show that the new representation automatically satisfies direct-channel threshold constraints and can be made to reproduce reasonable behavior of the discontinuity across the crossed-channel cut. A scalar model is investigated for low energies, using this new representation. In this discussion, we obtain a relation between the mass of the lowest bound state and the slope of the Regge trajectory.

PART I

SECTION I

GENERAL REMARKS

Suppose that there exists a system of strongly interacting particles obeying dynamical equations which have as solutions two sets of masses and coupling constants. We are interested here in the problem of spontaneous SU_3 symmetry breaking. In this case, one of the conjectured solutions to the full dynamical equations would be an SU_3 symmetric arrangement of particle masses and coupling constants, while the other solution would be the arrangement found in nature.

It is a moot point whether a complete and self-consistent theory of elementary particles would have any solution except the experimentally observed masses and coupling constants. Approximate theories exist which have SU_3 symmetric solutions.[2] If we include the features of an approximate model with an SU_3 symmetric solution, the calculation will be internally consistent on this point. The complete internal consistency of an incomplete theory is not necessarily a recommendation, however, as we will see later in the discussion of an overdetermined system of equations obtained in the theory of spontaneous symmetry breaking.

Let A_1 and A_2 be the scattering amplitudes corresponding to the two solutions, where we have specialized to the partial wave, spin, isospin, and strangeness appropriate to the bound states involved. Using the N over D Method of Chew and Mandelstam,[3] we decompose these amplitudes into numerator and denominator functions:

$$A_i \ (W) = N_i \ (W) \ D_i^{-1} \ (W) \qquad i = 1, \ 2$$

We frame our theory using W, the center of mass energy, as the energy variable. For each value of i, N_i has the same left hand cut (LHC) as A_i but has no right hand cut (RHC), while D_i similarly has a right hand cut but no left hand cut. The unitarity relation is

$$\text{Im } A_i \ (W) = A_i^+ \ \rho_i \ A_i \qquad (RHC), \ i = 1, \ 2$$

from which follows

$$\text{Im } D_i \ (W) = -\rho_i \ N_i \qquad (RHC), \ i = 1, \ 2$$

$$\text{Im } N_i \ (W) = \text{Im } A_i \ D_i \qquad (LHC), \ i = 1, \ 2$$

where ρ is a diagonal kinematic matrix, which is determined by the definition of the amplitude in terms of the unitary S-matrix.

The D_i will have simple zeros at the positions of the bound states and resonances. For simplicity, suppose that there is only one bound state[4] and that the D functions are normalized to have unit derivative at the energy of the bound state:

$$D_i \ (W) \ \cong \ (W-M_i) \ 1 + 0 \ ((W-M_i)^2)$$

$$\text{for } W \cong M_i, \ i = 1, \ 2$$

Now consider the function

$$J \ (W) = D_2^T \ (W) \ [A_2 \ (W) - A_1 \ (W)] \ D_1 \ (W)$$

At the bound states, the scattering amplitudes have poles

$$A_i \ (W) \cong \frac{R_i}{(W-M_i)} + \text{smooth function}$$

$$\text{for } W \cong M_i \qquad i = 1, \ 2$$

and, as a consequence,

$$J \ (M_1) \ = \ -D_2^T \ (M_1) \ R_1$$

and

$$J \ (M_2) \ = \ R_2 \ D_1 \ (M_2)$$

Writing a dispersion relation for J(W) we obtain

$$J \ (M_i) \ = \ \frac{1}{\pi} \int_{\text{LHC}} \frac{\text{Im} J(W) dW}{W-M_i} + \frac{1}{\pi} \int_{\text{RHC}} \frac{\text{Im} J(W) dW}{W-M_i} \qquad i = 1, \ 2$$

where LHC and RHC designate the left-hand and right-hand cuts of J(W), respectively. Evidently, J(W) will have the cuts of both A_1(W) and A_2(W).

Recalling that N(W) has no right-hand cut and that $A = ND^{-1} = D^{T-1}N^T$ (A is a symmetric matrix due to time reversal invariance), we can compute Im J(W) on the right-hand cut:

$$\text{Im} \ J(W) \ = \ \text{Im} \ [D_2^T \ (A_2 - A_1) \ D_1]$$

$$= \ \text{Im} \ [N_2^T D_1 \ - \ D_2^T \ N_1]$$

$$= \ N_2^T \ (\rho_2 \ - \ \rho_1) \ N_1$$

On the left-hand cut,

$$\text{Im } J(W) = D_2^T \text{ Im } (A_2 - A_1) \ D_1$$

where we have used the fact that D has no left-hand cut.

Finally, we obtain the equations

$$J(M_i) = \frac{1}{\pi} \int_{LHC} \frac{D_2^T \text{ Im } (A_2 - A_1)}{(W - M_i)} \ D_1 \ dW + \frac{1}{\pi} \int_{RHC} \frac{N_2^T (\rho_2 - \rho_1) \ N1}{(W - M_i)} \ dW$$

$$i = 1, \ 2$$

Defining two new matrices as follows:

$$K_1 = (M_2 - M_1) \ [D_1 \ (M_2)]^{-1}$$

$$K_2 = (M_1 - M_2) \ [D_2^T \ (M_1)]^{-1}$$

we obtain residue shift and mass shift equations:

$$R_2 \ (M_2 - M_1) = J(M_2) \ K_1$$

$$R_1 \ (M_2 - M_1) = K_2 \ J \ (M_1)$$

$$R_2 - R_1 = - \frac{1}{(M_2 - M_1)} \ [K_2 \ J(M_1) - J(M_2) \ K_1]$$

Evidently,

$$K_1^{-1} = 1 + \frac{1}{2} (M_2 - M_1) D_1'' (M_1) + \ldots .$$

and

$$K_2^{-1} = 1 + \frac{1}{2} (M_1 - M_2) D_2^{T''} (M_2) + \ldots .$$

Note that to solve the mass shift relations written above, we would have to take weighted averages over $2N^2$ equations, where N is the number of channels in the problem. There are obviously many ways to construct these averages, and if there are errors present in the original system of $2N^2$ equations, then there may be an optimum weighting. Furthermore, the N^2 elements of a residue matrix are not all independent, but are completely determined by N coupling constants, according to the factorization property:

$$R^{ij} = -g_1^i g_1^j \qquad i,j = 1, 2, \ldots, N$$

$$R_2^{ij} = -g_2^i g_2^j$$

In any calculation, the equations are approximated and the overdeterminancy of the system requires serious consideration, independent of assumptions about the size of the mass shifts and coupling shifts. Again, what is indicated is a procedure for optimizing the process of selecting information from the overdetermined system with errors.

As a step towards the solution of this problem, suppose that some approximation to the residue shift equations were to yield a real symmetric "residue matrix," R_2. In a calculation of spontaneous

SU_3-breaking, R_1 and M_1 would be the residues and masses corresponding to the SU_3-symmetric limit, while R_2 and M_2 would represent the corresponding quantities actually observed. In this case, R_1, M_1, M_2, and any other necessary parameters might be specified initially or determined elsewhere in the general problem.

We can determine the factorizable matrix which is the closest approximation to R_2, thus extracting from R_2 a set of "coupling constants." For simplicity, we choose the Euclidean metric as a criterion of approximation. In other words, we want to determine a set of numbers γ_i, $i = 1, 2, \ldots, N$ such that we minimize the expression

$$\epsilon = \sum_{\substack{i,j=1}}^{N} (R_2^{ij} - \gamma_i \, \gamma_j)^2$$

Now observe that any matrix of the form

$$M_{ij} = \gamma_i \, \gamma_j$$

has two important properties. First, only one of the eigenvalues is non-zero. Secondly, the vector γ_i is the eigenvector associated with the non-zero eigenvalue. Evidently, a matrix which is intended to be an approximation to a factorizable matrix would have to be characterized by having one eigenvalue much larger than the rest. We will assume this to be the case for R_2 in the following discussion.

At a minimum, ϵ considered as a function of the $\{\gamma_i\}$ will possess a set of first partial derivatives all equal to zero. Explicitly,

$$\sum_{j=1}^{N} (R_2^{ij} - \gamma_i \gamma_j) \; \gamma_j = 0 \qquad i = 1, 2, \ldots, N$$

Decomposing R_2 into invariant sub-matrices, we obtain

$$R_2^{ij} = \sum_{K=1}^{N} \rho_K \; r_i^K \; r_j^K$$

where the numbers ρ_K are the eigenvalues of R_2 and the vectors r^K are the unit-normalized eigenvectors associated with those eigen-values.

Transforming to a basis where the matrix R_2 is diagonal, we see that the optimization equations may be written as follows:

$$\tilde{\gamma}_i \; (\rho_i - \sum_{j=1}^{N} \tilde{\gamma}_j^2) = 0 \qquad i = 1, 2, \ldots, N$$

and

$$\in = \sum_{K=1}^{N} \left[\rho_K^2 - 2\rho_K \; \tilde{\gamma}_K^2 + \tilde{\gamma}_K^2 \sum_{\ell=1}^{N} \tilde{\gamma}_\ell^2 \right]$$

where $\tilde{\gamma}$ is the transformed vector γ.

It is now evident that the criteria for a minimum imply

$$\gamma_i = \pm \sqrt{\rho_{K_{max}}} \quad \gamma_i^{K_{max}} \qquad i = 1, 2, \ldots, N$$

where by K_{max} we mean that value of K for which $|\rho_{K_{max}}|$ attains the maximum value. The overall sign of the vector γ_i cannot be

determined from the residue matrix.

In summary, we have shown that a good approximation scheme to the residue shift equations must produce a real symmetric residue matrix which has one eigenvalue of much larger magnitude than the rest. Furthermore, the best way to obtain a set of coupling constants from this matrix, assuming our criterion for error, is to equate the coupling constants with the elements of the properly normalized eigenvector corresponding to the single largest eigenvalue. We also have obtained a measure of the deviation from factorizability in our approximate calculation

$$\epsilon_{min} = \sum_{K \neq K_{max}} \rho_K^2$$

Factorizability is an important requirement for two reasons. First, it expresses the fact that a single particle intermediate state is present in the system, a dynamical condition that is central to our theory. Second, it communicates information among the N^2 elements of the residue matrix. Thus, if we have some way of extracting a preferred subset of equations out of the original N^2 relations, we can partially compensate for lack of information about the remaining elements by the imposition of factorizability using our eigenvector method. Specifically, we can search for a set of residue matrix elements which is consistent with our preferred set of residue shift relations and which, at the same time, most nearly satisfies factorizability, minimizing ϵ_{min} .

The mathematical development so far has placed no restriction on the size of the mass shifts or residue shifts. We have required only that the system possess two solutions and that the integrals involved be well-defined.[5] The accuracy of any calculation using this mathematical framework is fundamentally limited by two things: first, by our knowledge of the amplitudes A_i (and their decompositions N and D) on the left-hand and right-hand cuts; second, by the extent of the cuts we decide to include in the integrals for $J(M_i)$ together with the rapidity with which those integrals converge. In the actual calculation of coupling constants in spontaneous SU_3 symmetry breaking, we will use a model in which only single particle intermediate states are considered, whether in the direct or crossed channels. We will make many of the approximations characteristic of the so-called static model: static crossing relations, for example.

Part II is devoted to the discussion of a model which is not necessarily limited by many of these approximations and which treats all partial waves simultaneously. As an illustration of the techniques we have developed for dealing with overdetermined systems with errors, however, we will use only the simpler model.

PART I

SECTION II

THE MODEL

We will consider two body scattering of the baryon SU_3 octet B_8 ($J^\pi = 1/2^+$) with the pion SU_3 octet P_8 ($J^\pi = 0^-$):

$$\text{s-channel:} \quad B_8 + P_8 \rightarrow B_8' + P_8'$$

$$\text{t-channel:} \quad B_8 + \overline{B}_8' \rightarrow P_8' + \overline{P}_8$$

$$\text{u-channel:} \quad B_8 + \overline{P}_8' \rightarrow B_8' + \overline{P}_8$$

We will specialize to the $\ell = 1$ partial wave. In this case, the total angular momentum can assume two values: $J^\pi = 1/2^+$ and $J^\pi = 3/2^+$. For $J^\pi = 3/2^+$, there are ten states grouped in the baryon SU_3 decuplet, B_{10}. The baryon octet itself has $J^\pi = 1/2^+$.

We will assume isospin symmetry and strangeness conservation to hold in our calculation. Accordingly, it is not necessary to differentiate different members of the same isospin multiplet. The isospin doublet (n,p) is referred to as N, the triplet (Σ^+, Σ^0, Σ^-) is called Σ, and so forth.

We will define a set of isospin coupling constants. The coupling constant for a particular set of particles is obtained by multiplying our isospin coupling constant by the appropriate SU_2 Clebsch-Gordon coefficient. For example,

$$g^{\text{particle}}_{pp\pi^0} = g^{\text{isospin}}_{NN\pi} \langle \tfrac{1}{2} \tfrac{1}{2} \mid \tfrac{1}{2}, \tfrac{1}{2}; 1, 0 \rangle$$

The description of the $B_8 B_8 P_8$ and $B_8 B_{10} B_8$ vertices evidently requires twenty-nine coupling constants.

$$g_{NN\pi}, \ g_{NN\eta}, \ g_{N\Sigma K}, \ g_{N\Lambda K}, \ g_{\Sigma N\bar{K}}, \ g_{\Sigma\Sigma\pi}, \ g_{\Sigma\Sigma\eta}, \ g_{\Sigma\Lambda\pi}, \ g_{\Sigma\Xi K}, \ g_{\Lambda\Lambda\eta},$$

$$g_{\Lambda N\bar{K}}, \ g_{\Lambda\Sigma\pi}, \ g_{\Lambda\Xi K}, \ g_{\Xi\Sigma\bar{K}}, \ g_{\Xi\Lambda\bar{K}}, \ g_{\Xi\Xi\pi}, \ g_{\Xi\Xi\eta}, \ g_{N^*N\pi}, \ g_{N^*\Sigma K}, \ g_{Y^*\Sigma\pi}, \ g_{Y^*\Sigma\eta},$$

$$g_{Y^*\Lambda\pi}, \ g_{Y^*N\bar{K}}, \ g_{Y^*\Xi K}, \ g_{\Xi^*\Sigma\bar{K}}, \ g_{\Xi^*\Lambda\bar{K}}, \ g_{\Xi^*\Xi\pi}, \ g_{\Xi^*\Xi\eta}, \ g_{\Omega\Xi\bar{K}}$$

Five pairs of coupling constants, however, are constrained by charge conjugation:

$$g_{N\Sigma K} = \sqrt{3/2} \ g_{\Sigma N\bar{K}}$$

$$g_{N\Lambda K} = -\frac{1}{\sqrt{2}} g_{\Lambda N\bar{K}} \qquad\qquad g_{\Sigma\Lambda\pi} = -\frac{1}{\sqrt{3}} \ g_{\Lambda\Sigma\pi}$$

$$g_{\Sigma\Xi K} = -\sqrt{2/3} \ \ g_{\Xi\Sigma\bar{K}}$$

$$g_{\Lambda\Xi K} = \sqrt{2} \ \ g_{\Xi\Lambda\bar{K}}$$

We will not impose this constraint on the calculation; instead, we will test whether it is satisfied by our solution. DDFS found that their "enhanced eigenvector" of coupling constants was not markedly changed when they projected out the parts violating charge conjugation. We might expect to find a similar result. Of course, the charge conjugation information could easily be added to the list of preferred equations, or it could be a constraint imposed on the minimization of the deviation from factorizability.

Table 1 lists the particles in these three SU_3 families, each with its mass, spin, isospin, and strangeness. For the two baryon families, there is a tabulation of the channels in our scattering system which can contain these particles as bound states or resonances. Our channels contain other resonances at higher energies, but we will limit our discussion to the two sets of states: B_8 and B_{10}.

It is characteristic of the low-energy limit of baryon-pion scattering that the $\ell = 1$ s-channel crosses into the $\ell = 1$ u-channel. This statement means that for $\ell = 1$ scattering the most influential u-channel states are precisely those particles bound in the s-channel. We assume that this low-energy behavior suitably represents the behavior of the amplitudes at all energies involved in our calculation. We will neglect t-channel processes. Table 2 presents a list of all the channels in our model, together with the resonances and bound states for each channel, and in every case the exchanged particles present as intermediate states in the u-channel.

We define our amplitudes by the following kinematic convention:

$$A = \frac{M^2}{2iq^3} (S-1)$$

Since we are considering the case of broken SU_3 symmetry, we should in principle make some allowance for different kinematics in the incoming and outgoing channels. Our calculation will drop all but the lowest terms in the mass shift, however, so this problem will not be discussed here. Many improvements in the details of this calculation are possible.

It was not considered worthwhile, however, to invest effort in improving

the detailed treatment of a model, such as the static model, whose basic

philosophy is defective. Instead, in Part II, an alternative "simple"

model is developed which is more reasonable. The basic techniques of

Part I can be applied to any model. We use the static model mainly

because it offers a simple illustration of these techniques and

secondarily, because it allows us to make a direct comparison with the

calculation of DDFS, which is also based on the static model.

A salient feature of our model is the assumption that, of

all the left-hand cuts, we need retain only the nearby short cuts

arising from baryon exchange. The left-hand cut contributions to the

$J(M_i)$ are then written as functions of the masses and residues of the

exchanged particles. Since the system of particles that is exchanged

is the same as the system that appears as bound states, the mass-shift

and residue-shift equations form a closed algebraic system which can be

solved to determine the masses and residues of the natural set of

baryons in terms of a fictitious SU_3 symmetric baryon system. If the

equations derived from this approximate model were completely self-

consistent, then the overdeterminancy of the system would be no problem.

In general, however, we expect errors to be present which render our

approximate equations inconsistent.

If the mass shifts and residue shifts are assumed to be

sufficiently small, then we could use a perturbative approach, such as

that investigated by DDFS. The experimental baryon octet and decuplet

masses vary less than about fifteen percent from their average values.

Therefore, it seems justifiable to write the equations as power series

in the mass shifts. Corresponding experimental measurements of couplings are less precise, but the calculations performed in DDFS[6] yielded coupling shifts as large as the SU_3 symmetric couplings. This situation would seem to rule out perturbative or power series approaches for the coupling shifts.

In their linearized theory, DDFS noted that the integrals in their coupling shift equations would converge faster than those in their-mass-shift equations, by a power of W. This feature may carry over into our theory. The residue shift equations could be more accurate than the mass shift equations, since they are one higher order in the perturbation. This possibility would be realized only if all orders in the coupling shifts were kept for each order in the mass shift expansion. Within the limits of our approximate model this is the case. If symmetry breaking is relatively larger at low energies than at high energies, this effect would be enhanced. Accordingly, we will perform only the residue shift calculation, since our model does not adequately treat distant cuts. Whenever they are needed, the mass shifts will be taken from experimental data. After we have obtained the residue shifts, we will determine the errors in the mass shift equations when we make the same approximations used in the coupling shift calculation. This procedure will provide a rough check on the self-consistency of the approximations involved in our calculation.

In the linearized theory, the right-hand cut contributes only to terms proportional to the mass shift. In the exact theory, if we expand our equations in powers of the mass shift, the contribution

of the right-hand cut appears in first and higher orders, but not in zeroth order. Several authors have remarked that the calculation of the contribution of the right-hand cut is extremely model-dependent.[7] DDFS, in their treatment of residue shifts, avoided explicit treatment of the right-hand cut.

Near the bound state we can expand the $D_i(W)$ in a power series:

$$D_i(W) = (W-M_i) \, 1 + \frac{1}{2} \, (W-M_i)^2 \, D_i{}'' \, (M_i) + \ldots \, .$$

The nearest singularity of $D_i(W)$ is at threshold. In an exact calculation, the second and higher order derivatives of $D_2(W)$ would include effects of the residue shifts, as well as mass-shift effects.

Following DDFS, we choose to ignore the cut in $D_i(W)$ for purposes of computations on the left-hand cuts of A_i. We retain only the nearby short left-hand cut resulting from bayon octet and decuplet exchanges. If the scattering process involves a baryon of mass M_a and meson of mass μ_a scattering to form a baryon of mass M_b and meson of mass μ_b, an exchange of a baryon of mass M_{exch} will produce a short cut running from $\ell_{exch} = \sqrt{S_-}$ to $\mu_{exch} = \sqrt{S_+}$ where (8)

$$S_{\pm} = \frac{-\sigma^4 + \frac{1}{2} \, (\alpha^2+\beta^2+\gamma^2+\delta^2) + \alpha\beta\gamma\delta \pm \sqrt{(\sigma^2-\alpha^2)(\sigma^2-\beta^2)(\sigma^2-\gamma^2)(\sigma^2-\delta^2)}}{2\sigma^2}$$

$$\alpha = M_1 - \mu_2$$

$$\beta = M_1 + \mu_2$$

$$\gamma = M_2 + \mu_1$$

$$\delta = M_2 - \mu_1$$

$$\sigma = M_{exch}$$

For W on this left-hand cut, $|W-M_i|$ is of the same order of magnitude as the observed mass shifts.

In the following calculation, we will keep only the lowest terms in (M_1-M_2). Accordingly, we drop the second and higher order terms in the expansion of $D_i(W)$ on the short left-hand cut, thus obtaining the so-called "linear-D" approximation. Within any specific model, of course, $D_i(W)$ can be calculated and included accurately, necessitating a nonessential modification of the following discussion. Evidently, we can set $K_1 = K_2 = 1$ consistent with keeping (M_1-M_2) only to lowest order. This assumption also allows us to neglect the right hand cut.

In the above approximations, the residue shift equations become:

$$\delta R = R_2 - R_1 = \sum_{exch} \frac{1}{\pi} \int_{\ell_{exch}}^{\mu_{exch}} dW \, [Im \, A_2 - Im \, A_1]$$

where by X we mean all terms not specifically included.

The mass shift equations become:

$$R_1 (M_2 - M_1) = \sum_{exch} \frac{1}{\pi} \int_{\ell_{exch}}^{\mu_{exch}} dW \, (W-M_2)(Im \, A_2 - Im \, A_1)$$

$$+ X$$

$$R_2 (M_2 - M_1) = \sum_{exch} \frac{1}{\pi} \int_{\ell_{exch}}^{\mu_{exch}} dW \, (W-M_1)(Im \, A_2 - Im \, A_1)$$

$$+ X$$

In the static model, the short left-hand cut is approximated by a pole:

$$\frac{1}{\pi} \int_{\ell}^{u} \frac{\mathrm{Im}\ A(\acute{W})d\acute{W}}{(\acute{W}-W)} \cong \frac{1}{<W>\ -\ W} \ \frac{1}{\pi} \int_{\ell}^{u} \mathrm{Im}\ A\ (\acute{W})\ d\acute{W}$$

$$\cong \frac{1}{<W>\ -W}\ R_{exch}$$

or

$$\frac{1}{\pi}\ \mathrm{Im}\ A_2\ (\acute{W})\ \cong\ \frac{R_{exch}}{(u-\ell)}$$

where R_{exch} is the residue of the amplitude in the u-channel.

So we can write:

$$\delta R = \delta R_{exch} + X$$

Using the static crossing relations, which relate states of angular momentum $\ell = 1$ in the s-channel to states of $\ell = 1$ in the u-channel, we can determine R_{exch} from the residue of the bound state in the crossed channel.

$$\delta R_{exch} = C\delta R$$

where C depends on the spin and isospin of the direct and crossed channels.

In writing this equation, we have assumed the crossing matrix is the same for the SU_3 symmetric and unsymmetric cases. This assumption is equivalent to neglecting higher orders in $(M_2 - M_1)$ in the crossing matrix.

Finally, our equations become

$$\delta R = C\delta R + X$$

Except for terms in the vector X, these equations along with the factorization constraint are unchanged if all residues R_2 and R_1 are multiplied by the same factor; they are likewise independent of the particle masses.

As an illustration, consider the process $\Sigma\pi \to N\overline{K}$ for $\ell = 1$. In the direct reaction are channels having isospins $I = 0, 1$ and spins $J = 1/2, 3/2$. Of the particles in the baryon octet and decuplet, Σ, Λ, Y^* are found as intermediate states. The crossed reaction with nonzero baryon number is $\Sigma K \to N\pi$. Possible isospin and spin states with $\ell = 1$ are $I = 1/2, 3/2$ and $J = 1/2, 3/2$. N and N^* are found in the crossed channel. Consequently, we say that the scattering amplitudes for $\Sigma\pi \to N\overline{K}$ have two short left-hand cuts which arise from the exchange of N and N^*. To calculate the crossing matrix, consider a particular charge state of the process in the s-channel:

$$\Sigma^+ \pi^o \to p\overline{K}_0$$

This channel is purely $I = 1$. Consulting a table of Clebsch-Gordon coefficients, we obtain

$$\langle \Sigma^+ \; \pi^o \; |A| \; p\overline{K}o \rangle = \frac{1}{\sqrt{2}} \; A^s_{I=1}$$

Crossing, we obtain the u-channel process:

$$\Sigma^+ K_0 \to p\pi^o$$

This reaction is evidently a mixture of $I = 1/2$ and $I = 3/2$. From a table we obtain

$$\langle \Sigma^+ \; K_0 \; |A^u| \; p\pi^o \rangle = \frac{\sqrt{2}}{3} A^u_{I=3/2} - \frac{\sqrt{2}}{3} A^u_{I=1/2}$$

Consequently we can write

$$A^2_{I=1} = \frac{2}{3} A^u_{I=3/2} - \frac{2}{3} A^u_{I=1/2}$$

Similar calculations applied to the process $\Sigma^0 \pi^0 \rightarrow n\bar{K}_0$ allow us to obtain the behavior of $A^s_{I=0}$ under crossing. States of orbital angular momentum $\ell = 1$ cross into themselves in the static limit, so we want to calculate the crossing of s-channel states with $J = 1/2, 3/2$ into u-channel states with $J = 1/2, 3/2$. Spin crosses the same way as isospin in the static limit, and a claculation similar to the isospin calculation above yields

$$A^s_{J=3/2} = \frac{2}{3} A^u_{J=1/2} + \frac{1}{3} A^u_{J=3/2}$$

$$A^2_{J=1/2} = -\frac{1}{3} A^u_{J=1/2} + \frac{4}{3} A^u_{J=3/2}$$

Combining the crossing relations for spin with those for isospin, we obtain crossing relations for the particle states in the direct and crossed channels:

$$A^s_{Y*} = \frac{2}{9} A^u_{N*} - \frac{4}{9} A^u_{N}$$

$$A^s_{\Sigma} = \frac{8}{9} A^u_{N*} + \frac{2}{9} A^u_{N}$$

$$A^2_{\Lambda} = \frac{8\sqrt{6}}{9} A^u_{N*} - \frac{\sqrt{6}}{9} A^u_{N}$$

Consequently, the residue shift equations for this particular set of particles can be written as follows:

$$\delta R(Y^* | \Sigma\pi, \ N\overline{K}) = \frac{2}{9} \delta R(N^* | N\pi, \ \Sigma K) - \frac{4}{9} \delta R(N | N\pi, \ \Sigma K) + X(Y^* | \Sigma\pi, \ N\overline{K})$$

$$\delta R(\Sigma | \Sigma\pi, \ N\overline{K}) = \frac{8}{9} \delta R(N^* | N\pi, \ \Sigma K) + \frac{2}{9} \delta R(N | N\pi, \ \Sigma K) + X(Y^* | \Sigma\pi, \ NR)$$

$$\delta R(\Lambda | \Sigma\pi, \ N\overline{K}) = \frac{8\sqrt{6}}{9} \delta R(N^* | N\pi, \Sigma K) - \frac{\sqrt{6}}{9} \delta R(N | N\pi, \ \Sigma K) + X \ (\Lambda | \Sigma\pi, \ N\overline{K})$$

A complete list of our residue shift equations for baryon-pion scattering is given in Table 3. Note that there are 74 equations but, assuming factorization, 29 independent unknowns (assuming charge conjugation invariance, this number drops to 24).

DDFS did not explicitly consider the problems associated with the inconsistency of the residue shift equations. They made the approximation

$$R_2^{ij} - R_1^{ij} = g_i^1 \ \delta g_j + g_j^1 \ \delta g_i + \delta g_i \ \delta g_j \approx g_i^1 \ \delta g_j + g_j^1 \delta g_i$$

thus linearizing the residue shift equations in δg (discarding terms which were not negligible), and then projected the g_i^1 out against itself (an averaging process which is not necessarily optimal). The resulting equations were treated by matrix methods. In this approximation the matrix R_2 is automatically factorizable. The equations for the coupling shifts were written in the form

$$\delta g_i = A_{ij}^{gg} \ \delta g_j + X_i$$

where the vector X contains all the terms not specifically included in $A^{gg} \ \delta g$: contributions from non-linear effects in δg; from the effects of the mass shifts; from distant cuts which were excluded in

the treatment of the equations; and possibly, from interactions present in nature which break SU_3 in the same way that the presence of electromagnetic interactions break isospin symmetry. Not expecting to be able to calculate X accurately, DDFS noted that if A^{gg} has an eigenvalue near one, the projection of the corresponding eigenvector on the vector X will be much larger than projections of X on the other eigenvectors, except for the case, of low probability, where the unknown vector X happens to be orthogonal to the favored eigenvector. The eigenvector corresponding to the unit eigenvalue of A^{gg} is said by DDFS to be "enhanced." The elements of this eigenvector will probably be nearly in the same ratio as the coupling shifts observed in nature. The overall magnitude of the coupling shifts, however, can be determined only from unattainable knowledge about X. This procedure is suspect for finite coupling shifts if X is itself a rapidly varying function of the coupling shifts.

DDFS, in selecting an enhanced eigenvector of A^{gg}, arrived at a process of filtering information out of the over-determined system with errors. Their method, however, derives from an invalid linearization of the original equations as well as an averaging of these equations which is not necessarily optimal. We expect it to be accurate, at best, in the limit of small coupling shifts; it may give only a rough estimate of the full-size coupling shifts.

Our method, on the other hand, is not limited to linear systems. The factorizability of R_2 appears as a constraint on the solution, rather than an automatic feature at the expense of accuracy in the equations. Since the factorizability condition is a highly

non-linear feature, we might expect to obtain some information about the size of δg. As we shall see in the next section, our calculation preserves the enhancement mechanism in an altered form.

PART I

SECTION III

THE CALCULATION

In the following pages, we apply the principles developed in Section I to the model discussed in Section II. In Table 3, the residue shift equations are arranged in closed systems of linear equations, the coefficients being determined from the crossing matrix elements. As before, the equations are written in the form

$$\delta R = A \delta R + X$$

so that the homogeneous equations have a solution when the matrix A has an eigenvalue equal to one. Table 3 lists the eigenvalues of the matrices A, and in those cases where an eigenvalue is near one, the eigenvector corresponding to that eigenvalue is also tabulated.

Note that in almost every case,[9] there is a clear differentiation between systems with an eigenvalue near one and systems with no eigenvalue near one. The single exception is a system with an eigenvalue $\lambda \cong .69$, which was assumed to be close enough to one to warrant including the corresponding eigenvector in the set of preferred equations.

Proceeding by the same logic as DDFS, we assign a special significance to the eigenvectors corresponding to the eigenvalues near one; we expect that the residue shifts are roughly proportional to the elements of these eigenvectors, subject to the constraint that the final residue matrix, R_2, is factorizable.

Table 4 contains a list of equations obtained by assuming that the residue shifts are proportional to the enhanced eigenvectors. Note that in going from the equations in Table 3 to the set in Table 4, we have reduced the number of equations from 74 to 38. Assuming that the equations in Table 3 explicitly include all the important terms varying with δR, we expect a reduction of errors concomitant with the reduction in the number of equations.

Following DDFS, we refer to the selection of the smaller number of equations as "enhancement." Not every residue shift is enhanced; some residue shifts are not determined by the equations in Table 4. We shall require that the unenhanced elements of the residue matrix R_2 be chosen to minimize the deviation of R_2 from factorizability. In this respect, we will be concerned with a second set of eigenvectors: the eigenvectors of the matrix R_2.

The equations in Table 4 can be arranged so that the enhanced elements of the baryon octet residue shifts are determined by the decuplet residue shifts. There are twelve decuplet-baryon-pion coupling constants. Writing the decuplet residues in terms of the decuplet coupling constants, we insure that the decuplet residue matrices are factorizable; the octet residues are determined by these twelve parameters, but are not necessarily factorizable.

One decuplet coupling constant, for $Y^* \rightarrow \Lambda \pi$, is fixed at an experimental value, and the other eleven decuplet couplings are varied until the octet residue matrices are most nearly factorizable, as determined by our factorizability criterion. If we believed our model to be very good, then we could optimize with respect to the twelfth

decuplet coupling constant as well. Fixing this number at an experimental value corresponds to specifying the size of the perturbation in the calculation of DDFS.

In summary, the original problem involving 74 equations in 29 unknowns has been reduced to a minimization problem in eleven variables. The actual calculation proceeded by an iteration scheme. The results of the DDFS calculation were used as a starting point for the matrix R_2. The unperturbed residue matrix R_1 was fixed according to the SU_3 symmetric model.

The enhanced octet matrix elements were replaced by the values indicated by the equations in Table 4, the present values of the decuplet residue elements being taken as input.

The R_2 resulting from this modification was then diagonalized and an optimum factorized approximation was computed, according to the methods discussed in Part I. We designate by Q this factorized approximation to R_2. Briefly,

$$(R_2)_{ij} = \sum_K \rho_K \lambda_i^K \lambda_j^K \quad \text{where} \quad \sum_i (\lambda_i^K)^2 = 1$$

and

$$Q_{ij} = \rho_1 \lambda_i^1 \lambda_j^1 \quad \text{where} \quad |\rho_1| = \max \left\{ |\rho_i| \right\}$$

If the choice of the eleven decuplet couplings were perfect, and the original equations were completely self-consistent, then Q and R_2 would be identical. The discussion in Part I indicated that a reasonable measure of the deviation of Q from R_2 would be the Euclidean norm of their difference:

$$\epsilon = \sum_{ij} (Q_{ij} - (R_2)_{ij})^2$$

In our actual calculation, we used another measure of the deviation:

$$\epsilon_{min} = \sum_{ij} |Q_{ij} - (R_2)_{ij}|$$

This step was taken because it was felt that the quadratic measure was insensitive to the behavior of couplings whose absolute magnitudes are much smaller than the average. Even with a linear measure, some insensitivity was evidenced (see Table 5).

The eleven-dimensional gradient of the error criterion, ϵ_{min}, was then computed by varying slightly the eleven free decuplet coupling constants and computing the values of R_2, Q, and ϵ_{min} at each point.

The unenhanced matrix elements of R_2 were then replaced by the corresponding elements of Q, and the decuplet couplings were moved a reasonable mesh step along the gradient of ϵ_{min}.

The iteration consisted of returning to the calculation of the enhanced matrix elements of R_2 from the equations in Table 4. This process was continued until the norm of the gradient of the error criterion fell below a satisfactory level, indicating that R_2 had been optimized with respect to factorizability. One cycle of this iteration process required from six to ten seconds of 7094 computation time. Sixty iterations were performed in the calculation.

Notice that the computation centers around the diagonalization of one 5 x 5 and three 4 x 4 matrices. Table 5 contains these four R_2

matrices, before and after application of the optimum factorization procedure. Also listed are the eigenvalues of each residue matrix. Ideally, only one eigenvalue would be non-zero. Our optimization procedure makes one eigenvalue much larger than the rest.

Table 6 contains a list of the SU_3 symmetric couplings, the couplings obtained in DDFS, and the couplings obtained in this calculation. In most cases, this calculation agrees with DDFS on the direction of coupling shifts away from the SU_3 symmetric limit; we obtain, however, different magnitudes of shifts. This result is consistent with our expectations.

As a check of the charge conjugation properties of our couplings, Table 7 compares the theoretical ratios with the results of our calculation. The charge conjugation ratios could have been taken as additional constraints on our set of eleven free decuplet couplings. Otherwise, we could follow the example of DDFS and average out the charge conjugation errors.

As an additional check on the residue calculation, we investigated the consistency of the mass shift equations. Table 8 lists the masses computed from the experimental masses and the calculated coupling constants. To test the sensitivity of our calculation to the neglect of kinematic effects in the crossing matrix, we performed the same computation using the static model crossing matrices including the correct kinematic factors determined by experimental masses. As can be seen in Table 8, the masses were not very sensitive to these changes.

No attempt was made to optimize the mass-shift equations. Instead, the redundant system was averaged by projecting the set of equations against the residue matrices appearing on the left hand side, in a manner exactly analogous to the calculation of DDFS.

PART II

SECTION I

GENERAL DISCUSSION

Consider the two body elastic scattering of spinless particles of identical nonzero mass, M. There are three physical channels:

$$\text{s-channel:} \quad 1 + 2 \rightarrow 3 + 4$$
$$\text{t-channel:} \quad 1 + \overline{3} \rightarrow \overline{2} + 4$$
$$\text{u-channel:} \quad 1 + \overline{4} \rightarrow 3 + \overline{2}$$

We will find it convenient to use the standard Mandelstam variables: s, t, and u, the squares of the total CM energies in the s-channel, t-channel, and u-channel, respectively. We will also use the squares of the CM momenta: q_s^2, q_t^2, q_u^2. Finally, we will use the cosines of the CM scattering angles in the various channels: $\cos \theta_s$, $\cos \theta_t$, $\cos \theta_u$.

These variables are related by equations such as the following:

$$s = 4(q_s^2 + M^2)$$
$$t = -2q_s^2(1 - \cos \theta_s)$$
$$u = -2q_s^2(1 + \cos \theta_s)$$

The Mandelstam variables are constrained as follows:

$$s + t + u - 4 M^2$$

This relation is a manifestation of the fact that a two body scattering

amplitude is a function of only two independent variables.

We assume that the scattering amplitudes are analytic func-
tions of the Mandelstam variables, except for cuts and poles, and that
the scattering amplitude for any channel can be obtained by analytic
continuation of the amplitude for any other channel, so that one
amplitude is sufficient to determine the scattering in all three
channels. We do not admit the possibility of natural boundaries in our
scattering amplitude.

In any channel, the scattering amplitude can be expanded in
a Legendre series. For example, in the s-channel

$$A\ (s,\ t,u) = \sum_{\ell=0}^{\infty}\ (2\ell + 1)\ a_\ell\ (s)\ P_\ell\ (\cos\ \theta_s)$$

$$s \geq 4\ M^2$$

$$-\ 1 \leq \cos\ \theta_s \leq 1$$

The sum converges for all physical s-channel angles, provided that all
crossed-channel intermediate states have nonzero mass. This require-
ment means that our idealized scattering process does not include
electromagnetic interactions, for example.

It is convenient to work with kinematic singularity free
amplitudes. In this case, the scattering amplitude will have a singu-
larity if and only if one of the Mandelstam variables attains such a
value that a physical intermediate state is possible. For example, if
there is a single particle state of mass M_x, whose quantum numbers are
compatible with the s-channel, then the amplitude will have a pole at

$s = M_x^2$. A trivial set of multiparticle states are the two-body

intermediate states consisting of particles 1 and 2 in the s-channel.

These states cause the scattering amplitude to have a cut running from

$s = 4M^2$ to $s = \infty$. In general, an s-channel multibody intermediate

state of N particles with masses M_i, i = 1, 2, ..., N will produce a

cut in the amplitude running from s = $(\sum_{i=1}^{N} M_i)^2$ to $s = \infty$. We will

take all such cuts along the real axis.

Of particular interest is the case where the scattering is

defined in terms of a set of partial wave amplitudes. For physical

s-channel angles, the set completely specifies the total amplitude

according to the convergent Legendre series. This set is thus suf-

ficient to determine the scattering amplitude everywhere, by means of

analytic continuation. The various techniques of this analytic

continuation are a central topic of our later discussion.

At this point, it is appropriate to review briefly the

Sommerfeld-Watson transformation, a classic technique for the continu-

ation of the Legendre series.[10] An analytic function can be found

which interpolates the partial wave set $\{ a_\ell(s) \}$ in a strip containing

the positive real ℓ-axis. We designate this function by $a_\ell(s)$, and

henceforth our notation will not differentiate between the set of

partial wave amplitudes and any interpolation we might choose. Then

the Legendre series can be written as a contour integral:

$$\sum_{\ell = 0}^{\infty} (2\ell+1)\, a_\ell(s)\, P_\ell(s) = \frac{i}{2} \int_C d\lambda \; \frac{a_\lambda(s)\, P_\lambda(-\cos\theta_s)\,(2\lambda + 1)}{\sin\pi\lambda}$$

where the contour C is a circuit coming from ∞ below the real axis,

counterclockwise around the origin and back to ∞ above the real axis.
C is chosen to lie entirely inside the strip of analyticity of $a_\ell(s)$.
It should be evident that interpolation is not unique. We will require,
however, that $a_\ell(s)$ be chosen in such a way that

$$\int_{C'} \frac{d\lambda \; (2\lambda+1) \; a_\lambda(s) \; P_\lambda \; (-\cos \theta_s)}{\mathrm{Sin} \; \pi \; \lambda} \;\; = \;\; 0$$

where C' is the arc of infinite radius centered on $\lambda = -1/2$, extending
clockwise from $\lambda = -1/2 + i \; \infty$ to $\lambda = -1/2 - i \; \infty$. It has been demon-
strated[11] in the theory of potential scattering that there is at
most one function $a_\ell(s)$ which satisfies all these requirements, and
that such a function will be analytic in the ℓ-plane except for poles.
Then we can express our Legendre series in terms of a finite series
and another contour integral:

$$\sum_{\ell=0}^{\infty} (2\ell+1) \; a_\ell(s) \; P_\ell \; (\cos \theta_s) = \pi \sum_n \frac{2\alpha_n+1}{\sin \; \pi\alpha_n} \; \beta_n \; P_{\alpha_n} \; (-\cos \theta_s)$$

$$+ \int_{C''} \frac{d\lambda}{2i} \; \frac{a_\lambda(s) \; P_\lambda(-\cos \theta_s)}{\sin \; \pi \; \lambda}$$

C" is a straight line running from $\lambda = -1/2 + i \; \infty$ to $\lambda = -1/2 - i \; \infty$.
$\{a_n(s)\}$ is the set of poles of $a_\ell(s)$ lying to the right of C", and
$\{\beta_n(s)\}$ is the set of corresponding residues. The poles are called
"Regge poles." Their paths in the ℓ-plane traced as functions of s
are called "Regge trajectories." The integral is called the "back-
ground integral."

These trajectories have a special physical significance. As we vary s, the set of Regge poles will move along their trajectories. Fixing ℓ at some non-negative integer, we see that the partial wave amplitude $a_\ell(s)$ appears to go through a resonance as any of the trajectories passes near ℓ. Evidently, there is pole dominance near a resonance. As we shall see later, however, it would be incorrect to assume that any pole or finite collection of poles in this expansion accurately represents non-resonant amplitudes.

Of particular consequence is the importance of the Regge pole terms relative to the contribution of the background integral. It can be shown that the Regge pole terms dominate the background integral as $|\cos \theta_s| \to \infty$. In fact, the asymptotic behavior in $\cos \theta_s$ is determined by the asymptotic expansion of the leading pole terms, for which $\mathrm{Re}\ \alpha_n$ is maximum:

$$A(s,t,u) \underset{|\cos \theta_s| \to \infty}{\sim} \frac{2\pi\ \beta_n}{\sin \pi\alpha_n} \frac{\Gamma(\alpha_n+3/2)}{\Gamma(\alpha_n + 1)}\ (2 \cos \theta_s)^{\alpha_n}$$

For finite $\cos \theta_s$, however, the other trajectories and the background integral are important. If we are concerned with low-energy behavior in the t-channel, the Sommerfeld-Watson transformation is especially clumsy.

Suppose that M_x is the mass of the lowest-energy inter-mediate state in the crossed channels (not necessarily a single particle state). Without any essential loss of generality, we can consider the only crossed channel to be the t-channel.[12] The s-channel partial

wave expansion will converge inside an ellipse in the complex $\cos \theta_s$-plane with focii at $\cos \theta_s = \pm 1$ and whose boundary includes the nearest singularity, $\cos \theta_s = 1 + \dfrac{M_x^2}{2q_s^2}$. This point corresponds to an unphysical angle.

It is convenient to define a function $\xi(s)$:

$$\cosh \xi(s) = 1 + \frac{M_x^2}{2q_s^2}$$

$$\xi(s) > 0$$

The function represented by our Legendre series then has a singularity at $\cos \theta_s = \cosh \xi(s)$. For simplicity, suppose that this singularity is a pole. Later on, we can integrate over a distribution of poles to represent a cut.

The contribution of the pole to the partial wave amplitude is

$$\frac{\rho(s)}{2q_s^2} \, Q_\ell \, (\cosh \xi(s))$$

where $\rho(s)$ is the residue of the pole in t:

$$A(s,t,u) \cong \frac{\rho(s)}{t - M_x^2} + \text{regular function}$$
$$\text{for } t \cong M_x^2$$

The nearest singularity dominates the asymptotic behavior of the partial wave amplitudes as $\ell \to \infty$, Re $\ell > -1/2$. From the asymptotic behavior of Q_ℓ we obtain[13]

$$a_\ell(s) \underset{\substack{\ell \to \infty \\ \mathrm{Re}\ \ell > -1/2}}{\sim} \frac{\rho(s)\sqrt{\pi}}{2q_s^2} \frac{\exp\left[-(\ell+1/2)\,\xi(s)\right]}{\sqrt{2\ell}\ \sinh \xi(s)}$$

The more distant singularities contribute terms whose magnitudes decrease at exponentially faster rates as $\ell \to \infty$.

Approximating the Sommerfeld-Watson expansion with a single Regge pole results in the following partial wave amplitudes:

$$a_\ell \cong \frac{\beta_n\,(2\alpha_n+1)}{(\alpha_n-\ell)\,(\alpha_n+\ell+1)}$$

Evidently this approximate amplitude has incorrect asymptotic behavior as $\ell \to \infty$. This property corresponds to an improper positioning of singularities in the $\cos \theta_s$-plane. $P_\alpha(-\cos \theta_s)$ has a cut running from $\cos \theta_s = 1$ to $\cos \theta_s = \infty$. This extraneous cut from $\cos \theta_s = 1$ to $\cos \theta_s = \cosh \xi(s)$ can be removed by adjustment of terms between the Regge poles and the background integral.[14] In this case, the problems remain of imposing direct-channel unitarity and determining the background integral in terms of physically relevant quantities. The behavior of the amplitude near $\cos \theta_s = \cosh \xi(s)$ is not well approximated by the Sommerfeld-Watson representation, and for physical s-channel angles we would expect the method to be even worse.

We adopt the customary definitions of phase shift δ_ℓ and elasticity η_ℓ in terms of the S-matrix projection S_ℓ, as follows:

$$\delta_\ell = \frac{1}{2}\ \mathrm{Im}\ \log S_\ell(s) \qquad \ell = 0,\ 1,\ 2,\ \ldots$$

$$\eta_\ell = \exp\left[\mathrm{Re}\ \log S_\ell(s)\right] \qquad s \geqslant 4\ M^2$$

Log S_ℓ is purely imaginary above threshold for a process with no open inelastic channels.

In every case,

$$0 \leq \eta_\ell \leq 1 \qquad\qquad \ell = 0, 1, 2, \ldots$$

Definition of the amplitude in terms of a unitary scattering matrix is a matter of convention. With some choice of kinematic factor, $K(s)$, we can write

$$a_\ell(s) = \frac{1}{2iK(s)} [S_\ell(s) - 1] .$$

From the asymptotic behavior of the scattering amplitude, we obtain

$$\log S_\ell \underset{\substack{\ell \to \infty \\ \mathrm{Re}\, \ell > -1/2}}{\sim} \frac{i\,\rho(s)\,K(s)}{q_s^2} \sqrt{\pi}\, \frac{\exp[-(\ell + 1/2)\,\xi(s)]}{\sqrt{2\ell \sinh \xi(s)}}$$

We could generalize this asymptotic formula by writing an expansion of $\log S_\ell$, which explicitly exhibits the relationship between the detailed behavior as $\ell \to \infty$ and the singularity structure of the amplitude in the $\cos \theta_s$-plane:

$$\log S_\ell = \sum_n \sigma(\xi_n)\, Z(\ell, \xi_n)$$
$$+ \int_\xi^\infty d\xi'\, \sigma(\xi')\, Z(\ell, \xi')$$

where the sum is taken over the $\xi_n(s)$ corresponding to single particle states and the integral is taken over multi-particle cuts in the

cos θ_s plane. Evidently for the nearest singularities

$$Z \quad (\ell, \xi) \sim 0(e^{-\ell \xi} / \sqrt{\ell})$$

$$\ell \rightarrow \infty$$

$$\text{Re } \ell > -1/2$$

but the precise form of $Z(\ell, \xi)$ would have to be determined by a more careful study of the asymptotic properties of log S_ℓ . If the scattering in a certain energy region of the crossed-channel process were dominated by a resonance, it would be valid to write a resonance approximation to the integral:

$$\int_\xi d\xi' \; \sigma(\xi') \; Z(\ell, \xi) \stackrel{\sim}{=} R(\xi_R) \; Z(\ell, \xi_R) \; .$$

For a wide class of potential scattering problems, it has been demonstrated[15] that the asymptotic behavior of S_ℓ in the left-half ℓ-plane is

$$S_\ell \sim \exp \left[2i \; \pi(\ell + 1/2) \right] \qquad \ell \rightarrow \infty$$

$$\text{Re } \ell < -1/2$$

Some investigators have speculated[16] on the possibility of pushing the background integral contour farther into the left half plane, possibly all the way to infinity, and replacing it by a sum of terms corresponding to the Regge poles lying between the new contour and the old contour. The asymptotic behavior of S_ℓ in the left half

ℓ-plane, however, indicates that the background integral would thereby become more important, rather than diminish.[17] Such a process would therefore not be convergent. We are forced to the conclusion that the background integral is important and is not simply related to the Regge poles that lie to the left of the background integral contour.

The elastic unitarity condition for the partial wave amplitude is

$$\operatorname{Im} a_{\ell}(s) = K(s) \, |a_{\ell}(s)|^{2} \qquad \ell = 0, \ 1, \ 2, \ \dots \ .$$

This equation is a hopeless tangle of Regge poles and background terms, unless we restrict our consideration to a small number of terms in the Sommerfeld-Watson expansion. In channels with no inelasticity, the unitarity condition can be written for complex ℓ

$$S_{\ell*}^{*}(s) \, S_{\ell}(s) = 1 \qquad\qquad s, \geqslant 4 \, M^{2}$$

Therefore elastic unitarity implies that if $S_{\ell}(s)$ has a pole at $\ell = a(s)$, then it must have a zero at $\ell = \alpha^{*}(s)$, and under no other circumstances. The Regge pole structure of the S-matrix determines in a trivial way the positions of all the poles and zeros of the S-matrix. The corresponding statement is not true for the amplitude, however.

The most natural way to incorporate this information into the amplitude is to use a product form[18] for S_{ℓ} :

$$S_{\ell} = \prod_{n} \left(\frac{\ell - \alpha_{n}^{*}(s)}{\ell - \alpha_{n}(s)} \right) e^{\phi_{\ell,n}(s)}$$

where the product is taken over the Regge poles of the amplitude. The $\phi_{\ell,n}$ are convergence factors. We could write this relation as follows:

$$\log S_\ell = \sum_n \psi_{\ell,n}(s)$$

where

$$\psi_{\ell,n} = \log \left[(\ell-\alpha_n^*(s)) \right] - \log \left[\ell-\alpha_n(s) \right]$$

$$+ \phi_{\ell,n}(s)$$

$$s \geqslant 4 M^2$$

From our previous discussion, we impose asymptotic conditions on $\{\psi_{\ell,n}\}$:

$$\sum_n \psi_{\ell,n} \underset{\ell \to \infty}{\sim} \frac{i\rho(s) K(s)}{q_s^2} \sqrt{\pi} \frac{\exp \left[-(\ell + 1/2)\xi \right]}{\sqrt{2\ell \sinh \xi}}$$
$$\text{Re } \ell > -1/2$$

$$\sum_n \psi_{\ell,n} \underset{\ell \to \infty}{\sim} 2i \pi(\ell + 1/2)$$
$$\text{Re } \ell < -1/2$$

Elastic unitarity is equivalent to

$$\text{Re } \sum_n \psi_{\ell,n} = 0 \qquad\qquad \ell = 0, 1, 2, \ldots .$$

In the general case, we must have

$$\text{Re } \sum \psi_{\ell,n} \leq 0 \qquad\qquad \ell = 0, 1, 2, \ldots .$$

The only finite singularities allowed for $\psi_{\ell,n}$ are logarithmic singularities at the Regge pole and Regge zero. The requirement that the Regge singularity in the amplitude be a simple pole fixes the overall multiplicative constant for $\psi_{\ell,n}$. This fact will have a bearing on the size of $\rho(s)$, the t-channel residue of the whole amplitude. $\psi_{\ell,n}$ is not defined as an analytic function of s unless we replace α_n^* by an analytic function agreeing with $\alpha_n^*(s)$ for real s above threshold. Such a function is $\alpha_n^{II}(s)$, the anlytic continuation of $\alpha_n(s)$ defined by taking a counterclockwise circuit around the threshold branch point and onto the second physical sheet. To avoid any confusion, we denote the function $\alpha_n(s)$ on the first physical sheet by $\alpha_n^I(s)$. We should then express $\psi_{\ell,n}(s)$ in terms of the boundary values of the analytic functions

$$\psi_{\ell,n}(s) = \lim_{\epsilon \to 0} \{\log [\ell-\alpha^{II}(\sigma)] - \log [\ell-\alpha^I(\sigma)]$$
$$+ \phi_{\ell,n}(\sigma)\}|_{\sigma = s + i\epsilon}$$
$$s \geq 4 M^2$$

This point is important, as we will see later in a discussion of the effects of open inelastic channels.

Just as in Part I, our concern here should be to make maximum use of the information we possess about our scattering process, and to cast the approximation scheme in such a way as to minimize the consequences of errors we will inevitably make in formulating a model for a practical calculation.

In order to satisfy unitarity, we have introduced a "Regge zero" as well as a Regge pole, and thereby have lost the possibility of independently specifying a Regge residue. Near a Regge pole, in fact:

$$
S(\ell,s) = e^{\phi_n(\alpha_n^I, s)} \left(\frac{\alpha_n^I - \alpha_n^{II}}{\ell - \alpha_n^I} \right) \prod_{m \neq n} \left[\left(\frac{\alpha_n^I - \alpha_m^{II}}{\alpha_n^I - \alpha_m^I} \right) \exp(\phi_{\ell,m}) \right]
$$

$$
+ \text{ regular function}
$$

$$
\text{for } \ell \stackrel{\sim}{=} \alpha_n^I
$$

As we remarked earlier, all that is necessary for a complete specification of the total scattering amplitude is knowledge of the set of partial wave amplitudes $\{a_\ell(s)\}$ for non-negative ℓ, along with a viable method of analytic continuation. We have rejected the Sommerfeld-Watson transformation for practical reasons: it is clumsy in dealing with direct-channel unitarity and in determining the behavior of the amplitude around nearby crossed-channel singularities, and there is no simple way to approximate the background integral. Another reason for searching for different techniques is that the Sommerfeld-Watson method involves the use of unphysical scattering amplitudes. It is fashionable in S-matrix theory to take care to talk only about physically relevant quantities; at the critical step, the relation of one channel to another, it seems odd to resort to unphysical entities, such as the values of a_ℓ for $\text{Re}\,\ell = -1/2$.

We shall, however, utilize certain information abstracted from the Sommerfeld-Watson method. For example, we restrict our

consideration to a class of representations for the scattering ampli-
tudes for which Regge poles are manifest, thereby treating whole
sequences of resonances in a unified way. We also incorporate non-
Regge information, insisting on certain asymptotic behavior of our
amplitudes, independent of the level of approximation.

We will make use of representations in which $\log S_\ell$ is
specified in terms of physically relevant quantities. In this case,
$\log S_\ell$ is a simpler function than S_ℓ, from the point of view of
practical analytic methods. Nevertheless, we must continue the sum:

$$A(S, \cos \theta_s) = \frac{1}{2i\ K(s)} \sum_{\ell=1}^{\infty} (2\ell + 1) \{\exp [\log S_\ell(s)]-1\} P (\cos \theta_s)$$

Let us therefore consider a class of methods for the continuation of
functions defined in terms of Legendre series. It will be obvious that
these methods, with appropriate modification, can be used for expansions
in terms of any set of orthogonal functions.

Consider the analytic continuation of

$$f(z) = \sum_{\ell=0}^{\infty} (2\ell + 1)(e^{b_\ell}-1)\ P_\ell(z)$$

where the related function

$$g(z) = \sum_{\ell=0}^{\infty} (2\ell + 1)\ b_\ell\ P (z)$$

will yield more readily to analysis. Writing Cauchy formulas for
$f(z)$ and $g(z)$:

$$f(z) = \frac{1}{\pi} \int_{z_0}^{\infty} \frac{dz' \; \Delta f(z')}{z'-z}$$

$$g(f) = \frac{1}{\pi} \int_{z_0}^{\infty} dz' \; \frac{\Delta g(z')}{z'-z}$$

we want to determine $\Delta f(z)$ in terms of $\Delta g(z)$. We define a new function;

$$f_{\lambda}(z) = \sum_{\ell=0}^{\infty} (2\ell + 1)(e^{\lambda b_{\ell}} -1) \; P_{\ell}(z) \; ,$$

which for $0 < \lambda \leq 1$ evidently converges within the same region as the sum for $f(z)$. Trivially, $f_0(z) = 0$ and $f_1(z) = f(z)$. Differentiating the new function, we obtain

$$\frac{\partial}{\partial \lambda} \; f_{\lambda}(z) = g(z) + \sum_{\ell=0}^{\infty} (2\ell + 1) \; b_{\ell} \; (e^{\lambda b_{\ell}} -1) \; P_{\ell}(z)$$

Now we have obtained a new Legendre series whose coefficients are products of coefficients belonging to two other series.

Recall the addition theorem[19] for Legendre polynomials:

$$P_{\ell}(z'') = P_{\ell}(z) \; P_{\ell}(z') + 2 \sum_{m=1}^{\ell} \frac{(\ell-m)!}{(\ell+m)!} \; P_{\ell}^{m}(z) \; P_{\ell}^{m}(z') \cos m \; \phi$$

where $z'' = z \; z' + (z^2-1)^{1/2}(z^2{}'-1)^{1/2} \cos \phi$

Also recall the orthogonality condition[20] for the Legendre polynomials:

$$\int_{-1}^{1} P_\ell(z) \, P_\ell{}'(z) \, dz = \frac{2 \, \delta_{\ell\ell'}}{2\ell + 1}$$

These two properties imply that our new series can be expressed as follows:

$$\sum_{\ell=0}^{\infty} (2\ell + 1) \, b_\ell (e^{\lambda b_\ell} - 1) \, P_\ell(z)$$

$$= \frac{1}{4\pi} \int_{-1}^{1} dz' \int_{0}^{2\pi} d\phi \, f_\lambda(z') g(z'') \Bigg|_{z''=zz'+(z^2-1)^{\frac{1}{2}}(z'^2-1)^{\frac{1}{2}}\cos \phi}$$

Consequently, we have reduced the problem of continuation of f(z) to the solution of an integrodifferential equation:

$$\frac{\partial}{\partial\lambda} \, f_\lambda(z) = g(z) + \frac{1}{4\pi} \int d\Omega' f_\lambda(z') \, g(z'')$$

with the boundary condition $f_0(z) = 0$.

The quantity of real physical interest is the discontinuity of f(z), since the cut in f(z) is related to physical intermediate states in the crossed-channel. In fact, to complete the dynamical specification of an amplitude defined in terms of direct-channel Regge poles, we would impose unitarity in the crossed channel, and consequently we would have to know the discontinuity across the crossed-channel cut.

The following identity[21] will be useful here:

$$\frac{1}{4\pi} \int d\Omega_p \; [\tau_1 - \hat{p}_1 \cdot \hat{p}][\tau_2 - \hat{p}_2 \cdot \hat{p}]^{-1}$$

$$= \int_{\eta_\infty}^{\infty} \frac{d\eta}{\eta - p_1 \cdot p_2} \; K^{-1/2}(\eta, \tau_1, \tau_2)$$

$$\text{where } \eta_0 = \tau_1 \tau_2 + (\tau_1^2 - 1)^{\frac{1}{2}} (\tau_2^2 - 1)^{\frac{1}{2}}$$

$$\text{and } K(x, \tau_1, \tau_2) = [(\tau_1 \tau_2 - x)^2 - (\tau_1^2 - 1)(\tau_2^2 - 1)]$$

Using the relation we obtain an equation to determine the discontinuity in $f(z)$ in terms of the discontinuity in $g(z)$:

$$\frac{\partial}{\partial \lambda} \Delta f_\lambda(z) = \Delta g(z) + \frac{1}{\pi} \int\int_{K > 0} \frac{dz' dz'' \; \Delta f_\lambda(z') \Delta g(z'')}{[K(z, z', z'')]^{\frac{1}{2}}}$$

$$\Delta f_0(z) = 0$$

$$\Delta f(z) = \Delta f_1(z)$$

This relation is a linear integral equation with the kernel being the form $K^{-\frac{1}{2}}$, familiar from the potential theory Mandelstam iteration scheme, integrated over the known discontinuity, Δg. This method should not be confused with the Mandelstam scheme, however, since the latter involves a non-linear integral equation which determines the singularities of the scattering amplitude from a partial knowledge of those singularities. Such a determination is on a

dynamical footing and is equivalent to imposing direct-channel
unitarity. Our method involves a linear equation which determines
the singularities of a function, hopefully an approximation to the
scattering amplitude. In any case, the function is entirely specified
beforehand by the set $\{b_\ell\}$. Our method is purely mathematical; it is
correct independent of direct-channel unitarity. After we determine
the analytic continuation of a partial wave expansion, we could com-
pare its behavior with the requirements of crossed-channel unitarity
and crossing. For example, if the direct and crossed channels were
identical, then we could bootstrap by requiring that the crossed
channel amplitude have resonances which correspond to the Reggeized
resonances in the direct channel.

It should be clear that our method and the Mandelstam scheme
have one important feature in common: the cuts propagate in exactly
the same way. If $g(z)$ has a singularity at $z = \cosh \xi$, then our
equation requires $f(z)$ to have an infinite sequence of singularities
at the points $z = \cosh n\xi$, $n = 1, 2, \ldots$. This fact makes iterative
methods of solution possible. Even more important, it means that the
nearest singularity of $f(z)$ is exactly the same as that of $g(z)$.

Of course, the success of this approach depends on our being
able to sum the series:

$$g(z) = \sum_{\ell=0}^{\infty} b_\ell \ (2\ell + 1) \ P_\ell(z)$$

representing it in some form that can be analytically continued to find
$g(z)$. Later, we will present some explicit examples of this sort of
summation, using representations for $b_\ell = \log S_\ell$ which have practical

significance. Should it happen that our methods of analysis are not sufficiently powerful to continue the input function g(z), however, we might still be able to find some function which relates the Legendre coefficients in our sum to the coefficients in a tractable sum. In our previous example, the function was an exponential. We were able to introduce a spurious parameter, λ, which "turned on" our unknown sum and its cut structure.

Another example is a rational function:

$$f(z,t) = \sum_{\ell=0}^{\infty} (2\ell+1) \frac{b_\ell}{1-tb_\ell} P_\ell(z)$$

$$g(z) = \sum_{\ell=0}^{\infty} (2\ell+1) b_\ell P_\ell(z)$$

It is quite straightforward to obtain an integral equation to determine f:

$$f(z,t) = g(z) + \frac{t}{4\pi} \int d\Omega' g(z') \left. f(z'',t) \right|_{\substack{z'' = zz' \\ + (z^2-1)^{1/2}(z'^2-1)^{1/2} \cos\phi}}$$

Evidently,

$$\sum_{\ell=0}^{\infty} (2\ell+1) \log(1-b_\ell t) P_\ell(z) = -\int_0^t f(z,t')dt'$$

If we are willing to consider second-order differential equations, we enter the realm of complete sets of functions, which can be used to expand an arbitrary continuous function of our basic partial wave amplitude, b_ℓ. For example, if our unknown function is

$$f(z,\lambda) = \sum_{\ell=0}^{\infty} (2\ell + 1) [J_0(\lambda b_\ell)-1] P_\ell(z)$$

where $J_0(x)$ is the Bessel function of zero order, regular at $x = 0$, then we obtain the following equation:

$$\lambda \frac{\partial^2 f}{\partial \lambda^2} (z,\lambda) + \frac{\partial}{\partial \lambda} f(z,\lambda) = -\lambda h(z)$$

$$- \frac{\lambda}{4\pi} \int d\Omega' \; h(z')f(z'',\lambda)$$

$$z''=zz +(z^2-1)^{\frac{1}{2}}(z'^2-1)^{\frac{1}{2}}\cos \phi$$

where

$$h(z) = \sum (2\ell + 1) b_\ell^2 \; P_\ell(z)$$

$$f(z,0) = 0$$

$$\frac{\partial}{\partial \lambda} f(z,\lambda)\Big| = 0$$
$$\lambda = 0$$

Our method of analytic continuation makes no mention of continuation in angular momentum. Our integral equation, however, involves nonphysical partial wave amplitudes in intermediate steps.

In cases where we do not have an adequate knowledge of the analytic structure of the partial wave amplitude to carry out the integral equation scheme, we can still continue the Legendre series, since in principle all that is needed for complete specification of the scattering amplitude is the set of numerical values of the partial

wave amplitude. We will illustrate this fact by investigating a particular method of numerical continuation of the divergent Legendre series.

Consider the set of partial sums of our Legendre series:

$$\sigma_L(z) = \sum_{\ell=0}^{L} (2\ell + 1) \, a_\ell \, P_\ell(z), \quad L = 1, 2, \ldots$$

$$\sigma_0(z) = 0$$

If the sum converges then we have $\lim_{L \to \infty} \sigma_L(z) = f(z) < \infty$. If the sum fails to converge, we still expect that the set $\{\sigma_L(z)\}$ contains enough information to specify the analytic continuation of $f(z)$.

We have seen that $a \sim K \cdot Q_\ell(\cosh \xi)$ as $\ell \to \infty$, Re $\ell > -1/2$. If Re $(\eta - \xi) > 0$, the sequence of partial sums $\{\sigma_L(\cosh \eta)\}$ will not converge. In any case, for large enough L, [22]

$$\sigma_L \sim \text{const} + K' \sum_{\ell=0}^{L} (2\ell + 1) \, Q_\ell(\cosh \xi) \, P_\ell(\cosh \eta)$$

$$\sim \text{const}' + \frac{K' \, (L + 1)}{\cosh \xi - \cosh \eta} \{ Q_{L+1}(\cosh \xi) \, P_L(\cosh \eta)$$

$$- Q_L(\cosh \xi) \, P_{L+1}(\cosh \eta) \}$$

$$\sim \text{const}' + K'' \, e^{L(\eta - \xi)} \cdot L$$

or

$$\lim_{L \to \infty} \frac{\log \sigma_L}{L} = \text{const} < \infty \text{ as } L \to \infty$$

Asymtotically, at least, σ_L resembles an exponential function.

Most methods for summing divergent series involve a linear transformation of the sequence $\{\sigma_L(z)\}$ to obtain a new sequence which converges to $f(z)$. We refer the reader to a standard text[22] in this field for discussion of the linear methods.

Little attention seems to have been paid to nonlinear transformations as summation methods for partial wave expansions. In a remarkable paper, Shanks[23] investigated a class of nonlinear transformations of nonconvergent and slowly convergent sequences.

If $\{A_n\}$ is a sequence, Shanks defines the k-th order transform of $\{A_n\}$:

$$B_{K,n} = \frac{\begin{vmatrix} A_{n-K} & \cdots & A_{n-1} & A_n \\ \Delta A_{n-K} & \cdots & \Delta A_{n-1} & \Delta A_n \\ \Delta A_{n-K+1} & \cdots & \Delta A_n & \Delta A_{n+1} \\ \vdots & & & \\ \Delta A_{n-1} & \cdots & & \Delta A_{n+K-1} \end{vmatrix}}{\begin{vmatrix} 1 & \cdots & 1 \\ \Delta A_{n-K} & \cdots & \Delta A_n \\ \vdots & & \\ \Delta A_{n-1} & \cdots & \Delta A_{n+K-1} \end{vmatrix}}$$

where

$\Delta A_n = A_{n+1} - A_n$

$K = 1, 2, \ldots$

$n = K, K+1, \ldots$

$B_{0,n} = A_n$

Shanks showed that if $A_n = B + \sum\limits_{i=1}^{K} a_i q_i^n$, then $B_{K,n} = B$.

If the sequence converges, $|q_i| < |$ for all i, and B is called the limit of the sequence. If the sequence diverges, $|q_i| > |$ for at least one i, and Shanks calls B the <u>anti-limit</u> of the sequence.

Thus the transform removes exponential behavior from a sequence. Application of a transform will generate a new sequence, so that transforms can be compounded. Shanks defined a number of special transforms, but we are most interested in the "diagonal transform":

$$e_d (A_n) = B_{n,n}$$

Shanks showed that if $\{A_n\}$ is the set of partial sums of a power series, then the diagonal transform obtains the diagonal of the Pade table for the power series. Roughly speaking, the diagonal transform sequence is a set of attempts to fit the partial sums of the series with increasing numbers of exponential components. Asymptotically, we expect this to be a justifiable characterization for a Legendre series.

The simplest example of a Legendre series representing a function with a "Regge pole" is the partial wave expansion of the Legendre function itself:[24]

$$P_\alpha (z) = \frac{\sin \alpha\pi}{\pi} \sum_{\ell=0}^{\infty} (-)^\ell \left[\frac{1}{\alpha-\ell} - \frac{1}{\ell+\alpha+1} \right] P_\ell(z)$$

Computing the diagonal transform of the partial sum sequence for this series, we have compared the result with a contour integral determination of $P_\alpha(z)$ for several values of complex α and z. These results are presented in Appendix A. Inside or outside the ordinary

region of convergence, the agreement is excellent within the range of practical applicability of Shanks' diagonal transform and one would expect improvement with the introduction of multiple precision arithmetic.

One way to use Shanks' method in a bootstrap calculation would be to expand the total amplitude in partial wave sums in two identical channels. Continuing to a region in complex s and t where the diagonal transform sequence can be applied to both sums, we would then compare the two results.

The application of Shanks' technique is limited by the numerical accuracy of the input sequence as well as the precision retained in the intermediate arithmetic steps. Errors will propagate, and in general, the accuracy of the determination of the anti-limit is less than the accuracy of the defining sequence.

P. Wynn[25] simplified the computations involved in applications of Shanks' transforms. Wynn's algorithm eliminates the need for calculating determinants in Shanks' formulas:

if

$$\epsilon_{2m}(S_n) = e_m(S_n)$$

and

$$\epsilon_{2m+1}(S_n) = 1/e_m(\Delta S_n)$$

then

$$\epsilon_{K+1}(S_n) = \epsilon_{K-1}(S_{n+1}) + 1/[\epsilon_K(S_{n+1}) - \epsilon_K(S_n)]$$

provided that none of the quantities $\epsilon_{2m}(S_n)$ becomes infinite.

Having argued that a partial wave expansion is a practical way to specify a scattering amplitude, we return to the discussion of general properties of partial wave amplitudes. Previously, we had restricted our considerations to representations of the product form:

$$S(s) = e^{G(\ell,s)} \;\; \prod_n \left[\frac{\ell - \alpha_n^{II}(s)}{\ell - \alpha_n^{I}(s)} \right] e^{\phi_n(\ell,s)}$$

In generalizing to relativistic scattering problems, we propose to use this general form, explicitly exhibiting the pole- and zero-behavior of S_ℓ in the ℓ-plane. Below the elastic threshold, Im $\alpha^{I}(s) = 0$; at the elastic threshold, Im $\alpha^{I}(s)$ = IM $\alpha^{II}(s)$ = 0 and Re $\alpha^{I}(s)$ = Re $\alpha^{II}(s)$; for real s above the elastic threshold and below the first inelastic threshold, $\alpha_n^{I*}(s) = \alpha_n^{II}(s)$; above the first inelastic threshold, $\alpha_n^{I*}(s) \neq \alpha_n^{II}(s)$. Consequently, we need to know the Regge trajectory defined on two sheets in order to determine the behavior of the scattering amplitude for a process with inelastic channels or for a description of the amplitude below the elastic threshold.

In principle, we could determine the Regge trajectory on the second sheet by analytic continuation of the trajectory on the first sheet. In practice, however, knowledge of the analytic structure of the $\{\alpha_n(s)\}$ is equivalent to a complete solution of the scattering problem with many-body production processes. As a consequence, a practical Regge parametrization of two-body elastic scattering will involve specification of a new set of trajectory functions for every new threshold; to the extent of our ability to determine them, these new functions will be arbitrary, within certain limits.

As an illustration of the relation between the multi-sheeted Regge trajectory and the behavior of the partial wave amplitudes, consider a partial wave amplitude in an energy region for which only one resonance dominates the amplitude

$$S_\ell = \eta_\ell \, e^{2i\delta_\ell} \approx \frac{\ell - \alpha^{II}(s)}{\ell - \alpha^I(s)} \cdot Z_\ell$$

$$\text{for } s \cong S_R$$

Evidently,

$$\eta_\ell = \frac{|\ell - \alpha^{II}(s)|}{|\ell - \alpha^I(s)|} \, |Z_\ell|$$

and

$$\delta_\ell = \frac{1}{2} \arg(Z_\ell) + \frac{1}{2} \arg\left(\ell - \alpha^{II}(s)\right)$$

$$- \frac{1}{2} \arg\left(\ell - \alpha^I(s)\right)$$

If this energy is below the first inelastic threshold, then $\alpha^{I*} = \alpha^{II}$ and $|Z_\ell| = 1$. Figure 1a shows the trajectories, phase shift, and elasticity we expect in this case. As the energy rises through resonance, the two trajectory functions pass on either side of Re $\alpha = \ell$, with Im $\alpha^I(s) = -$Im $\alpha^{II}(s)$. Consequently, the elasticity factor remains constant:

$$\eta_\ell = 1$$

and the phase shift follows the pattern characteristic of an elastic resonance, rising from $\delta_\ell = \frac{1}{2} \arg Z_\ell$, through $\delta_\ell = \frac{1}{2} \arg Z_\ell + \pi/2$ at

resonance, and reaching $\delta_\ell = \frac{1}{2} \arg Z_\ell + \pi$ at energies well past the resonance.

Now consider the case where the resonance energy is above one or more inelastic thresholds. There are two cases which appear quite different in terms of the behavior of the phase shift, but which appear very similar when interpreted in terms of the behavior of the multi-sheeted Regge trajectory.

First, there is the case where the two trajectory functions pass on opposite sides of $\alpha = \ell$. Figure 1b illustrates this case. For simplicity, let us assume that Re $\alpha^I(s) = $ Re $\alpha^{II}(s)$. The condition $\eta_\ell < |$ then implies $|\text{Im } \alpha_I| > |\text{Im } \alpha_{II}|$. In order to have a rising phase shift as the energy goes through resonance, we must have Im $\alpha_I(s) > 0$. Evidently, the inelasticity will have a dip at resonance. The phase shift will rise through $\delta_\ell = \frac{1}{2} \arg Z_\ell + \pi/2$ to $\delta_\ell = \frac{1}{2} \arg Z_\ell + \pi$ at energies past resonance, just as in the completely elastic case.

The second possibility is for the two trajectories to pass on the same side of $\alpha = \ell$. In this case, Im $\alpha^I > $ Im $\alpha^{II} > 0$. Figure 1c indicates the expected behavior. Again, the inelasticity will dip at resonance. Slightly before resonance, the phase shift will rise to a value smaller than $\delta_\ell = \frac{1}{2} \arg Z_\ell + \pi/2$; exactly at resonance, it will pass downward through $\delta_\ell = \frac{1}{2} \arg Z_\ell$, going lower at energies slightly past resonance; finally, the phase shift will approach the value it had for energies well before resonance, $\delta_\ell = \frac{1}{2} \arg Z_\ell$.

Evidently, the difference between a "slightly inelastic" and a "very inelastic" resonance is simply that the trajectory on

the second sheet passes $\alpha = \ell$ on different sides of the real axis. Roughly speaking, the first elastic threshold causes equal and opposite increments in the imaginary part of α^{I} and α^{II}, whereas any inelastic threshold causes increases in Im α^{I} greater than the increase in $-$Im α^{II}. As mere inelastic channels open, Im α^{I} and Im α^{II} come to have the same sign.[26]

Examples of the three different kinds of resonances can be taken from elastic N_{π} scattering at low energy. Up to about 2000 MeV kinetic energy this scattering has been analyzed in terms of phase shifts and elasticity factors.[27] First, consider scattering in the $I = 3/2$ channel. In the P_{33} amplitude, there appear to be two resonances; one, the well-known 1238 MeV resonance at about 200 MeV above threshold, is completely elastic; the other, at about 900 MeV above threshold, is very inelastic, and shows up as a dip in the elasticity factor. In the F_{37} amplitude, there is a very inelastic resonance at about 1400 MeV above threshold, which produces a dip in the elasticity factor and an oscillation of the phase shift about zero (this resonance is presumably the Regge recurrence of the 1238 resonance). An example of a "slightly inelastic" resonance can be seen in the $I = \frac{1}{2}$ channel; in the D_{13} amplitude at about 600 MeV, the phase shift rises through ninety degrees and there is a large dip in the elasticity factor. In a schematic fashion, Figure 2 shows Regge trajectories which will account for this behavior.

Unitarity constrains the behavior of the trajectory on the two sheets. For example, if we assume Re $\alpha^{I} = R \, \alpha^{II}$ and that a one-trajectory approximation is valid, then the unitary bound on this

approximation amplitude implies

$$|\text{Im } \alpha^{II}| \leq |\text{Im } \alpha^{I}|$$

The precise effect of unitarity is modified by the presence of other trajectories. In any approximation, the precise consequences of unitarity will appear to depend on the form of the functions $G(\ell,s)$ and $\phi_n(\ell,s)$ in our amplitude.

Note that there does not seem to be any difficulty in principle with the phase shift because of infinitely rising trajectories. As more inelastic channels open, the $\alpha_n^{II}(s)$ cross the real axis and the resonances cease causing the phase shifts to jump by π. Furthermore, since the effect of a Regge pole is negated by a Regge zero, any of the other difficulties appearing to arise from infinitely rising Regge trajectories could be eliminated by the corresponding poles and zeros approaching coincidence. Since $|\alpha^{I}(s) - \alpha^{II}(s)| \rightarrow 0$ does not imply $\text{Im } \alpha^{I}(s) \rightarrow 0$, there is considerable freedom in the allowed representations for the Regge trajectory functions.

Now consider the partial wave amplitudes for a fixed and $\ell \rightarrow \infty$, $\text{Re } \ell > -1/2$. We have already seen that $\log S_\ell \sim 0(e^{-\ell\xi} \Lambda\!/\!\ell)$. A simple way to ensure this behavior would be to choose the $\phi_n(\ell,s)$ so that:

$$\phi_n(\ell,s) = \phi_n^{I}(\ell,s) - \phi_n^{II}(\ell,s)$$

and

$$\phi_n^{i}(\ell,s) - \log\,(\ell-\alpha_n^{i}(s)) \sim 0\,\,(e^{-\ell\xi}\,\Lambda\!/\!\ell) \qquad i = I,II$$
$$\substack{\ell \rightarrow \infty \\ \text{Re } \ell > -1/2}$$

We can specialize to a convenient class of representations without
losing too much generality as follows:

$$\phi_n^i \ (\ell,s) = g(\ell-\alpha_n^i(s)) \qquad\qquad i = I, II \ .$$

Taking $\alpha_n^i(s)$ as the origin for the ℓ-plane, we can write our asymptotic
condition as follows:

$$g(z,s) - \log \ (z) \underset{z \to \infty}{\sim} 0(e^{-z\xi} \sqrt{\ell} \ )$$

$$z = (\ell-\alpha)$$

If we assume that $g(z)$ is an entire function, we have constructed a
representation which has only Regge singularities and automatically
has the correct asymptotic behavior in the right half ℓ-plane, regard-
less of the number of terms kept in the product representation.

In the case of realistic particle scattering, it is often
supposed that the real part of a Regge trajectory rises indefinitely
with rising energy. To study the effect of this behavior on our
representation, we fix ℓ and allow α to rise, causing the variable
$z = (\ell-\alpha)$ to become large and negative. If $g(z)$ is an entire function,
then exponential fall-off for large positive z would imply exponential
growth for large negative z. At first sight, this class of repre-
sentations would therefore appear to have the unfortunate feature that
partial wave amplitudes are influenced more by remote Regge trajec-
tories than by nearby trajectories. We expect the opposite effect to
be the actual case: since the leading Regge trajectories correspond
to intermediate states with high spins, these trajectories should

become decoupled from the amplitude.

In our approximate model, the full contribution of a single Regge pole would be

$$\frac{\ell - \alpha^{II}(s)}{\ell - \alpha^{I}(s)} \quad \exp \left[g(\ell - \alpha^{I}(s), s) - g(\ell - \alpha^{II}(s), s) \right]$$

This formula indicates that the high-energy difficulties of our model would be resolved if any of the following three conditions were satisfied:

First, $\alpha(s)$ might rise but still be bounded by $s^{1/2}$. Since $\xi(s) \sim s^{-1/2}$, the product $\xi \cdot \alpha$ would remain bounded.

Second, $\alpha^{II}(s)$ might approach $\alpha^{I}(s)$ rapidly enough for $|\alpha^{I}(s) - \alpha^{II}(s)| \sim |e^{-\alpha \cdot \xi}|$. The remote trajectories would fade away as the pole-trajectory approaches coincidence with the zero-trajectory. This situation would contrast with potential theory, where the trajectories turn around rather than disappear.

Third, the relativistic problem allows Regge cuts as well as poles. Cuts in $g(z)$ might shield lower partial waves from distant trajectories. For example,[27a]

$$h(z) = \int_{0}^{1} \frac{dt}{t} (1 - e^{-\left[\frac{1}{2} \cdot \xi z + \frac{1}{2} \sqrt{z^2 \xi^2 + iA} \right] t}) - \gamma - \log z$$

$$= g(z) - \log z$$

is a function falling off exponentially for Re $z > 0$ and not blowing up exponentially for Re $z < 0$. In this particular case, the contribution from the distant Regge pole would reduce to

$$\frac{\ell-\alpha^{II}(s)}{\ell-\alpha^{I}(s)}$$

A priori, we have no idea how to approximate $\phi_n(\ell,s)$ when ℓ is in the midst of a cluster of Regge poles and cuts. Presumably, the $\phi_n(\ell,s)$ would be developed in a full dynamical calculation; considerations such as the above would be helpful, however, in arriving at a reasonable first approximation.

As is well known, the simplest way to describe high-energy s-channel scattering is to Reggeize the crossed-channel amplitude using the Sommerfeld-Watson expansion. In this case the leading t-channel Regge trajectories dominate scattering in the forward direction, and leading u-channel trajectories dominate backward scattering. Consequently in order to explore the general features of high energy s-channel partial wave amplitudes, we analyze a Reggeized exchange into partial waves.

A simple Born amplitude has the expansion

$$\frac{1}{t-m^2} = \frac{1}{2q^2} \sum_{\ell=0}^{\infty} (2_\ell + 1) \, Q_\ell \, (1 + \frac{m^2}{2q^2}) \, P_\ell \, (\cos \theta_s)$$

with "fixed poles" in the Q_ℓ functions at negative integral values of ℓ. We will now show that if we instead decompose $S^{\alpha(t)}/(t-m_\rho^2)$ into Legendre series, we obtain partial wave amplitudes which are entire functions of ℓ, assuming $\alpha(t)$ is linear in t.

A well known expansion for the exponential function is[28]

$$e^{az} = \sum_{\ell = 0}^{\infty} (2\ell + 1) \sqrt{\frac{\pi}{2a}} \; I_{\ell + \frac{1}{2}} (a) \; P_{\ell} (z)$$

where the I_{ℓ} are modified Bessel functions of the first kind. I_{ℓ} is an entire function of ℓ.

To expand $e^{bt} S^{\alpha(0) + \alpha'(0)t}$, for example, we would take

$$a = 2q_s^2 (b + \alpha'(0) \; \log s)$$

The expansion of $e^{az}/(z-z_0)$ follows from the expansion of e^{az}:

$$\frac{e^{az}}{z-z_0} = e^{az_0} \int_{a}^{\infty} e^{x(z-z_0)} dx$$

$$= \sum_{\ell = 0}^{\infty} (2\ell + 1) \left[e^{az_0} \int_{a}^{\infty} \sqrt{\frac{\pi}{2x}} \; I_{\ell+1/2}(x) \; e^{-z_0 x} \; dx \right] P_{\ell}(z)$$

A representation for I_ν valid in this range is[29]

$$I_\nu(x) = \frac{1}{\pi} \int_{o}^{\pi} e^{x \cos \theta} \cos \nu \, \theta d\theta - \frac{\sin \nu \pi}{\pi} \int_{o}^{\infty} e^{-x \cosh t - \nu t} dt$$

Consequently we obtain after a straightforward integration:

$$\int_a^\infty \sqrt{\frac{\pi}{2x}}\, I_{\ell+1/2}(x)\, e^{-z_0 x} dx = \sqrt{\frac{1}{2}} \int_0^\pi \frac{\cos\left[(\ell+1/2)\theta\right]\, \mathrm{Erfc}\left(\sqrt{a(z_0-\cos\theta)}\right) d\theta}{\sqrt{z_0-\cos\theta}}$$

$$- \frac{\sin\left[(\ell+1/2)\pi\right]}{\sqrt{2}} \int_0^\infty \frac{e^{-(\ell+1/2)x}\mathrm{Erfc}\left(\sqrt{a(z_0+\cosh x)}\right) dx}{\sqrt{\cosh x + z_0}}$$

where Erfc(x) is the complementary error function[30] normalized so that Erfc(0) = 1. The first integral poses no problem for continuation in ℓ , since it is taken over a finite interval with no singularities. The second integral converges for all ℓ due to the fact that integrand is asymptotic to

$$\frac{2}{\sqrt{\pi}} \frac{e^{-(\ell+1/2)x}\, e^{-z_0 a - a\cosh x}}{\sqrt{\cosh x + z_0}}$$

for large x.

Setting a = 0 in our partial wave amplitude for $e^{az}/(z-z_0)$ we obtain

$$\frac{1}{\sqrt{2}} \int_0^\pi \frac{\cos\left[(\ell+1/2)\theta\right] d\theta}{\sqrt{z_0-\cos\theta}} - \frac{\sin\left[(\ell+1/2)\pi\right]}{\sqrt{2}} \int_0^\infty \frac{e^{-(\ell+1/2)x} dx}{\sqrt{\cosh x + z_0}}$$

which is an integral representation[31] for the Legendre function of the second kind, $Q_\ell(z_0)$. Thus our partial wave amplitude for

$e^{az}/(z-z_0)$ reduces to the partial wave amplitude for $1/(z-z_0)$ as $a \to 0$, but unless $a = 0$, the partial wave amplitudes are entire functions of ℓ. For $a = 0$, we recover the "fixed poles" of the Born term expansion.

It is simple to explain the apparent discrepancy in behavior between the cases $a \neq 0$ and $a = 0$. Note that these partial wave amplitudes do not have the large ℓ behavior required to expand the contour in the Sommerfeld-Watson transformation: a valid Froissart-Gribov continuation is possible only for the case $a = 0$. In any case, these amplitudes are of interest only for non-negative integral ℓ, where they approximate the correct partial wave amplitudes; the exact amplitudes, presumably, can be interpolated in a suitable continuation with appropriate Regge poles. Certainly, however, there appears to be no easy and unique way to associate definite s-channel trajectories, either rising or fixed, with crossed-channel Regge behavior at high energy; simple identification of poles, as occurred in the partial wave analysis of the Born term, does not carry over to the relativistic high energy case. The exponential behavior in t near the forward direction appears to be a constraint on the behavior of the entire set of direct channel Regge poles, but a unique individual specification would come only with a treatment of crossing in more detail.

In order to get a rough picture of the distribution of s-channel Regge poles, we consider the partial wave amplitudes of $s^{\alpha}(t)$ for large s. For small ℓ we can use an expansion of Bessel functions of large argument:[32]

$$\log \left(\frac{a_\ell(s)}{a_0(s)} \right) = \log \left[\frac{I_{\ell + 1/2}(a)}{I_{1/2}(a)} \right] = \log \left[1 - \frac{\mu-1}{8a} + \frac{(\mu-1)(\mu-9)}{2!(8a)^2} + \cdots \right]$$

$$\cong - \frac{\mu-1}{8a} = - \frac{\ell(\ell+1)}{2a}$$

where $\mu = 4(\ell + 1/2)^2$ and $a = 2q_s^2 \, \alpha'(0) \, \log(s)$ and the approximation is valid for $\mu-1 \ll 8a$ or $\ell(\ell+1) \ll 2a$.

Examining the behavior of the amplitudes around $\ell^2 \approx 2a$, we consider the function

$$\log \left[\frac{I_{\sqrt{2a}+\delta}(a)}{I_{1/2}(a)} \right]$$

For large a we can replace the numerator by an asymptotic expansion of Bessel functions of large order:[33]

$$I_\nu(z) \sim \frac{1}{\sqrt{2\pi\nu}} \frac{e^{\nu\eta}}{(1+z^2)^{1/4}} \left\{ 1 + \sum_{k=1}^{\infty} \frac{u_k(t)}{\nu^k} \right\}$$

$$\eta = \sqrt{1+z^2} + \log \left(z/(1 + \sqrt{1+z^2}) \right)$$

$$t = 1/(1+z^2)^{1/2}$$

where $u_k(t)$ is a kth order polynomial in t.

The expansion holds uniformly with respect to z in the sector $|\arg z| \leq 1/2\,\pi - \epsilon$, $\epsilon > 0$.

Making the replacements $\nu z = a$, $\nu = \sqrt{2a} + \delta$ and $z = \sqrt{\frac{a}{2}} - \frac{\delta}{2}$, we obtain

$$\left[\frac{I_{\sqrt{2a}+\delta}(a)}{I_{1/2}(a)}\right] \simeq \frac{\exp\left[-a + a\sqrt{1 + v^2/x^2} - v/z\right]}{(1 + v^2 (a^2)^{1/4}}$$

$$\simeq \frac{\exp\left[\frac{-v^2}{2a}\right]}{(1 + v^2/a^2)^{1/4}}$$

or

$$\log\left[\frac{I_{\sqrt{2a}+\delta}(a)}{I_{1/2}(a)}\right] \simeq -1 - \delta\sqrt{\frac{2}{a}} = -1 - \frac{2\delta}{\sqrt{2a}}$$

$$+ 0\left(\frac{1}{a}\right) + 0\left(\left(\frac{\delta}{\sqrt{a}}\right)^2\right)$$

For $\ell + 1/2 \cong \sqrt{2a}$, we obtain

$$\log\left[\frac{a_\ell(s)}{a_0(s)}\right] \simeq -1$$

which is the result we would have obtained from a naive extrapolation of our formula for small ℓ:

$$\log\left[\frac{a_\ell(s)}{a_0(s)}\right] \cong -\frac{\ell^2}{2a}$$

For $\ell \approx \sqrt{2a}$ we have demonstrated that

$$\log\left[\frac{a_\ell(s)}{a_0(s)}\right] \simeq -1 - 2\frac{\ell - \sqrt{2a}}{\sqrt{2a}}, \left|\frac{\ell - \sqrt{2a}}{\sqrt{a}}\right| << 1$$

For $\frac{\ell - \sqrt{2a}}{\sqrt{2a}} >> 1$, it is easy to show[34] that the partial wave

amplitudes decrease at an even faster rate.

Figure 3 shows a plot of $\log \frac{a_\ell(s)}{a_0(s)}$ vs. $x = \ell / \sqrt{2a}$,

illustrating our conclusion that the significant partial waves are

concentrated in the region $\ell \lesssim \sqrt{2a} = L$. For $\ell \approx L$ the partial waves

are decreasing with an exponential factor

$$\exp\left[- \frac{(\ell - L)}{\sqrt{4\, q_s^2\, \alpha'(0)\, \log s}} \right]$$

for large s. It is appropriate to compare this behavior with the

exponential factor obtained in our earlier discussion of large-ℓ

behavior:

$$\exp\left[-(\ell - L)\, \xi(s) \right] \approx \exp\left[-(\ell - L) \sqrt{\frac{m_{ex}^2}{q_s^2}} \right]$$

where m_{ex} is the mass of the lowest-mass exchanged system. Equality

for all s is evidently impossible:

$$m_{ex}^2 \neq \frac{1}{4\, \alpha'(0)\, \log s}$$

This failure is not particularly important because the important

properties of the partial wave expansion of $s^{\alpha(t)}$ are related to the

lower partial waves. $s^{\alpha(t)}$ has no t-channel cut for linear $\alpha(t)$

and therefore its Legendre coefficients necessarily have incorrect

behavior as $\ell \to \infty$. Log S is not a rapidly varying function; if we

were to speculate on a correct form of the above equation we could assume

$$m_{ex}^2 \approx \frac{const.}{\alpha'(0)}$$

Later, we will see that this equation arises in a more reasonable calculation.

In summary, we conclude that in order to construct a Reggeized amplitude reproducing the essential behavior of $s^{\alpha(t)}$, we need a distribution of Regge poles only for Re $\ell \lesssim \sqrt{\alpha(0)s \, \log s}$.

A more intuitive way to arrive at this result derives from a study of the Legendre polynomials near the forward direction. At $\theta = 0$, $P_\ell (\cos \theta) = 1$ for all ℓ. As the order increases, the largest zero of the Legendre polynomials moves closer to $\cos \theta = 1$. An expression for the largest zero of the Legendre polynomials is[35]

$$n \, \theta_n \cong 2.4 \cong \frac{3\pi}{4}$$

where $\cos \theta_n$ is the largest root of $P_n(\cos \theta) = 0$ and n is large. Therefore, we could say that the Legendre polynomials have a "forward peak" between $\theta = 0$ and $\theta \cong \frac{3\pi}{2(2\ell + 1)}$. Approximating an exponential peaked in the forward direction requires Legendre polynomials of order sufficiently high so that the peak is accurately represented. Consequently, we can get a rough estimate of the maximum order required if we determine the order of a Legendre polynomial whose largest zero coincides with the angle in which the exponential decreases by one e-fold: i.e.,

$$\theta_0 \approx \frac{1}{\sqrt{\alpha'(0) \; q_s^2 \; \log \; s}}$$

implies

$$\ell_{max} \approx \frac{3\pi}{4} \sqrt{\alpha'(0) \; q_s^2 \; \log \; s}$$

$$\approx \frac{3\pi}{8} \sqrt{\alpha'(0) \; s \; \log \; s}$$

which is consistent with our previous estimate.[36]

Investigating a third way to arrive at this conclusion, we consider an elastic scattering process whose amplitude has the expansion

$$A(s,z) = \sum_{\ell = 0}^{\infty} (2\ell + 1) \frac{(\eta_\ell \; e^{2i\delta_\ell} - 1) \; P_\ell(z)}{2iK(s)}$$

We assume that the scattering is determined by a collection of singularities in the ℓ-plane, and that these singularities are confined to a region left of a "leading trajectory" at $\ell = L(s)$. Figure 4 shows a schematic picture of the ℓ-plane for this amplitude. For physical reasons, we expect that the scattering in the lower partial waves is highly inelastic. Exactly how η_ℓ behaves in this region is relatively unimportant, since it is small compared to one, and the quantity of interest is $\eta_\ell \; e^{2i\delta_\ell} - 1$. According to our earlier discussion, $a_\ell \sim 0(e^{-\ell\xi} \sqrt{\ell})$ for $\ell \gg L$, in order that the partial wave expansion have a singularity corresponding to the crossed channel

state of lowest mass. We will assume that the partial wave amplitude attains this asymptotic behavior in ℓ shortly after $\ell = L(s)$. This assumption allows us to estimate the relative importance of the tail of the partial wave sum; later we will see that this behavior is characteristic of a large class of representations of the product form.

The amplitude for forward scattering is then

$$A(s, \cos \theta_s)\Big|_{\theta_s=0} \cong \sum_{\ell = 0}^{L} (2\ell + 1)a_\ell + \frac{C(s)}{K(s)} \sum_{L + 1}^{\infty} \frac{e^{-\ell\xi}(2\ell + 1)}{\sqrt{\ell - L}}$$

$$\text{where } \left| C(s) \, e^{-(L + 1)\xi} \right| < 1$$

In order to estimate the contribution of the tail of the sum, we can approximate:

$$\sum_{L + 1}^{\infty} \frac{e^{-\ell\xi}(2\ell + 1)}{\sqrt{\ell - L}} \approx \int_{L + 1}^{\infty} \frac{e^{-\ell\xi}(2\ell + 1)}{\sqrt{\ell - L}} \, dl$$

$$= 2 \int_{L + 1}^{\infty} e^{-\ell\xi} \sqrt{\ell - L} \, dl + (2L + 1) \int_{L + 1}^{\infty} \frac{e^{-\ell\xi} dl}{\sqrt{\ell - L}}$$

$$= \frac{2e^{-L\xi}}{\xi^{3/2}} \int_{\xi}^{\infty} e^{-x} \sqrt{x} \, dx + \frac{(2L + 1) \, e^{-L\xi}}{\xi^{1/2}} \int_{\xi}^{\infty} \frac{e^{-x} dx}{\sqrt{x}}$$

We thus obtain a bound on the contribution of the tail of the sum:

$$\left| \frac{1}{K(s)} \sum_{\ell = 1 + 1}^{\infty} a_\ell \, (2\ell + 1) \right| < \frac{1}{K(s)} \left| \frac{f_1}{\xi^{3/2}} + \frac{(2L+1) \, f_2}{\xi^{1/2}} \right|$$

where f_1, f_2 are constant in s, and $\xi \sim C\, s^{-1/2}$. If we take the kinematic factor to be $K(s) = q_s$, then assumption of Regge behavior in the crossed channel implies $A(S, \cos \theta_s)\big|_{\theta_s = 0} \sim \sqrt{S}$ (to the nearest power in s). In order for the tail of the sum to account for this growth rate, we would have $L \sim S^{3/4}$, at least. If the scattering in these partial waves were elastic, however, the scattering amplitude would have the wrong phase.

Now suppose that the partial waves with $\ell < L$ are characterized by very inelastic scattering, i.e., $a_\ell(s) \sim \dfrac{i}{2K(s)}$ for $\ell < L$. Even if this assumption is only roughly correct, we should be able to obtain a mean value for the inelastic partial wave amplitudes:

$$\sum_{\ell = 0}^{L} (2\ell + 1)\, a_\ell \sim <a_\ell> \sum_{\ell = 0}^{L} (2\ell + 1)$$

$$<a_\ell> \sim \frac{i}{2K(s)}$$

Noting that $\displaystyle\sum_{\ell = 0}^{L} (2\ell + 1) = (L + 1)^2$, we can estimate the contribution of the inelastic part of the sum:

$$A(S, \cos \theta_s)\bigg|_{\theta_s = 0} \approx\; <a_\ell> (L + 1)^2$$

from which we obtain the estimate $L \sim \text{const.}\sqrt{S}$, to the nearest power in s.

This growth rate for $L(s)$ is consistent with the exponential behavior in t which is dictated by the crossed-channel

Regge formalism. Making use of the formula

$$\frac{d}{d \cos \theta} P_\ell (\cos \theta) \Big|_{\theta=0} = \frac{(\ell + 1)}{2}$$ we can evaluate the logarithmic

derivative of the amplitude in the forward direction:

$$\frac{\dfrac{dA (s, \cos \theta_s)}{dt}}{A (s, \cos \theta_s)} \Bigg|_{\theta_s = 0} \cong \frac{const.\ L^2}{S} \sim \begin{array}{l} \text{constant to the nearest} \\ \text{power of S.} \end{array}$$

This result is satisfactory. There may be some dispute

concerning the exact behavior of the experimental forward peak;

furthermore, we have used an argument valid for determining asymptotic

behavior accurate only to the nearest power of s. As higher moments

of the partial wave amplitudes are considered,

$$\mu_N = \sum_{\ell = 0}^{\infty} (2\ell + 1)\ a_\ell\ \ell^{2N},$$ the initial assumptions and approxi-

mations become more critical. In any case, there does not seem to

any way for $L^{(s)}$ to grow any slower than $\sqrt{s}$ and still provide the

proper growth rate for the whole amplitude. As we pointed out earlier,

however, it does not necessarily follow that all trajectories are

strictly constrained by this asymptotic behavior; the influence of

the higher trajectories could be reduced by the associated Regge pole

and Regge zeros approaching coincidence.

We have demonstrated that an amplitude can be parametrized by

direct-channel Regge poles and cuts and still have behavior appropriate

to crossed-channel Reggeization. It should be clear, however, that

such amplitudes necessitate a collection of direct channel Regge singu-

larities; this observation means that a simple bootstrap could work

only at values of the Mandelstam variables for which the amplitude
is dominated by a single trajectory in all channels, in which case
the calculation should resemble the old-fashioned bootstraps involving
particles having fixed spins. In a later discussion, we will require
that a direct-channel Reggeized amplitude reduce, for low energy, to
a conventional fixed-spin amplitude for which such a bootstrap calcu-
lation is possible.

Finally, it is instructive to consider another consequence
of direct-channel Reggeization: the nature of the deviations from
idealized crossed-channel Regge behavior. In the forward direction,
all Legendre polynomials have the same sign, while away from the
forward direction, the Legendre polynomials of different order oscillate
with different frequencies and may tend to cancel. In the previous
discussion, we constructed a forward peak by imposing constraints on an
otherwise unspecified set of partial wave amplitudes. As we considered
increasing angles, conformation to exponential behavior implied con-
straints on higher moments of our partial wave amplitudes. Recall that
we have assumed that there is a fundamental change in the nature of the
partial wave amplitudes as ℓ increases past L(s), the "leading edge"
of the resonance region. It would be possible to arrange the set of
Regge trajectories and cuts to produce some desired set of amplitudes
$a_\ell(s)$ for $\ell \lesssim L$, but there would be little possibility of variation in
a (s) for $\ell > L$. In other words, it is possible to satisfy the con-
straints on the moments of the partial wave amplitudes.

$$\mu_N = \sum_{\ell = 0}^{\infty} (2\ell + 1)\, a_\ell\, \ell^{2N}$$

only for $0 \lesssim N \lesssim L$. As a consequence, for large angle scattering there would be deviation from the behavior expected from a simple crossed-channel Reggeized model. This deviation would be an oscillating term similar to a Legendre polynomial of order roughly equal to L. In addition, there might be a small spike or dip in the forward direction coming from the tail of the partial wave sum, whose behavior is determined by the non-Reggeized singularity structure of the total amplitude, rather than by the requirements of the crossed-channel Regge pole approximation.

The magnitude of these deviations is related to the discontinuity in the behavior of the partial wave amplitudes between the resonance and non-resonance region. Speaking very qualitatively, the ℓ-plane appears to be swept by Regge poles and branch points clustered behind a "shock front" whose intersection with the real axis is L(s). At low energies, a Regge pole close to the real axis can produce discernible resonances, assuming that the effect of the Regge pole is not diminished by the presence of a nearby Regge zero. If the Regge singularities were not of sufficient strength to produce resonant effects in low-energy scattering amplitudes, however, it is plausible that for ℓ on the real axis there would be a fairly smooth transition across $\ell = L$, in which case there would be small deviation from angular behavior smoothly extrapolated from the crossed-channel Regge pole approximation. Experimentally, this appears to be the case. For example, high energy $p\bar{p}$ scattering has dips and peaks at non-forward angles, whereas pp scattering does not;[37] our qualitative picture would associate these results with the presence of resonances in $p\bar{p}$

scattering and the absence of resonances in pp scattering, whereas the conventional crossed-channel Regge picture would associate these dips with interference between terms from several crossed-channel trajectories.

PART II

SECTION II

THE CHENG REPRESENTATION AND MODIFICATIONS

Hung Cheng constructed the first reasonable product representation as an outgrowth of a study of the asymptotic behavior of the S-matrix in a certain class of potential scattering problems.[38] Briefly, recalling this result:

$$S_\ell \sim \exp\left[2i\pi\,(\ell + 1/2)\right] \text{ as } \ell \to \infty\,,\ \text{Re } \ell < -1/2$$

and, of course,

$$\log S_\ell \sim 0(e^{-(\ell + 1/2)\xi}/\sqrt{\ell}) \text{ as } \ell \to \infty \quad \text{Re } \ell > -1/2$$

$$\text{where } \cosh \xi = 1 + M^2/2q^2$$

Cheng[39] then considered the integral

$$\oint \frac{d\lambda}{\lambda - \ell}\ e^{\lambda\xi}\ \log S_\lambda$$

The integral vanishes as the contour is expanded to infinity, assuming the asymptotic behavior of $\log S_\ell$ is uniform. The only singularities in ℓ are logarithmic branch points corresponding to the Regge poles and Regge zeros. The following representation is obtained:

$$\log S_\ell = \sum_n \int_{\alpha_n^{I}}^{\alpha_n^{II}} \frac{d\lambda}{\lambda - \ell}\ e^{(\lambda - \ell)\xi}$$

$$= \sum_n [E_1 ((\ell - \alpha_n^I(s))\xi(s)) - E_1 ((\ell - \alpha_n^{II}(s)) \cdot \xi(s)]$$

where the sum is taken over the Regge poles of the S-matrix and where

$$E_1(z) = \int_1^\infty e^{-zt} \frac{dt}{t}$$

where the integral converges, and elsewhere by analytic continuation.[40]

It is immediately apparent that, for any finite number of Regge poles, the asymptotic behavior of this representation is $\log S_\ell \sim 0(e^{-\ell \xi}/\ell)$, rather than $\log S_\ell \sim 0(e^{-\ell \xi} \sqrt{\ell})$, as $\ell \to \infty$, Re $\ell > -1/2$. This fact means that the nearest singularity of the total amplitude is not automatically in the form of a pole or cut with finite discontinuity. Consequently, the Cheng representation is not powerful enough to use in a practical calculation. Its simple analytic form, however, makes it interesting as a study of the application of some of the techniques developed in the previous section.

Recall that we have reduced the problem of summing

$$f(z) = \sum_{\ell = 0}^\infty (2\ell + 1) \{\exp [\sum_n (E_1(\ell - \alpha_n^I) \cdot \xi) - E_1((\ell - \alpha_n^{II}) \cdot \xi))]$$

$$- 1\} P_\ell(z)$$

to the problem of summing

$$g(z) = \sum_{\ell = 0}^\infty (2\ell + 1) \{\sum_n (E_1((\ell - \alpha_n^I) \cdot \xi) - E_1((\ell - \alpha_n^{II}) \cdot \xi))\} P_\ell(z)$$

and solving an integro-differential equation. We have also seen that leading singularities of the two functions, $f(z)$ and $g(z)$, are exactly the same. In a straightforward manner, we can continue the Legendre expansion for $g(z)$ in the Cheng representation. We perform the summation by considering a function $F(\alpha, z)$ which is simply related to $g(z)$:

$$F(\alpha, z) = \sum_{\ell = 0}^{\infty} (2\ell + 1) \, E_1 \left((\ell - \alpha) \cdot \xi \right) P_\ell (z)$$

for Re $\alpha < 0$, we obtain

$$F(\alpha, z) = \sum_{\ell} \int_1^{\infty} (2\ell + 1) e^{-\ell \xi x} e^{\alpha \xi x} P_\ell(z) \frac{dx}{x}$$

$$= \int_{\xi}^{\infty} \frac{e^{\alpha x}}{x} \left[\sum_{\ell} (2\ell + 1) e^{-\ell x} P_\ell(z) \right] dx$$

Using the generating function for Legendre polynomials,[41] it is easy to show that:

$$\sum_{\ell = 0}^{\infty} e^{-\ell x} (2\ell + 1) P_\ell(z) = \frac{e^{\frac{x}{2}} \sinh x}{\sqrt{2} \, (\cosh x - z)^{3/2}}$$

which implies:

$$F(\alpha, z) = \int_{\xi}^{\infty} \frac{e^{\alpha x}}{x} \frac{e^{\frac{x}{2}} \sinh x \, dx}{\sqrt{2} \, (\cosh x - z)^{3/2}}$$

and thus:

$$\frac{\partial F}{\partial \alpha} = \frac{1}{\sqrt{2}} \int_{\xi}^{\infty} e^{(\alpha+1/2)x} \frac{\sinh x \; dx}{[\cosh x - z]^{3/2}}$$

Integrating by parts we obtain

$$\frac{\partial F}{\partial \alpha} = +\frac{\sqrt{2} \; e^{(\alpha+1/2)\xi}}{[\cosh \xi - z]^{1/2}} + \sqrt{2}(\alpha + 1/2) \int_{\xi}^{\infty} \frac{e^{(\alpha + 1/2)x} \; dx}{[\cosh x - z]^{1/2}}$$

For $-1 < \operatorname{Re} \alpha < 0$, the following representation of the Legendre function is valid: (42)

$$P_{\alpha}(-z) = \frac{-\sin \alpha \pi}{\pi \sqrt{2}} \int_{-\infty}^{\infty} \frac{e^{(\alpha + 1/2)x} \; dx}{[\cosh x - z]^{1/2}}$$

For $-1 < \operatorname{Re} \alpha < 0$, we can therefore write

$$\frac{\partial F}{\partial \alpha} = \sqrt{2} \; \frac{e^{(\alpha + 1/2)\xi}}{[\cosh \xi - z]^{1/2}} + (2\alpha + 1)\pi \left\{ -\frac{P_{\alpha}(-z)}{\sin \pi \alpha} - \frac{1}{\pi \sqrt{2}} \int_{-\infty}^{\xi} \frac{e^{(\alpha + 1/2)x} \; dx}{[\cosh x - z]^{1/2}} \right\}$$

Evidently, this form can be continued to all $\operatorname{Re} \alpha > -1$.

Now,

$$F(\alpha, z) = F(-1/2, z) + \int_{-1/2}^{\alpha} d\alpha' \; \frac{\partial F(\alpha', z)}{\partial \alpha'}$$

and

$$F(-1/2,z) = \frac{1}{\sqrt{2}} \int_{\xi}^{\infty} \frac{\sinh x \, dx}{x \, [\cosh x - z]^{3/2}}$$

so putting in the conjugate trajectories α_n^I and α_n^{II} and summing over n we obtain the analytic continuation of our input function, $g(z)$, defined in terms of an arbitrary set of Regge poles and zeros:

$$g(z) = \frac{1}{\sqrt{2}} \int_{\xi}^{\infty} \left\{ \sum_{\substack{\text{Re } \alpha_n \\ < -1/2}} [e^{\alpha_n^I x} - e^{\alpha_n^{II} x}] \right\} \frac{e^{\frac{x}{2}} \sinh x \, dx}{x \, [\cosh x - z]^{3/2}}$$

$$+ \left[(\text{Number of Re } \alpha_n^I > -1/2) - (\text{Number of Re } \alpha_n^{II} > -1/2) \right] \frac{1}{\sqrt{2}} \int_{\xi}^{\infty} \frac{\sinh x \, dx}{x [\cosh x - z]^{3/2}}$$

$$+ \frac{\sqrt{2}}{[\cosh \xi - z]^{1/2}} \cdot \frac{1}{\xi} \sum_{\text{Re } \alpha_n > -1/2} [e^{(\alpha_n^I + 1/2)\xi} - e^{(\alpha_n^{II} + 1/2)\xi}]$$

$$+ \pi \sum_{\text{Re } \alpha_n > -1/2} \int_{\alpha_n^{II}}^{\alpha_n^I} (2\alpha'+1) \left[\frac{P_{\alpha'}(-z)}{\sin \pi \alpha'} - \frac{1}{\pi\sqrt{2}} \int_{-\infty}^{\xi} \frac{e^{(\alpha'+1/2)x} \, dx}{[\cosh x - z]^{1/2}} \right] d\alpha'$$

This formula explicitly exhibits the singularity structure of $g(z)$. The contours of integration from α_n^I to α_n^{II} are immaterial for the purpose of finding the discontinuity, a reflection of the fact that the replacement $\log S_\ell \to \log S_\ell + 2\pi i$ produces no change in the value of the Legendre series for the whole amplitude.

Other investigations have indicated that analyticity of the amplitude requires every Regge trajectory at $S = 0$ to be associated with an infinite sequence of "daughter" trajectories evenly spaced below it in angular momentum.[43] It is worth considering an extrapolation of this arrangement of trajectories to physical $s > 4m^2$. Designate by α^I and α^{II}, the leading pole and zero of a family of daughters. By $\triangle^I$ and $\triangle^{II}$ we mean the spacings of the pole trajectory daughters and the zero trajectory daughters, respectively.

The Cheng representation for our amplitude is

$$\log S_\ell = \sum_{n=0}^{\infty} \{E_1((\ell-\alpha^I+n\triangle^I)\cdot\xi) - E_1((\ell-\alpha^{II}+n\triangle^{II})\cdot\xi)\}$$

It is straightforward to obtain a closed expression for this sum. If $\text{Re } \ell > \max(\text{Re } \alpha^I, \text{Re } \alpha^{II})$, then the defining integral for $E_1(z)$ converges for all the Regge poles. Evidently, the series under the integral sign is absolutely and uniformly convergent. Exchanging the summation and integration, we obtain:

$$\log S_\ell = \sum_{n=0}^{\infty} \left[\int_1^{\infty} e^{-(\ell-\alpha^I)\xi t} \, e^{-n\triangle^I\xi t} \frac{dt}{t} - \int_1^{\infty} e^{-(\ell-\alpha^{II})\xi t} \, e^{-n\triangle^{II}\xi t} \frac{dt}{t} \right]$$

$$= \int_1^{\infty} \left\{ \frac{e^{-(\ell-\alpha^I)\xi t}}{1-e^{-\triangle^I\xi t}} - \frac{e^{-(\ell-\alpha^{II})\xi t}}{1-e^{-\triangle^{II}\xi t}} \right\} \frac{dt}{t}$$

In order to find an analytic continuation of this formula valid for all ℓ, we use a representation of the E_1 function valid for all

values of the argument:[44]

$$E_1(z) = - \gamma - \log(z) + \int_0^1 (1-e^{-zt}) \frac{dt}{t}$$

where γ is the Euler-Mascheroni constant. Now we consider the Nth partial sum of the infinite series in the Cheng representation:

$$\log S^{(n)} = \sum_{n=0}^{N} \left[E_1((\ell-\alpha_n^{I})\xi) - E_1((\ell-\alpha_n^{II}) \cdot \xi) \right]$$

$$= - \sum_{n=1}^{N} \log\left(\frac{\ell-\alpha^{I}+n\triangle^{I}}{\ell-\alpha^{II}+n\triangle^{II}}\right) - \log\left(\frac{\ell-\alpha^{I}}{\ell-\alpha^{II}}\right)$$

$$+ \int_0^1 \left[e^{-(\ell-\alpha^{II})\xi x} (\sum_{n=0}^{N} e^{-n\triangle^{II}\xi x}) - e^{-(\ell-\alpha^{I})\xi x} (\sum_{n=0}^{N} e^{-n\triangle^{I}\xi x}) \right] \frac{dx}{x}$$

This form is not convergent as we take $N \to \infty$. Rearranging the sum and the integral, we obtain

$$\log S_\ell^{(N)} = -(N+1) \log \left(\frac{\triangle^{I}}{\triangle^{II}}\right) - \sum_{n=1}^{N} \log \left(\frac{1 + \dfrac{\ell-\alpha^{I}}{n\triangle^{I}}}{1 + \dfrac{\ell-\alpha^{III}}{n\triangle^{II}}}\right)$$

$$- \log\left[\frac{(\ell-\alpha^{I})/\triangle^{I}}{(\ell-\alpha^{II})/\triangle^{II}}\right] + \int_0^1 \frac{1}{x} \left[e^{-(\ell-\alpha^{II})\xi x} -1+(\ell-\alpha^{II})\xi x \right] (\sum_{n=0}^{N} e^{-n\triangle^{II}\xi x}) dx$$

$$- \int_0^1 \frac{1}{x} \left[e^{-(\ell-\alpha^I)\xi x} -1+(\ell-\alpha^I)\xi x \right] \left(\sum_{n=0}^{N} e^{-\triangle^I \xi x} \right) dx + \int_0^1 \frac{1}{x} \left(\sum_{n=0}^{N} e^{-n\triangle^{II}\xi x} - \sum_{n=0}^{N} e^{-n\triangle^I \xi x} \right) dx$$

$$- (\ell-\alpha^{II})\xi \int_0^1 \sum_{n=0}^{N} e^{-n\triangle^{II}\xi x} dx + (\ell-\alpha^I)\xi \int_0^1 \sum_{n=0}^{N} e^{-n\triangle^I \xi x} dx$$

substituting

$$\int_0^1 \left(\sum_{n=0}^{N} e^{-n\triangle\xi x} \right) dx = 1 - \frac{1}{\triangle\xi} \sum_{n=1}^{N} \left(\frac{e^{-n\triangle\xi} - 1}{n} \right)$$

as well as adding and subtracting

$$\left(\frac{\ell-\alpha^I}{\triangle^I} - \frac{\ell-\alpha^{II}}{\triangle^{II}} \right) \left(\gamma - \sum_{n=1}^{N} \frac{1}{n} \right)$$

we obtain

$$\log S_\ell^{(N)} = -(N+1) \log \left(\frac{\triangle^I}{\triangle^{II}} \right)$$

$$- \left\{ \sum_{n=1}^{N} \left[\log \left(\frac{1 + \frac{\ell-\alpha^I}{n\triangle^I}}{1 + \frac{\ell-\alpha^{II}}{n\triangle^{II}}} \right) - \left(\frac{\ell-\alpha^I}{n\triangle^I} \right) + \left(\frac{\ell-\alpha^{II}}{\triangle^{II}} \right) \right] \right.$$

$$+ \log \left[\frac{(\ell-\alpha^I)/\triangle^I}{(\ell-\alpha^{II})/\triangle^{II}} \right] + \gamma \left[\frac{\ell-\alpha^I}{\triangle^I} - \frac{\ell-\alpha^{II}}{\triangle^{II}} \right] \right\} + \sum_{n=1}^{N} \left[\frac{\ell-\alpha^{II}}{n\triangle^{II}} - \frac{\ell-\alpha^I}{n\triangle^I} \right]$$

$$+ \gamma \left(\frac{\ell-\alpha^I}{\triangle^I} - \frac{\ell-\alpha^{II}}{\triangle^{II}}\right) + \int_0^1 \frac{1}{x} \left[e^{-(\ell-\alpha^{II})\xi x} - 1 + (\ell-\alpha^{II})\xi x\right] \left(\sum_{n=0}^N e^{-n\triangle^{II}\xi x}\right) dx$$

$$- \int_0^1 \frac{1}{x} \left[e^{-(\ell-\alpha^I)\xi x} - 1 + (\ell-\alpha^I)\xi x\right] \left(\sum_{n=0}^N e^{-n\triangle^I\xi x}\right) dx - \frac{(\ell-\alpha^I)}{\triangle^I} \sum_{n=1}^N \left(\frac{e^{-n\triangle^I\xi}-1}{n}\right)$$

$$+ \left(\frac{\ell-\alpha^{II}}{\triangle^{II}}\right)\left(\sum_{n=1}^N\right) \frac{e^{-n\triangle^{II}\xi}-1}{n} + (\alpha^{II}-\alpha^I)\xi$$

$$- \int_0^1 \frac{dt}{t} \left(\sum_{n=0}^N e^{-n\triangle^I\xi t} - \sum_{n=0}^N e^{-n\triangle^{II}\xi t}\right)$$

Now notice that the expression in the curly brackets { } is the

logarithm of the Nth partial product of Euler's infinite-

product representation of the Gamma functions:[45]

$$\frac{1}{\Gamma(z)} = z \, e^{\gamma z} \prod_{n=1}^\infty \left[(1+\frac{z}{n}) \, e^{-\frac{z}{n}}\right]$$

valid for $|z| < \infty$.

Define $\Gamma_N(z) = \{z \, e^{\gamma z} \prod_{n=1}^N [(1 + \frac{z}{n}) \, e^{-z/n}]\}^{-1}$

so that $\lim_{N \to \infty} \Gamma_N(z) = \Gamma(z)$

Also define $\log_N (1-z) = - \sum_{n=1}^N z^n/n$

So that $\lim\limits_{N \to \infty} \log_N(1-z) = \log(1-z)$ where the series converges.

Finally, rewriting the integral

$$\int_0^1 \frac{1}{x} \sum_{n=0}^N \left[\left(e^{-n\triangle^{II}\xi x} - e^{-n\triangle^{I}\xi x} \right) \right] dx$$

$$= \int_{\triangle^I}^{\triangle^{II}} \frac{1}{x} \left(\sum_{n=0}^N e^{-n\xi x} \right) dx - (N+1) \log \left(\frac{\triangle^{II}}{\triangle^I} \right)$$

we obtain for our expression

$$\log S_\ell^{(N)} = \log \left[\frac{\Gamma_N \left(\frac{\ell-\alpha^I}{\triangle^I} \right)}{\Gamma_N \left(\frac{\ell-\alpha^{II}}{\triangle^{II}} \right)} \right] + \gamma \left(\frac{\ell-\alpha^I}{\triangle^I} - \frac{\ell-\alpha^{II}}{\triangle^{II}} \right)$$

$$+ \int_0^1 \frac{1}{x} \left[e^{-(\ell-\alpha^{II})\xi x} - 1 + (\ell-\alpha^{II})\xi x \right] \left(\sum_{n=0}^N e^{-n\triangle^{II}\xi x} \right) dx$$

$$- \int_0^1 \frac{1}{x} \left[e^{-(\ell-\alpha^I)\xi x} - 1 + (\ell-\alpha^I)\xi x \right] \left(\sum_{n=0}^N e^{-n\triangle^I\xi x} \right) dx$$

$$+ \int_{\triangle^I}^{\triangle^{II}} \frac{\sum_{n=0}^N e^{-n\xi x}}{x} dx + \frac{(\ell-\alpha^I)}{\triangle^I} \log_N \left(1-e^{-\triangle^I\xi} \right)$$

$$- \frac{(\ell-\alpha^{II})}{\triangle^{II}} \log_N (1-e^{-\triangle^{II}\xi}) + (\alpha^{II} - \alpha^I)\xi$$

Now all the terms are convergent as $N \to \infty$. Using the expansion

$$\sum_{n=0}^{\infty} x^n = \frac{1}{1-x}$$

we can write

$$\log S_\ell = \lim_{N \to \infty} \log S^{(N)} = \log \left[\frac{\Gamma \left(\frac{\ell - \alpha^I}{\Delta^I} \right)}{\Gamma \left(\frac{\ell - \alpha^{II}}{\Delta^{II}} \right)} \right]$$

$$+ \gamma \left[\frac{\ell - \alpha^I}{\Delta^I} - \frac{\ell - \alpha^{II}}{\Delta^{II}} \right] + \int_0^1 \frac{1}{x} \frac{e^{-(\ell - \alpha^{II})\xi x} - 1 + (\ell - \alpha^{II})\xi x}{1 - e^{-\Delta^{II}\xi x}} \, dx$$

$$- \int_0^1 \frac{1}{x} \frac{e^{-(\ell - \alpha^I)\xi x} - 1 + (\ell - \alpha^I)\xi x}{1 - e^{-\Delta^I \xi x}} \, dx$$

$$+ \int_{\Delta^I}^{\Delta^{II}} \frac{dx}{x(1 - e^{-\xi x})} + \frac{(\ell - \alpha^I)}{\Delta^I} \log (1 - e^{-\Delta^I \xi})$$

$$- \frac{(\ell - \alpha^{II})}{\Delta^{II}} \log (1 - e^{-\Delta^{II} \xi})$$

$$+ (\alpha^{II} - \alpha^I) \xi$$

This expression can be continued to any point in the ℓ-plane, except for the singularities of the Gamma functions. We have arrived at an elastic scattering "model" involving an infinite number of Regge trajectories.[46]

In Appendix B, we plot the angular cross-section defined by partial wave sums derived from these approximate phase shifts. Shanks method was applied to accelerate the convergence of the Legendre series, and in some cases, to allow numerical extrapolation of the amplitudes outside the region of convergence of the expansion. We have investigated the speed with which the Cheng representation converges by plotting in Figure 5 differential cross sections corresponding to increasing numbers of Regge poles, along with a graph of the limit curve as the number of Regge poles is taken to infinity. The Cheng representation converges fairly rapidly to the infinite-trajectory amplitude, which means that the representation is insensitive to the exact distribution of the trajectories far to the left of the imaginary ℓ-axis; for physical angles, and nearby crossed-channel singularities, the amplitude is critically dependent on the leading trajectories, and non-critically dependent on the background trajectories. The graphs also evidence a phenomenon discussed in the previous section; for large angles, the amplitudes have small oscillations at about the same rate as a Legendre polynomial of order equal to the leading trajectory. In the forward direction, the angular behavior is well approximated by an exponential, as an expanded logarithmic plot demonstrates in Figure 6.

Continuing outside the physical angles, we find that the exponential behavior persists in the forward direction; in the backward direction, however, the differential cross section appears to have a power law bound.[47] As we would expect, the phase of the amplitude in the forward direction can be varied over a wide range if

α^I and α^{II} are adjusted. As we consider higher energies, the Cheng representation is subject to the restrictions developed in the previous section, concerning the behavior of the low partial waves.

Although the Cheng representation places the crossed-channel cut in the correct position, the amplitude fails to have the proper analytic structure near this singularity. Consequently, it is difficult to define a crossed-channel amplitude as an analytic continuation of the direct channel Cheng amplitude. A sensible bootstrap calculation would therefore be impossible in the Cheng representation.

Abbe, Kaus, Nath, and Strivastava[48] devised a modification to the Cheng representation which, in a superficial sense, repairs the analytic structure of the Cheng amplitude, but at the expense of divorcing the complete specification of the crossed-channel singularity structure from the specification of the sequence of Regge trajectories.

AKNS considered the contour integral

$$\oint \frac{d\lambda}{\lambda-\ell} \left[\log S_\lambda - \frac{ig^2}{q_s} Q_\lambda (\cosh \bar{\xi}) \right] e^{\lambda\xi}$$

where

$$\cosh \xi = 1 + \frac{4M^2}{2q_s^2}$$

$$\cosh \bar{\xi} = 1 + \frac{m_{ex}^2}{2q_s^2}$$

and $-g^2$ is the t-channel residue. This integral tends to zero as the contour is expanded to infinity, assuming that $\log S_\ell$ tends uniformly to

the asymptotic behavior derived by Cheng. This equality implies the following representation:

$$S_\ell = \exp\left[\frac{ig^2}{q_s} \ Q_\ell \ (\cosh \bar{\xi})\right] \prod_n S_n \ (\ell,s)$$

where

$$S_n \ (\ell,s) = \exp\left[\int_{\alpha_n^I}^{\alpha_n^{II}} \frac{d\lambda}{\lambda-\ell} \ e^{(\lambda-\ell)\xi} \ \frac{ig^2}{q_s} \ \frac{e^{-(\ell+n)\xi}}{(\ell+n)} \ P_{n-1}(\cosh \bar{\xi})\right]$$

In this case, the scattering amplitude will have a cross-channel pole regardless of the disposition of the Regge trajectories. The crossed-channel residue is completely independent of the direct-channel trajectories. Therefore, as far as a bootstrap calculation is concerned, this representation is no improvement over the Cheng formula, although it may produce a better fit to angular distribution in the direct channel. AKNS noted that the modified Cheng representation is more rapidly convergent in determining the residues of the direct-channel Regge poles in potential theory.

Cheng and AKNS remarked that, as $q_s \to 0$ in their formulas, the phase shift behaved as follows:

$$\delta_\ell \sim \text{const. Im } \alpha \ q^{2\ell - 2 \text{ Re } \alpha}$$

Therefore, provided Im α has the threshold behavior required by potential theory,

$$\text{Im } \alpha \sim \text{cost } q_s^{2 \text{ Re } \alpha + 1} \qquad \text{as } q_s \to 0,$$

the phase shift will have the proper behavior at threshold:

$$\delta_\ell \sim \text{const. } q_s^{2\ell + 1}$$

This behavior is by no means automatic, however, since in these parametrizations, the threshold behavior of $\text{Im } \alpha$ is entirely arbitrary. In the AKNS representation, it is straightforward to calculate the input function $g(z)$ for our analytic continuation scheme. If the model includes an infinite number of trajectories, as for example in our evenly spaced trajectory model, then the effect of the AKNS modification is to add the term

$$\frac{ig^2}{q_s} \left[Q_\ell (\cosh \bar{\xi}) - \sum_{n=1}^{\infty} \frac{e^{-(\ell+n)\xi}}{(\ell+n)} P_{n-1} (\cosh \bar{\xi}) \right]$$

to the expression for $\log S_\ell$.

Consider

$$\sum_{n=1}^{\infty} \frac{e^{-(\ell+n)\xi}}{(\ell+n)} P_{n-1} (\cosh \bar{\xi})$$

Using the generating function for the Legendre polynomials, it is trivial to show that

$$\sum_{n=0}^{\infty} e^{-(\ell+n)x} P_n(z) = \frac{1}{\sqrt{2}} \frac{e^{-(\ell-1/2)x}}{\sqrt{\cosh x - z}}$$

where the sum converges. Integrating with respect to x, we find

$$\sum_{n=1}^{\infty} \frac{e^{-(\ell+n)\xi}}{(\ell+n)} P_{n-1} (\cosh \xi) = \frac{1}{\sqrt{2}} \int_{\xi}^{\infty} \frac{e^{-(\ell+1/2)x} \, dx}{\sqrt{\cosh x - \cosh \bar{\xi}}}$$

For Re $\ell > -1/2$, $Q_\ell (\cosh \bar{\xi})$ can be represented as follows:[49]

$$Q_\ell (\cosh \bar{\xi}) = \frac{1}{\sqrt{2}} \int_{\bar{\xi}}^{\infty} \frac{e^{-(\ell + 1/2)x} \, dx}{\sqrt{\cosh x - \cosh \bar{\xi}}}$$

Subtracting these two equations, we obtain

$$Q_\ell (\cosh \bar{\xi}) - \sum_{n=1}^{\infty} \frac{e^{-(\ell+n)\xi}}{(\ell+ n)} P_{n-1} (\cosh \bar{\xi}) = \frac{1}{\sqrt{2}} \int_{\bar{\xi}}^{\xi} \frac{e^{-(\ell + 1/2)x} \, dx}{\sqrt{\cosh x - \cosh \bar{\xi}}}$$

The integral vanishes as $\xi \to \bar{\xi}$ and the equation reduces to a representation[50] for the Legendre function of the second kind:

$$Q_\ell (\cosh \xi) = \sum_{n=0}^{\infty} \frac{e^{-(\ell+n+1)\xi}}{(\ell+n+1)} P_n (\cosh \xi)$$

convergent for all complex ℓ not equal to a negative integer.

We could have written down the summation formula from intuitive arguments. The presence of the exponential factor $e^{\lambda \xi}$ in the contour integral equation

$$\oint \left[\log S_\lambda - \frac{ig^2}{q_s} Q_\lambda (\cosh \bar{\xi}) \right] \frac{e^{\lambda \xi}}{(\lambda - \ell)} \, d\lambda = 0$$

has the effect of supressing exponential components $e^{-\mu\lambda}$ in a Laplace-transform representation of the function Q_λ for $\mu > \xi$. Accordingly, we write a convergent decomposition of Q_λ and simply drop the unwanted terms:

$$Q_\ell (\cosh \bar{\xi}) = \frac{1}{\sqrt{2}} \int_{\bar{\xi}}^{\infty} \frac{e^{-(\ell + 1/2)x} \, dx}{\sqrt{\cosh x - \cosh \bar{\xi}}} \quad \frac{1}{\sqrt{2}} \to \int_{\bar{\xi}}^{\xi} \frac{e^{-(\ell + 1/2)x} \, dx}{\sqrt{\cosh x - \cosh \bar{\xi}}}$$

Since this is a finite integral it is convergent for all ℓ. Approximating the sum

$$\sum_{n=1}^{\infty} \frac{e^{-(\ell+n)\xi}}{(\ell + n)} \, P_{n-1} (\cosh \bar{\xi})$$

by any finite number of terms, however, introduces spurious pole in the left-half ℓ-plane.

In order to calculate the added contribution of the AKNS modification to the input function $g(z)$ obtained in the Cheng representation, we need to perform the following sum:

$$\sum_{\ell=0}^{\infty} (2\ell+1) \frac{1}{\sqrt{2}} \int_{\bar{\xi}}^{\xi} \frac{e^{-(\ell + 1/2)x} \, dx}{\sqrt{\cosh x - \cosh \bar{\xi}}} \, P_\ell (z)$$

Using the generating function for $P_\ell (z)$ we can show that the AKNS contribution to the input function is

$$\frac{1}{2} \int_{\bar{\xi}}^{\xi} \frac{\sinh x \, dx}{\sqrt{\cosh x - \cosh \bar{\xi}} [\cosh x - z]^{3/2}} = \frac{1}{\cosh \bar{\xi} - z} - \frac{1}{2} \int_{\xi}^{\infty} \frac{\sinh x \, dx}{\sqrt{\cosh x - \cosh \bar{\xi}}}$$

$$\cdot \frac{1}{[\cosh x - z]^{3/2}}$$

in the case of an infinite number of trajectories. If we truncate the sum in the AKNS representation, the contribution to the input function becomes

$$\Sigma \ (2\ell + 1) \left[Q_\ell \ (\cosh \bar{\xi}) - \sum_{n=1}^{N} \frac{e^{-(\ell+n)\xi}}{(\ell + n)} \ P_{n-1}(\cosh \bar{\xi}) \right] P_\ell(z)$$

$$= \frac{1}{\cosh \bar{\xi} - z} - \sum_{n=1}^{N} P_{n-1} \ (\cosh \bar{\xi}) \int_{\xi}^{\infty} \frac{dx \ e^{-nx} \ e^{1/2x}}{\sqrt{2} \ [\cosh x - z]^{3/2}}$$

At this point, it should be apparent that the effect of the AKNS modification is to give the scattering amplitude reasonable analytic structure at the leading singularity simply by introducing a pole in an ad hoc fashion. Difficulty remains at the next singularity, however, and there is no provision for correction.

PART II

SECTION III

A NEW REPRESENTATION

Recall that in the first section, we indicated that a class of Reggeized representations for $\log S_\ell$ can be generated which have the proper asymptotic behavior as $\ell \to \infty$, $\mathrm{Re}\ \ell > -1/2$. Here, we reduce the specification of the representations to the choice of an entire function $\phi(\ell, s)$ with the following asymptotic properties:

$$\phi(\ell, s) \sim 0\ (e^{\ell\xi} / \sqrt{\ell}) \qquad \text{as } \ell \to \infty,\ \mathrm{Re}\ \ell > -1/2$$
$$\cosh \xi = 1 + M^2/2q_s^2$$

$$\phi(\ell, s) \sim 0\ (e^{\ell\xi'} \sqrt{\ell}) \qquad \text{as } \ell \to \infty\ \mathrm{Re}\ \ell < -1/2$$
$$\xi' > 0$$

We consider the integral

$$\oint \frac{\phi(\lambda, s)\ \log S_\lambda\ d\lambda}{(\lambda - \ell)}$$

as the contour is taken to infinity, just as in the case of the Cheng representation and the AKNS modification. In deriving the Cheng representation and the AKNS modification, we assumed that

$$e^{\ell\xi}\ \log S_\ell \to 0$$

uniformly as $\ell \to \infty$ in all directions. In our class of representations,

the requirement is relaxed somewhat:

$$\phi(\ell,s) \log S_\ell \to 0 \qquad \text{as } \ell \to \infty$$

or

$$\frac{e^{\ell\xi}}{\sqrt{\ell}} \log S_\ell \to 0 \qquad \text{Re } \ell > -1/2$$

$$\frac{e^{\ell\xi'}}{\sqrt{\ell}} \log S_\ell \to 0 \qquad \text{Re } \ell < -1/2$$

uniformly.

One choice for $\phi(\ell,s)$ is:

$$\phi(\ell,s) = e^{(1-a)\ell\xi} P_\ell(\cosh a\xi)$$

where a remains to be specified. Using the asymptotic expansion[51] of $P_\ell(x)$, we find that the asymptotic behavior of $\phi(\ell,s)$ is

$$\phi(\ell,s) \sim \frac{e^{\frac{a\xi}{2}} e^{\ell\xi}}{\sqrt{2\ell\pi\sinh a\xi}} \qquad \begin{array}{l} \ell \to \infty \\ \text{Re } \ell > -1/2 \end{array}$$

$$\phi(\ell,s) \sim \frac{e^{\frac{-a\xi}{2}} e^{(1-2a)\ell\xi}}{\sqrt{2\ell\pi}\ \sinh a\xi} \qquad \begin{array}{l} \ell \to \infty \\ \text{Re } \ell < -1/2 \end{array}$$

Evidently, we must require that $0 < a < 1/2$. If we set $a = 0$, then we obtain the Cheng representation since

$$P_\lambda(1) = 1 \text{ for all } \lambda,$$

and therefore

$$\phi(\ell,\xi)\Big|_{a=0} = e^{\ell\xi}$$

our representation for $\log S_\ell$ is

$$\log S_\ell = \sum_n P_\ell \frac{1}{(\cosh a\xi)} \int_{\alpha_n^I}^{\alpha_n^{II}} P_\lambda \frac{(\cosh a\xi) e^{(1-a)(\lambda-\ell)\xi} d\lambda}{(\lambda-\ell)}$$

The factor $[P_\ell(\cosh a\xi)]^{-1}$ has an interesting interpretation. The zeros in ℓ of the entire function $P_\ell(\mu)$ for $\mu > 1$ are all located on the line Re $\ell = -1/2;$ [52] there are an infinite number of zeros symmetrically distributed around the line Im $\ell = 0$. The positions of the zeros are functions of the argument of the Legendre function $\mu = \cosh a\xi$. If our representation converges, and if we correctly specify the positions of all the Regge poles and zeros, then the sum

$$\sum_n \int_{\alpha_n^I}^{\alpha_n^{II}} P_\lambda \frac{(\cosh a\xi) e^{(1-a)\lambda\xi} d\lambda}{(\lambda-\ell)}$$

should have zeros in ℓ at the same positions as the zeros of the function $P_\ell (\cosh a\xi)$. If we truncate the sum over Regge poles, the approximate expression for $\log S_\ell$ will have an infinite number of poles along the line Re $\ell = -1/2$, which is the location of the background integral of the conventional Sommerfeld-Watson representation.

Mathematically, the zeros along Re ℓ = -1/2 occur because

we have required $e\phi(\ell,s)^{-(\ell-a)\ell\xi}$ to be an analytic function of exponential growth in all directions away from the line Re ℓ = -1/2; this requirement was necessary so that our representation would converge and produce the correct asymptotic behavior as $\ell \to \infty$, Re $\ell > -1/2$, regardless of the number of trajectories retained in an approximation. Consequently, the poles along Re ℓ = -1/2 represent the effect of trajectories in the left half ℓ-plane which have been neglected and in this way are related to the background integral of the Sommerfeld-Watson transformation.

Now consider the direct-channel threshold behavior of our representation. We limit the discussion to a one-trajectory approximation to the amplitude, but it will be clear that the argument extends to any number of trajectories. The one-trajectory approximation for the phase shift is

$$\delta_\ell = \frac{1}{2i} \left[\int_{\alpha^I}^{\alpha^{II}} e^{(1-a)\lambda\xi} P_\lambda \frac{(\cosh a\xi)d\lambda}{\lambda-\ell} \left[e^{(1-a)\ell\xi} P_\ell(\cosh a\xi) \right]^{-1} \right.$$

The equation

$$\cosh \xi = 1 + M_x^2/2q_s^2$$

implies

$$e^\xi \sim \frac{M_x^2}{q_s^2} \quad \text{as } q_s^2 \to 0 .$$

For large positive values of the argument[53] and Re $\nu > 0$,

$$P_\nu(x) \sim x^\nu \cdot \text{const},$$

which implies that our expression may be replaced as follows:

$$\delta_\ell \cong \frac{1}{2i} \left(\frac{M_x^2}{q_s^2}\right)^{-\ell} \int_{\alpha^I}^{\alpha^{II}} \left(\frac{M_x^2}{q_s^2}\right)^\lambda \frac{d\lambda}{(\lambda-\ell)}$$

As $q_s^2 \to 0$, $\alpha^{II} \to \alpha^I$, so that a mean value approximation to the integral approaches the correct value

$$\int_{\alpha^I}^{\alpha^{II}} \left(\frac{M_x}{q_s^2}\right)^\lambda \frac{d\lambda}{(\lambda-\ell)} \cong \frac{(\alpha^{II}-\alpha^I)}{(\text{Re }\alpha-\ell)} \left(\frac{M_x^2}{q_s^2}\right)^{\text{Re }\alpha}$$

which implies

$$\delta_\ell \cong \text{const.} \; \text{Im }\alpha \cdot q^{2\ell-2 \text{ Re }\alpha} \qquad \text{as } q_s^2 \to 0$$

This result is independent of a in the range $0 < a < 1/2$, and it also is true for the original Cheng representation and the AKNS modification. All of these representations have the property that, <u>provided</u> Im α has the correct threshold behavior

$$\text{Im }\alpha \cong q^{2 \text{ Re }\alpha + 1} \cdot \text{const} \qquad \text{as } q_s^2 \to 0 \; ,$$

the phase shift has the correct threshold behavior:

$$\delta_\ell \cong \text{const} \cdot q_s^{2\ell + 1} \qquad \text{as } q_s^2 \to 0 \; .$$

In a practical calculation, the trajectory near threshold would be determined by the constraints placed on the amplitude by the nearby crossed-channel singularities. In potential theory, for example, the amplitude must contain singularities in $\cos \theta_s$ corresponding to the Born term, and a simple way to find the behavior of the trajectory is to solve the Schrödinger equation using this potential. Suppose that the nearest crossed-channel singularity is a pole. If our amplitude is correctly represented, the residue of the crossed-channel pole is

$$\text{Residue} = -\lim_{\ell \to \infty} \frac{\dfrac{1}{2iq_s} \log S_\ell}{\dfrac{1}{2q_s^2} Q_\ell (\cosh \xi)}$$

where the limit is taken along positive real values of ℓ.

Retaining only one trajectory and making a mean value approximation to the integral in anticipation of taking the limit $q_s \to 0$, we compute the asymptotic behavior of $\log S_\ell$:

$$\frac{\log S}{2iq_s} \underset{\ell \to \infty}{\sim} e^{-(1-a)\ell\xi} \; e^{-(\ell + 1/2)a\xi} \sqrt{2\pi\ell \, \sinh a\xi} \cdot \frac{\text{Im}\,\alpha}{q_s \cdot \ell} \cdot e^{(1-a)\xi \, \text{Re}\,\alpha} \; P_{\text{Re}\,\alpha}(\cosh a\xi)$$

Recalling the asymptotic behavior of $Q_\ell (\cosh \xi)$[54]:

$$Q_\ell (\cosh \xi) \underset{\ell \to \infty}{\sim} e^{-(\ell + 1/2)\xi} \sqrt{\frac{\pi}{2\ell \, \sinh \xi}}$$

We compute the residue:

$$\text{Residue} = -4 \ q_s \cdot \text{Im} \ \alpha \cdot e^{\xi(1-a)(\text{Re} \ \alpha \ + \ 1/2)} \ P_{\text{Re} \ \alpha} \ (\cosh \ a\xi) \ \sqrt{\sinh \ \xi \ \sinh \ a\xi}$$

Even in the crudest approximation, the crossed-channel residue should remain finite as $q_s^2 \to 0$. Imposing this condition we obtain a constraint on the behavior of the trajectory:

$$\text{Residue} = \text{const} \ \widetilde{=} \ - \ \text{Im} \ \alpha \cdot [q_s^2]^{-1/2 \ - \ \text{Re} \ \alpha} \cdot \text{const}$$

$$\text{as} \ q_s^2 \to 0$$

or

$$\text{Im} \ \alpha \ \widetilde{=} \ \text{const} \ \ q_s^{2 \ \text{Re} \ \alpha(s) \ + \ 1} \ \ \ \text{as} \ q_s^2 \to 0$$

Again, we have obtained a threshold condition independent of a in the range $0 < a < 1/2$.

In this respect our representation is a distinct improvement over those of Cheng and AKNS. Such a constraint on the threshold behavior of $\alpha(s)$ cannot automatically hold for these older formulations, since the first of these representations does not allow a reasonable crossed-channel singularity, and the second specifies the residue of the Born term a priori, as a parameter independent of the direct-channel Regge trajectories.

Our representation implies the following formula for the amplitude near the mth direct-channel Regge pole:

$$a \ = \ \frac{1}{2iq_s} \left\{ \left(\frac{\ell \ -\alpha_m^{II}}{\ell - \ \alpha_m^I} \right) \ \exp \left[\int_{\alpha_m^I}^{\alpha_m^{II}} \left(\frac{e^{(1-a)\lambda\xi} \ P_\lambda(\cosh \ a\xi)}{e^{(1-a)\ell\xi} \ P_\ell(\cosh \ a\xi)} - 1 \right) \frac{d\lambda}{(\lambda-\ell)} \right. \right.$$

$$+ \sum_{n \neq m} \int_{\alpha_n^I}^{\alpha_n^{II}} \frac{e^{(1-a)\lambda\xi} P_\lambda(\cosh a\xi)}{e^{(1-a)\ell\xi} P_\ell(\cosh a\xi)} \frac{d\lambda}{\lambda-\ell} \Bigg] -1 \Bigg\}$$

Generalizing our discussion to the case of many trajectories, we can write down the expression for the residue of the nearest crossed-channel pole:

$$\rho(s) = -4q_s \ e^{1/2 \ \xi(1-a)} \sqrt{\sinh \xi \ \sinh a\xi} \sum_n \frac{1}{2i} \int_{\alpha_n^{II}}^{\alpha_n^I} P_\lambda(\cosh a\xi) \ e^{(1-a)\lambda\xi} \ d\lambda$$

where $A(s,t,u) \sim \dfrac{\rho(s)}{t-m_\rho^2}$ near $t = m_\rho^2$

We could obtain the residue of the Born term pole by computing exactly the input function $g(z)$, which would give an identical answer. The problem of determining the input function $g(z)$ for our analytic scheme is only slightly more complicated in this case than in the Cheng or AKNS representation:

$$2iq_s g(z) = \sum_{\ell=0} (2\ell+1) \left\{ \frac{\sum_n \int_{\alpha_n^I}^{\alpha_n^{II}} e^{(1-a)\lambda\xi} P_\lambda(\cosh a\xi) d\lambda}{\lambda-\ell} \frac{}{e^{(1-a)\ell\xi} P_\ell(\cosh a\xi)} \right\} P_\ell(z)$$

This problem reduces to the analytic continuation of the following Legendre series:

$$R(\xi, z, \lambda) = \sum_{\ell=0}^{\infty} (2\ell + 1) \frac{e^{-(1-a)\ell\xi}}{(\lambda-\ell) P_\ell(\cosh a\xi)} P_\ell(z)$$

since

$$2iq_s g(z) = \sum_n \int_{\alpha_n^I}^{\alpha_n^{II}} e^{(1-a)\lambda\xi} P_\lambda(\cosh a\xi) R(\xi, z, \lambda) d\lambda$$

Consider the following contour integral: [55]

$$\underset{\ell_0 \to \infty}{\text{Lim}} \frac{1}{2\pi i} \oint \frac{e^{-(1-a)\lambda'\xi} d\lambda'}{P_{\lambda'}(\cosh a\xi) Q_{\lambda'}(\cosh \xi)(\lambda'-\ell)(\lambda'-\lambda)(\lambda'-\ell_0)}^{(-\ell_0)}$$

First taking the contour to infinity in a sequence of finite contours symmetric about the real axis and passing between zeros of the Legendre functions, and then taking the limit $\ell_0 \to \infty$, we obtain an equation for the quantity

$$\frac{e^{-(1-a)\ell\xi}}{P_\ell(\cosh a\xi) Q_\ell(\cosh \xi)(\lambda-\ell)} \qquad .$$

The zeros of the denominator of the integrand occur at $\lambda' = \lambda$, ℓ, ℓ_0, at the zeros of the $Q_{\lambda'}(\cosh \xi)$ function, which lie along the negative real axis between integers and half-integers: [56] $-n -1/2 < \Lambda_n^Q(\xi) < -n$, $n = 1, 2, 3,\ldots$ and at the zeros of the $P_{\lambda'}(\cosh a\xi)$ function, which lie along the line Re $\Lambda_n^P(a\xi) = -1/2$. [52] For any finite ℓ_0, the contribution of the infinite contour is zero,

as can be demonstrated using the asymptotic expansions of the two

Legendre functions. Finally, we obtain the following equation:

$$\frac{e^{-(1-a)\xi}}{P_\ell(\cosh a\xi)Q_\ell(\cosh \xi)(\ell-\lambda)} = 2\, e^{1/2\xi(1-a)}\frac{1}{\sqrt{\sinh \xi\, \sinh a\xi}}$$

$$+ \frac{e^{-(1-a)\xi\lambda}}{P_\lambda(\cosh a\xi)Q_\lambda(\cosh \xi)(\ell-\lambda)} + \sum_n \frac{e^{-(1-a)\xi\Lambda_n^Q}}{P_{\Lambda_n^Q}(\cosh a\xi)\frac{d}{d\lambda'}Q_{\lambda'}(\cosh \xi)\Big|_{\lambda'=\Lambda_n^Q}(\Lambda_n^Q-\lambda)(\ell-\Lambda_n^Q)}$$

$$+ \sum_n \frac{1}{\frac{d}{d\lambda'}P_{\lambda'}(\cosh a\xi)\Big|_{\lambda'=\Lambda_n^P}} \cdot \left[\frac{e^{-(1-a)\xi\Lambda_n^P}}{Q_{\Lambda_n^P}(\cosh\xi)(\Lambda_n^P-\lambda)(\ell-\Lambda_n^P)}\right.$$

$$\text{Im } \Lambda_n^P > 0$$

$$\left. - \frac{e^{-(1-a)\xi\Lambda_n^{*P}}}{Q_{\Lambda_n^{*P}}(\cosh\xi)(\Lambda_n^{*P}-\lambda)(\ell-\Lambda_n^{*P})}\right]$$

The two infinite series are absolutely convergent, so all
that remains is to perform the required Legendre series summations.
The first term is the pole which arose in our earlier simple treat-
ment of the crossed-channel cut:

$$\Sigma\ (2\ell + 1)\ Q_\ell\ (\cosh \xi)\ P_\ell\ (z) = \frac{1}{\cosh \xi - z}$$

The remaining terms are of the type:

$$\sum_{\ell=0}^{\infty}\ (2\ell + 1)\ \frac{Q_\ell(\cosh \xi)}{(\ell-\Lambda)}\ P_\ell(z)$$

Using the following representation (49) for $Q_\ell(\cosh \xi)$:

$$Q_\ell(\cosh \xi) = \frac{1}{\sqrt{2}} \int_\xi^\infty e^{-(\ell + 1/2)x} \frac{dx}{\sqrt{\cosh x - \cosh \xi}} \quad ,$$

we reduce our unknown series to the form:

$$\frac{1}{\sqrt{2}} \int_\xi^\infty \frac{e^{-1/2 \, x}}{\sqrt{\cosh x - \cosh \xi}} \sum_{\ell=0}^\infty (2\ell + 1) \frac{e^{-\ell x}}{\ell - \Lambda} P_\ell(z) \, dx \quad .$$

Summation of the series

$$\sum_{\ell=0}^\infty (2\ell + 1) \frac{e^{-\ell x}}{\ell - \Lambda} P_\ell(z)$$

is accomplished by manipulation of the generating function for $P_\ell(z)$:

$$\sum_{\ell=0}^\infty (2\ell + 1) \frac{e^{-\ell x}}{(\ell - \Lambda)} P_\ell(z) = e^{-\Lambda x} \int_x^\infty \frac{e^{t/2} \sinh t \, e^{\Lambda t} dt}{\sqrt{2}(\cosh t - z)^{3/2}} \quad .$$

Finally, to transform this function into a form valid for Re $\Lambda > -1/2$, consider the following representation (42) for $P_\Lambda(z)$ valid in the range $-1 < \text{Re } \Lambda < 0$.

$$P_\Lambda(-z) = \frac{-\sin \Lambda \pi}{\pi \sqrt{2}} \int_{-\infty}^\infty \frac{e^{(\Lambda + 1/2)x} \, dx}{\sqrt{\cosh x - z}} \quad .$$

Finally, we arrive at the formula

$$\sum_{\ell=0}^{\infty} (2\ell + 1) \frac{Q_\ell(\cosh \xi)}{(\ell - \Lambda)} \ P_\ell(z) = \frac{1}{\sqrt{2}} \int_\xi^\infty \frac{e^{-(\Lambda + 1/2)x}}{\sqrt{\cosh x - \cosh \xi)}} \cdot$$

$$\cdot \left\{ \frac{2e^{(\Lambda + 1/2)x}}{[\cosh x - z]^{1/2}} \right.$$

$$- (2\Lambda + 1) \left[\frac{\pi \sqrt{2}}{\sin \Lambda \pi} P_\Lambda(-z) - \int_{-\infty}^x \frac{e^{(\Lambda + 1/2)y}}{[\cosh y - z]^{1/2}} dy \right] \left. \right\} dx$$

which completes the analytic continuation of our input function in terms of a convergent infinite series.

Since our representation allows a specification of both direct-channel and crossed-channel behavior, we can attempt a boot-strap calculation. Our new representation has the same difficulties as the Cheng and AKNS representations for large s; moreover, we have not included all the effects of higher inelastic thresholds (al-though we still have more to say about this later); finally, our treatment of the crossed-channel cut will have to be modified at high energies, since we expect difficulties for high-spin exchanged systems unless we Reggeize the crossed-channel intermediate states. As a consequence, we will restrict our consideration for the moment to a low-energy calculation, encouraged by the fact that our representation satisfies direct-channel unitarity, threshold constraints in both direct and crossed channels, and will fit direct-channel resonances at any reasonable level of approximation.

We have in mind $\pi\pi$ scattering with a ρ resonance in both direct channel and crossed channels. We ignore the effects of isospin and inelastic thresholds. We do not intend this calculation to develop a reliable model of the ρ meson; instead, we are simply investigating the behavior of our representation, and we will be satisfield if we obtain dynamical quantities which are of the order of magnitude characteristic of the strong interactions.

Recalling that we have formulae for determining the residues of poles in the direct-channel and crossed-channel, we obtain a pair of equations by dropping all but the smallest number of Regge trajectories needed to approximate the quantities. The highest Regge trajectory lies at Re $\alpha = 1$ at the energy of the resonance:

direct-channel:

$$\rho_s \cong \frac{1}{2iq_s} \left. \frac{(\alpha^I - \alpha^{II})(2\alpha^I + 1)}{(-\frac{d\alpha^I}{ds})} \right|_{s = m_\rho^2}$$

$$\cong - \left. \frac{3 \text{ Im } \alpha}{q_s \left(\frac{d\alpha}{ds}\right)} \right|_{s = m_\rho^2}$$

crossed-channel:

$$\left. \rho_t \, P_\ell(\cos \theta_t) \right|_{\substack{\ell = 1 \\ t = m_\rho^2 \\ s = m_\rho^2}} \cong - 4q_s \, e^{1/2(1 - a)\xi} \sqrt{\sinh \xi \, \sinh a\xi} \cdot$$

$$\cdot \left. \text{Im } \alpha P_{\text{Re } \alpha}(\cosh a\xi) e^{\xi(1 - a)\text{Re } \alpha} \right|_{\substack{s = m_\rho^2 \\ \text{Re } \alpha \cong 1}}$$

where

$$A(s,t) \cong \frac{\rho_s P_1(\cos \theta_s)}{s - m_\rho^2} + \rho_t \frac{P_1(\cos \theta_t)}{t - m_\rho^2} + \text{non-pole terms} .$$

We would obtain another equation if we were to write a dispersion relation for $\alpha(s)$:

$$\alpha(s) = \frac{1}{\pi} \int\limits_{4m_\pi^2}^{\infty} \frac{\text{Im } \alpha(s')ds'}{s' - s}$$

In a more elaborate calculation, we would assume such a relationship between Re $\alpha(s)$ and Im $\alpha(s)$, and investigate our equations as functions of s. At this level, however, we fix s at a $s = m_\rho^2$; $\frac{d\alpha}{ds}$ and Im α are undetermined. Experimentally[57], $\alpha(s) = 0.57$ at $s=0$ so we can set $(d\alpha/ds) \approx (1 - .57)/m_\rho^2 \approx (1/65 \, m_\pi^2)$. By requiring equality between the direct-channel and crossed-channel residues, we will obtain a relation which determines m_ρ^2. Evidently, Im α factors out of the equation, and so its value is irrelevant at this level of approximation.

We still have a free parameter: a. In our approximation, this parameter has a straightforward physical interpretation. It appears to be a measure of the fundamental strength of the interactions. As $a \rightarrow 0$ with Im α and $d\alpha/ds$ held fixed, it can be shown that the value of m_ρ^2 goes to infinity while the residue goes to zero. The minimum value of m_ρ^2 and maximum value of residue occur as a approaches $1/2$. In accordance with an intuitive feeling that the strong interactions should be "as strong as possible", we set $a = 1/2$, although it should be pointed out that the value of m_ρ^2 that we obtain is still a

function of, indeed perhaps very sensitive to, the approximations we are making regarding the neglecting of the lower Regge trajectories; the choice of a value of a may have a bearing on this problem, and in principle, should we possess an exact knowledge of the disposition of all Regge poles and zeros, the value of a should be irrelevant, as long as it is in the range $0 < a < 1/2$. In this regard, we should recall once again the spirit in which we have constructed this representation. Specifically, we have arranged the mathematics so that it is possible to compensate for our ignorance of trajectories to the left of the background integral by introducing information about the crossed-channel cut. In general, in order to obtain more precise agreement between the behavior of our approximate amplitude and the requirements of crossing and unitarity, we will have to introduce an integration over a and ξ, with an appropriate integration density.

Our equation is:

$$\frac{-3 \cosh \xi}{q_s \frac{d\alpha}{ds}} = -4 q_s e^{3\xi/4} \sqrt{\sinh \xi \, \sinh \xi/2} \, \cosh(\xi/2) \Bigg|_{s = m_\rho^2}$$

or

$$q_s^2 \cong \frac{3}{4} \frac{\cosh \xi}{e^{3\xi/4} \cosh \xi/2 \sqrt{\sinh \xi \, \sinh \xi/2}} \left[\frac{d\alpha}{ds}\right]^{-1}$$

where

$$\frac{d\alpha}{ds} \approx 1/65$$

$$q_s^2 = \frac{m_\rho^2 - 4}{4}, \quad \cosh \xi = 1 + \frac{m_\rho^2}{2q_s^2} \ .$$

This equation can be solved by successive approximations, starting with $q_s^2 \approx [\frac{d\alpha}{ds}]^{-1}$. The solution is $m_\rho \cong 8.2\, m_\pi$ or $m_\rho \approx 1100$ MeV.

Reviewing our approximations, we might have more confidence in the direct-channel residue equation than in the crossed-channel equations. Separate investigations [58] have indicated that the approximation $\text{Im}\,\alpha = q_s \frac{d\alpha}{ds}$ may be quite good, in spite of the corrections one might expect from lower trajectories. Inclusion of the lower trajectories in the crossed-channel equation will lower the value of m_ρ obtained in our model. To obtain a quantitative evaluation of this correction, we would require knowledge of $\text{Im}\,\alpha_n$ and α_n for the lower trajectories in question.

All known Regge particle trajectories have approximately the same slope at the origin. Taking the rho trajectory as representative, we have

$$\frac{d\alpha}{ds}\bigg|_{s\,=\,0} \cong \frac{1}{65 m_\pi^2} \quad.$$

Evidently, the quantity $[\frac{d\alpha}{ds}\big|_{s\,=\,0}]^{-1/2}$ fixes a mass scale for strong interactions, at least in regions where one of the Mandelstam variables assumes a small value.

Even in this crude level of approximation, our bootstrap theory possesses an important feature in common with observed scattering processes. As we increase the mass of the external particles, holding $\frac{d\alpha}{ds}\big|_{s\,=\,0}$ fixed, the size of the self-consistent bound state mass decreases relative to the external mass. Thus, for example, a two pion system can bind a particle of mass $8.2\, m_\pi$, but if

we allow the external particles to have the mass of the K, the system
binds a particle whose mass satisfies the equation

$$q_s^{\;2} = \frac{3}{4} \; \frac{\cosh \xi}{e^{3/4\xi}\cosh(\xi/2)\sqrt{\sinh \xi \; \sinh \xi/2}} \left(\frac{m_\pi}{m_K}\right)^2 \; .65$$

for which we obtain the solution

$$"m_\rho" \cong 2.8 \; m_K.$$

In order to extend these results to a more interesting class
of reactions, the formalism must be generalized to allow for unequal
external masses, multiple exchanges, inelastic channels, external
particles with spin, and bound states lying at energies below thresh-
hold. It does not seem that these modifications would pose any
problems in principle, but they lie outside the scope of this work.
Unequal mass kinematics should be straightforward; extra compli-
cations arise from distinct t-channel and u-channel states, in which
case the different signature amplitudes must be treated independently.
Scattering of particles with spin requires the separation of scalar
amplitudes which are then Reggeized. Multiple exchanges could be
treated by the following substitutions in our formulas:

$$\int_\alpha^{\alpha^*} \frac{\varphi(\lambda,\xi)d\lambda}{\varphi(\ell,\xi)(\lambda-\ell)} \;\rightarrow\; \int_\alpha^{\alpha^*} \sum_i \frac{\varphi(\lambda,\xi_i)}{\varphi(\ell,\xi_i)} \, A_i \, \frac{d\lambda}{\lambda-\ell}$$

where $\cosh \xi_i = 1 + \dfrac{m_i^{\;2}}{2q_s^{\;2}}$ and $\displaystyle\sum_i A_i = 1,$

or, perhaps more naturally,

Page 116 is not missing; the pages are numbered
incorrectly.

$$\varphi(\lambda, \xi) \longrightarrow \sum_{i} A_i \; \varphi(\lambda, \xi_i)$$

$$\sum_{i} A_i = 1, \text{ etc.}$$

In our parametrization, the higher inelastic thresholds manifest themselves in various ways. The integral

$$\int_{\alpha^I}^{\alpha^{II}} \frac{\varphi(\lambda, s) d\lambda}{\lambda - \ell}$$

develops a new piece corresponding to each new open channel. Figure 7 shows a perspective sketch of the complex S-plane showing the paths of integration which lead to the introduction of the new pieces. Presumably, the integrands $\varphi^i(\lambda, s)$ in these new pieces would involve functions of q_{Rel}^i, the relative momentum of the in-elastically produced particles, just as the purely elastic pieces involve functions of the elastic CM momentum, q_s. The functions $\alpha(s)$ and $\varphi^i(\lambda, s)$ develop branch cuts in s corresponding to the in-elastic threshold branch cuts on the various sheets. The behavior of the functions $\varphi^i(\lambda, s)$ as $q_{Rel, i} \to 0$ would determine the inelastic threshold behavior of the $\alpha^i(s)$, just as in the elastic case.

Application of unitarity would involve detailed consideration of all the various channels involved in the problem. In an intuitive sense, however, we might expect the solution of the problem to follow certain patterns. Especially, we could speculate that quasi

two-body approximations could be made to represent the effects of inelastic channels on the scattering in the basic elastic channel. For example, a three pion channel would be represented as $\rho\pi$ two-body scattering, with an "effective" Regge trajectory equal to the original trajectory displaced in the ℓ-plane according to the rules for the addition of angular momemtum, by the value of the ρ trajectory at the relative CM energy of the two pions bound in the fictitious ρ. Evidently, the "effective" Regge trajectory would never rise much above $\alpha = 1$, and, in this sense, the scattering would always resemble a low-energy process, with the threshold behavior and rate of rise of the effective trajectory, and hence the original trajectory, being governed by the kind of two-body threshold considerations we described earlier. Therefore, the opening of new thresholds would allow the trajectories to rise indefinitely[59]; at the same time, the higher inelastic thresholds would influence the behavior of the Regge trajectory in different manners on different sheets, and the coupling of the Regge trajectory to the original elastic channel would decrease with rising energy, as $\alpha^{II}(s) \to \alpha^{I}(s)$.

APPENDIX A

$P_\alpha(z)$, the Legendre function of the first kind, was calculated for various values of α and z, in order to compare values obtained from three methods: first, the ordinary partial wave expansion; second, the sequence obtained from the partial wave expansion using Shanks' diagonal transform method; third, a contour integral representation.

The partial wave expansion of $P_\alpha(z)$ is:

$$P_\alpha(z) = \lim_{n \to \infty} S_n(z, \alpha) \quad \text{(where the limit exists)}$$

where

$$S_n(z, \alpha) = \frac{\sin(\alpha\pi)}{\pi} \sum_{\ell=0}^{n} (-)^\ell \left[\frac{1}{\alpha - \ell} - \frac{1}{\alpha + \ell + 1} \right] P_\ell(z)$$

This expansion converges for all z in the segment $-1 \leq z \leq 1$, and for all non integral α.

$\alpha = 1.5 + .5i$

$z = 2 + 2i$

From a contour integral calculation, $P_\alpha(z) = -1.32 + 3.47i$

Original Partial Wave Sequence	Diagonal Transform Sequence
0 + 0i	- .0087 + .0104i
-.17 + .098i	- .06128 + .05643i
2.51 - .285i	-1.74 - .514i
-7.33 + 11.0i	-2.20 + 3.38i
24.9 - 5.74i	-1.44 + 3.45i
-93.6 - 33.2i	-1.34 + 3.46i
162.8 + 365.5i	-1.32 + 3.46i
604.2 - 1590.9i	-1.32 + 3.47i
-7030.2 + 3047.7i	
32788.2 + 13718.5i	
-60537.2 - 157778.9i	
-351862.0 + 739498.4i	
3831230.4 - 1247462.1i	

        *   *
          '
          '
          '
          '

* * Absolute value of real or imaginary part greater than 10^7.

$\alpha = 2.5 + .5i$

$z = 2 + 2i$

From a contour integral calculation, $P_\alpha(z) = -16.1 + 5.71i$

Original Partial Wave Sequence	Diagonal Transform Sequence
0 + 0i	
.0836 - .0295i	.00433 - .00640i
-.805 - .357i	.00519 - .00638i
8.295 + 7.892i	.0415 - .0536i
-60.51 + 8.024i	2.083 + 1.614i
98.56 + 68.27i	-13.0 + 14.7i
-183.86 - 438.72i	-16.3 + 6.60i
-773.28 + 1783.3i	-16.1 + 5.81i
7779.4 - 3124.8i	-16.1 + 5.73i
-34930.5 - 15399.6i	-16.1 + 5.73i
61582.4 + 167881.7i	-16.1 + 5.70i
377298.6 - 770005.4i	
-3992259.7 + 1258998.1i	

```
        *   *
          '
          '
          '
          '
```

* * Absolute value of real or imaginary part greater than 10^7.

$\alpha = 1.5 + .5i$

$z = 1.5 + i$

From a contour integral calculation, $P_\alpha(z) = .283 + 1.95i$

Original Partial Wave Sequence	Diagonal Transform Sequence
$0 + 0i$	$-.0159 + .0128i$
$-.172 + .0983i$	$.0983 + .0918i$
$1.46 - .477i$	$-1.23 + 2.45i$
$-.710 + 4.98i$	$.230 + 2.02i$
$4.33 - 2.30i$	$.276 + 1.95i$
$-12.6 + 5.04i$	$.282 + 1.95i$
$31.2 + 14.4i$	$.283 + 1.95i$
$-46.4 - 74.5i$	$.283 + 1.95i$
$-24.7 + 252i$	
$498 - 529i$	
$-2131 + 349i$	
$5735 + 3113i$	
$-8046 - 18319i$	
$-15192 + 60241i$	
$153678 - 119808i$	
$-616533 + 70.4i$	
$1549716 + 1208627i$	

$\alpha = 1.5 + .5i$

$z = 1.5 + 1.5i$

From a contour integral calculation, $P_\alpha(z) = -.568 + 2.30i$

Original Partial Wave Sequence	Diagonal Transform Sequence
$0 + 0i$	$-.0115 + .0134i$
$-.172 + .0983i$	$-.0692 + .0774i$
$1.84 - .189i$	$-1.855 + .734i$
$-3.91 + 6.00i$	$-.782 + 2.29$
$10.16 - .315i$	$-.592 + 2.29i$
$-26.84 - 12.15i$	$-.570 + 2.30i$
$24.27 + 89.66i$	$-.568 + 2.30i$
$149.39 - 250.69i$	$-.568 + 2.30i$
$-973.8 + 213.1i$	
$2843 + 2011i$	
$-1543 - 12368i$	
$-29646 + 34498i$	
$168409 - 4274i$	
$-435034 - 458025i$	
$-185603 + 2386023i$	
$7251866 - 5573949i$	

        *   *
          '
          '
          '
          '

* * Absolute value of real or imaginary part greater than 10^7.

$\alpha = 1.5 + .5i$

$z = 1.5i$

From a contour integral calculation, $P_\alpha(z) = -1.06 + .334i$

Original Partial Wave Sequence	Diagonal Transform Sequence
0 + 0i	-.000215 + .0257i
-.172 + .0980i	-.0323 + .103i
.978 + .961i	-.646 + .227i
-2.80 - 2.06i	-.985 + .359i
-4.36 + 4.60i	-1.06 + .347i
8.93 + 6.21i	-1.06 + .335i
11.22 - 24.16i	-1.06 + .333i
-63.87 - 28.06i	-1.06 + .333i
-71.31 + 167.16i	
454.29 + 182.51i	
487.86 - 1269.49i	
-3603.7 - 1346.3i	
-3786.0 + 10366i	
30176.9 + 10811.8i	
31292.2 - 88726.1i	
-263077 - 91577i	
-270497 + 785741i	

APPENDIX B

Using the Cheng representation, scattering cross sections are calculated for infinite numbers of evenly spaced Regge pole and zero trajectories. α_I and α_{II} refer to the leading pole and zero trajectories, respectively, while $\triangle_I$ and $\triangle_{II}$ refer to the spacings of their respective daughters. ξ is a kinematic variable indicating the position of the nearest crossed channel cut (see text).

$\alpha_I = 4.1 + .4i$

$\alpha_{II} = 4.1 - .4i$

$\triangle_I = \triangle_{II} = 1.2$

$\xi = .35$
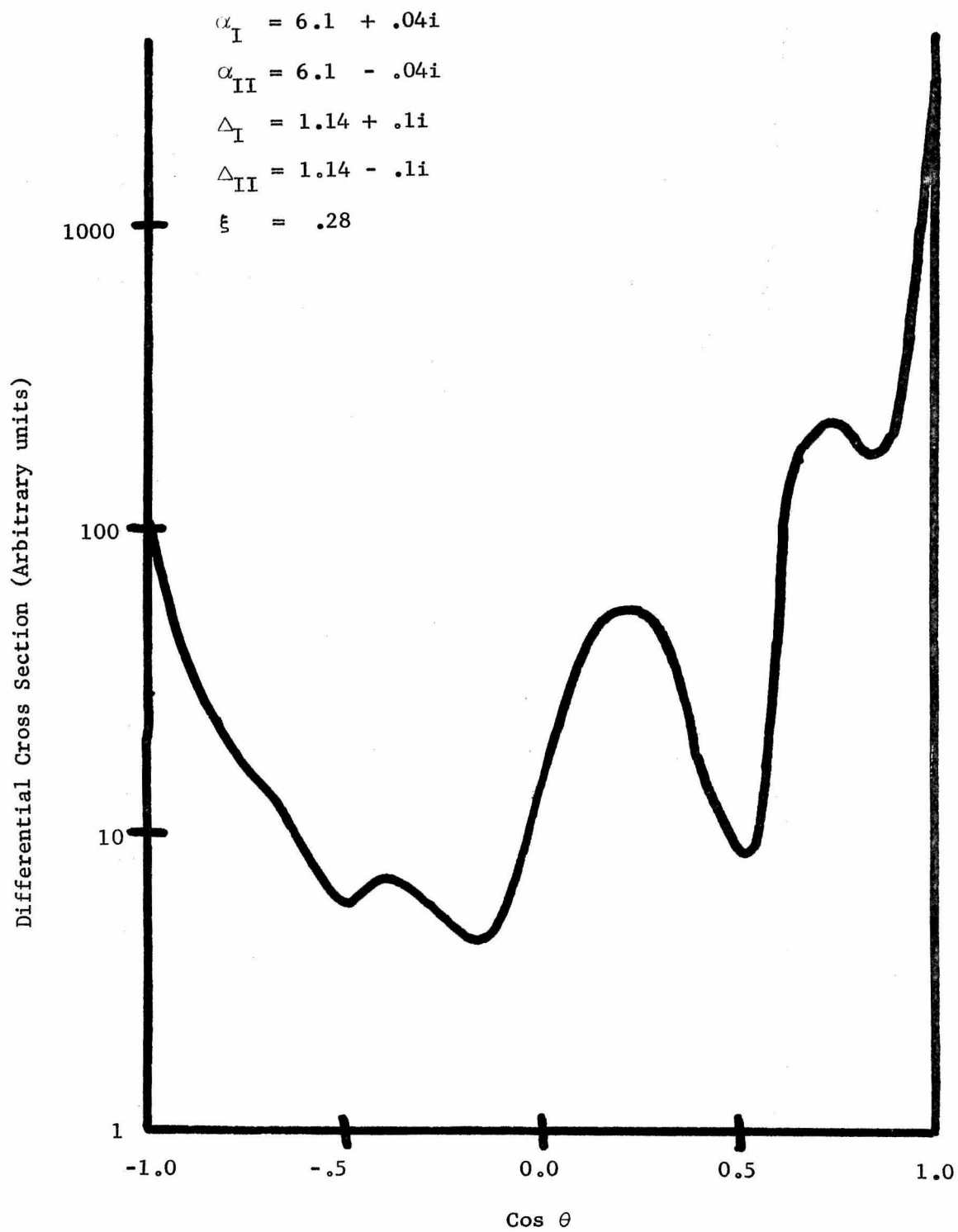
$\alpha_I = 5.7 + .04i$

$\alpha_{II} = 5.7 - .04i$

$\triangle_I = 1.15 + .1i$

$\triangle_{II} = 1.15 - .1i$

$\xi = .29$

α_I = 6.1 + .04i

α_{II} = 6.1 - .04i

$\triangle_I$ = 1.14 + .1i

$\triangle_{II}$ = 1.14 - .1i

ξ = .28
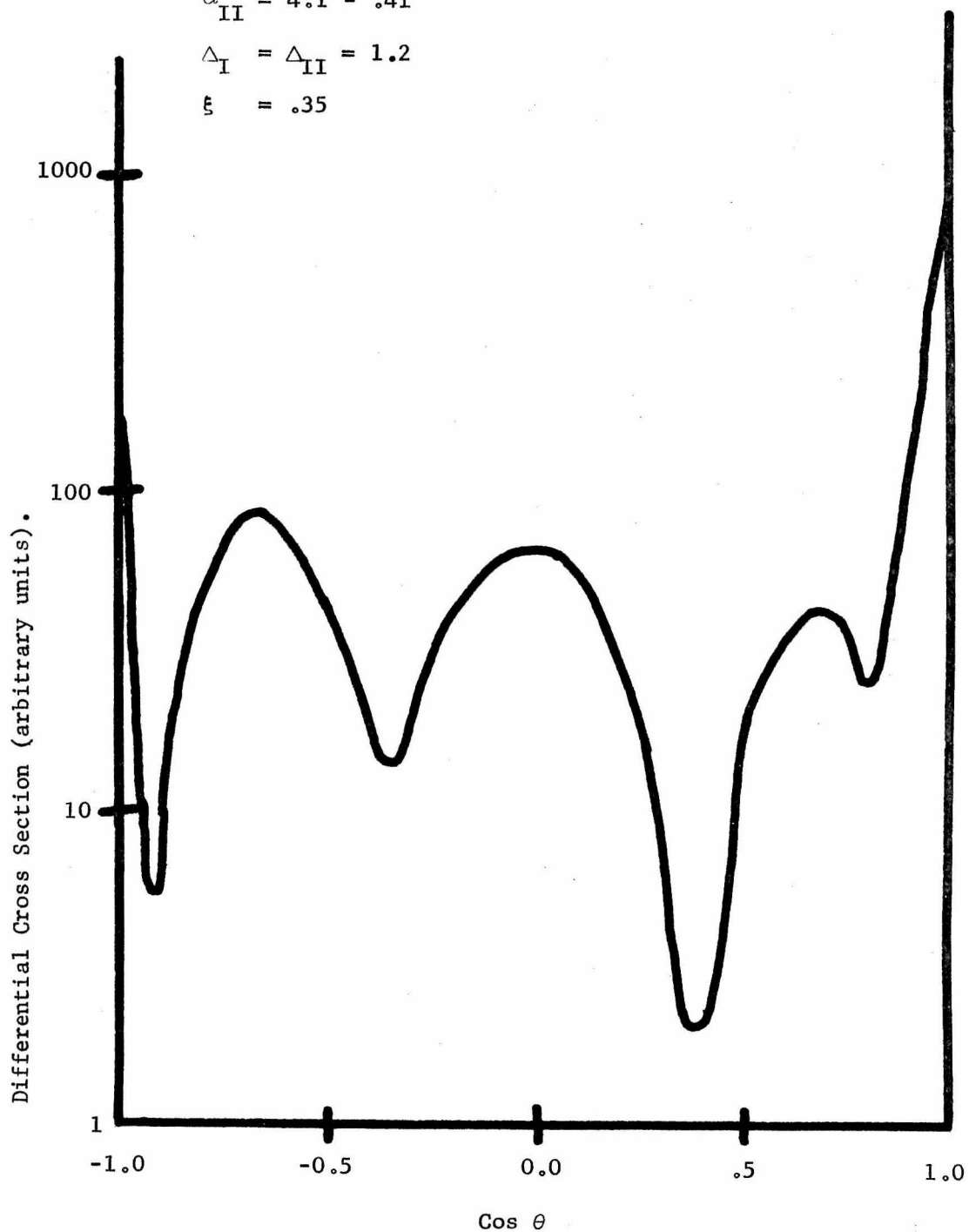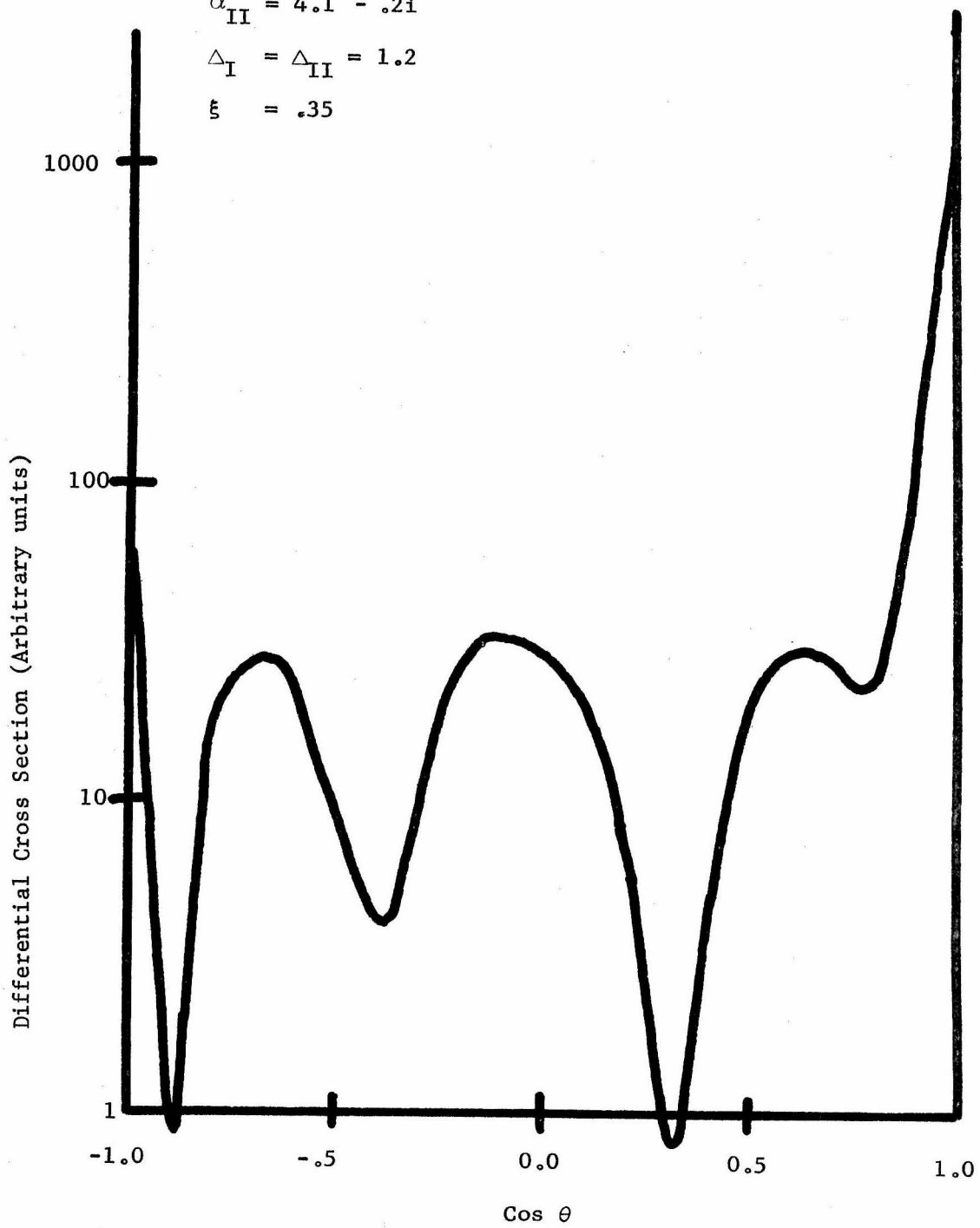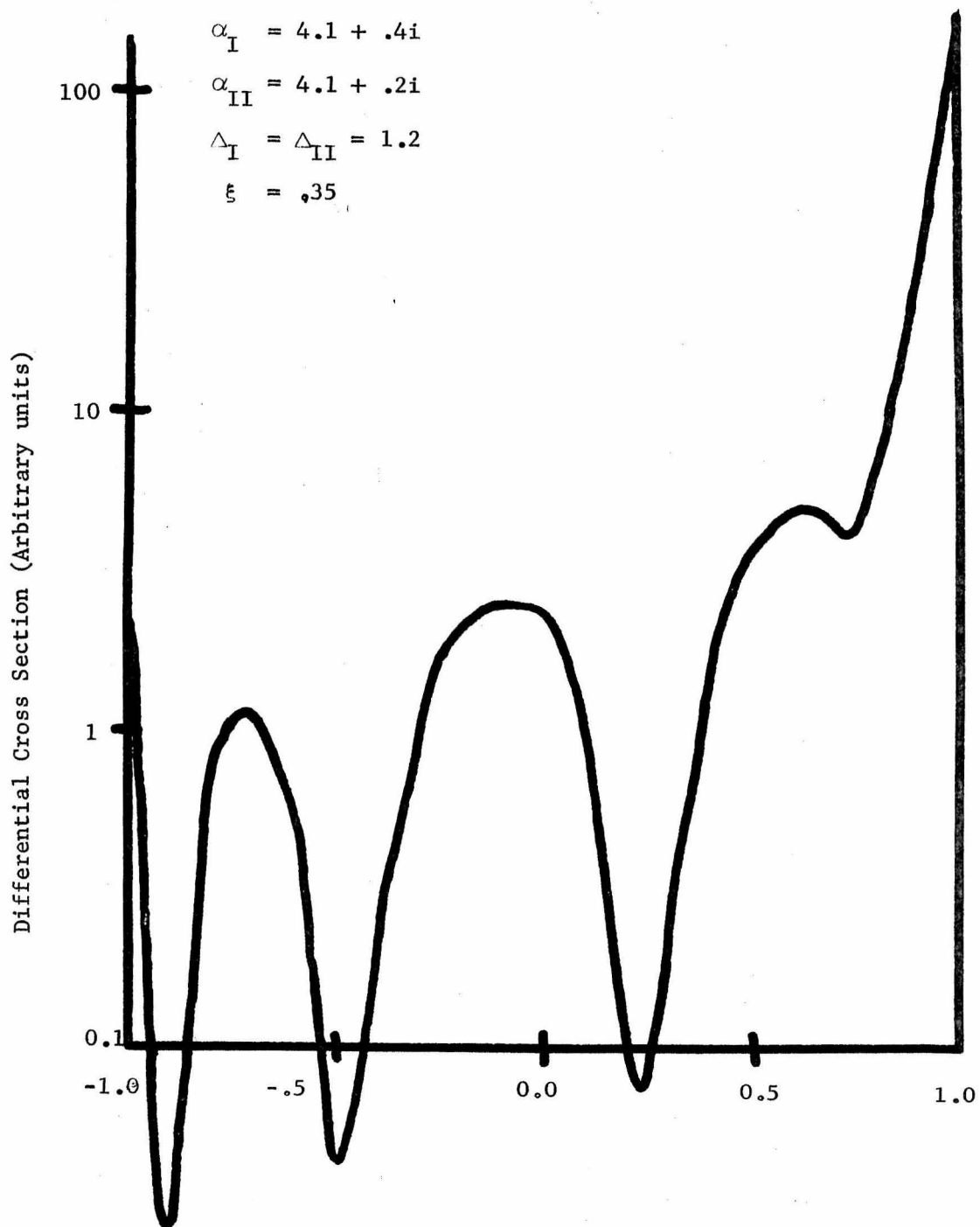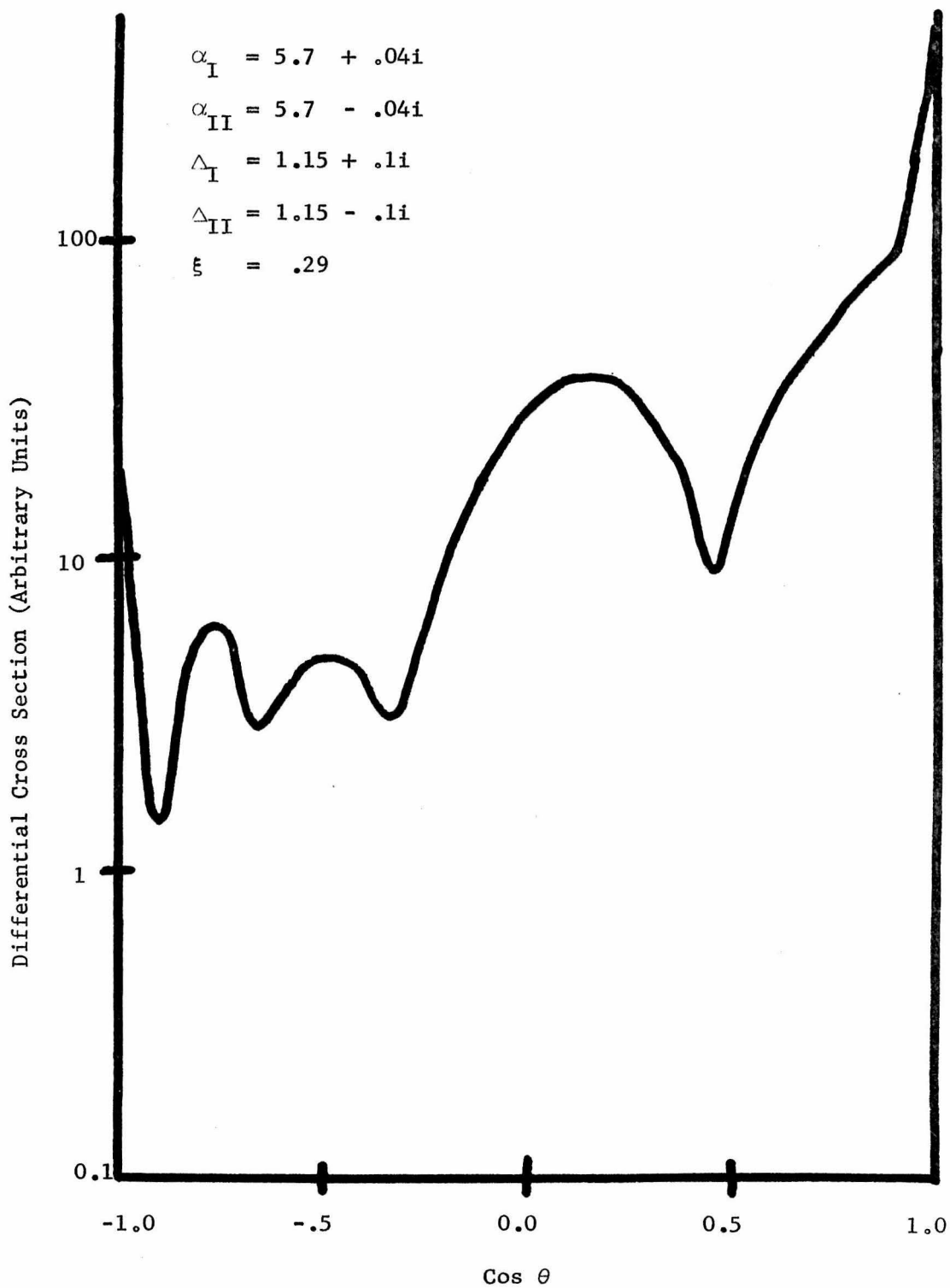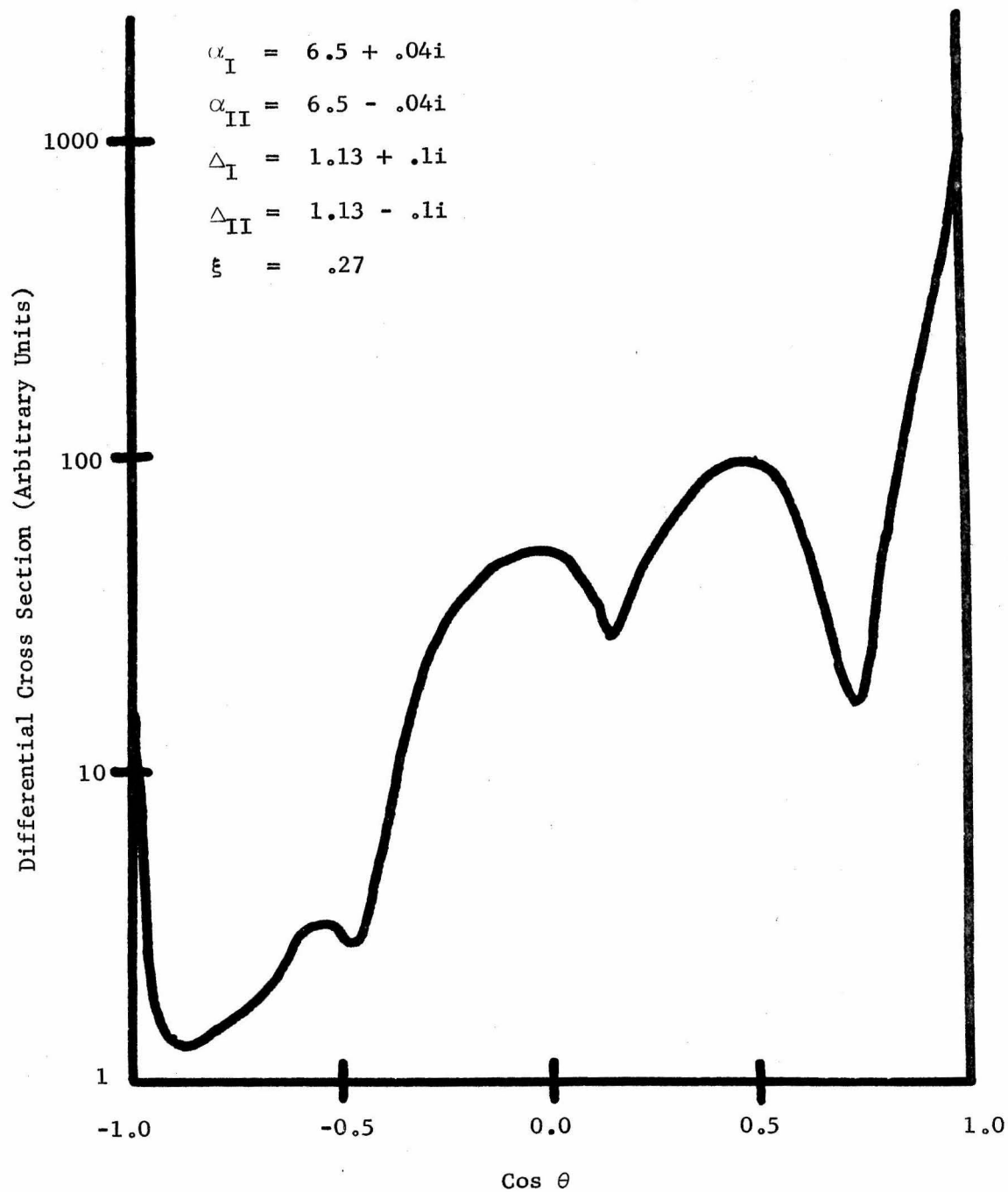
TABLE 1

PARTICLES IN THE PION-BARYON SCATTERING MODEL

<u>Pion Octet</u> π_8

Particle	Mass(MeV)	Spin-Parity	Isospin	Strangeness
π	138	0^-	1	0
K	496	0^-	1/2	1
$\bar{K}$	496	0^-	1/2	-1
η	548	0^-	0	0

<u>Baryon Octet</u> B_8

Particle	Mass(MeV)	Spin-Parity	Isospin	Strangeness
N	939	$1/2^+$	1/2	0
Σ	1193	$1/2^+$	1	-1
Λ	1115	$1/2^+$	0	-1
Ξ	1320	$1/2^+$	1/2	-2

<u>Baryon Decuplet</u> B_{10}

Particle	Mass(MeV)	Spin-Parity	Isospin	Strangeness
N^*	1238	$3/2^+$	3/2	0
Y^*	1385	$3/2^+$	1	-1
Ξ^*	1530	$3/2^+$	1/2	-2
Ω	1685	$3/2^+$	0	-3

TABLE 2

PION-BARYON CHANNELS WITH BOUND STATES

Bound State	Channel	Exchanged Particles
N	$N\pi \to N\pi$	N, N^*
	$N\pi \to N\eta$	N
	$N\pi \to \Sigma K$	Σ, Y^*, Λ
	$N\pi \to \Lambda K$	Σ, Y^*
	$N\eta \to N\eta$	N
	$N\eta \to \Sigma K$	Σ, Y^*
	$N\eta \to \Lambda K$	Λ
	$\Sigma K \to \Sigma K$	Ξ, Ξ^*
	$\Sigma K \to \Lambda K$	Ξ, Ξ^*
	$\Lambda K \to \Lambda K$	Ξ, Ξ^*
N^*	$N\pi \to N\pi$	N, N^*
	$N\pi \to \Sigma K$	Σ, Y^*, Λ
	$\Sigma K \to \Sigma K$	Ξ, Ξ^*
Σ, Y^*	$\Sigma\pi \to \Sigma\pi$	Σ, Y^*, Λ
	$\Sigma\pi \to \Sigma\eta$	Σ, Y^*
	$\Sigma\pi \to NK$	N, N^*
	$\Sigma\pi \to \Lambda\pi$	Σ, Y^*
	$\Sigma\pi \to \Xi K$	Ξ, Ξ^*
	$\Sigma\eta \to \Sigma\eta$	Σ, Y
	$\Sigma\eta \to NK$	N
	$\Sigma\eta \to \Lambda\pi$	Λ
	$\Sigma\eta \to \Xi K$	Ξ, Ξ^*
	$N\bar{K} \to N\bar{K}$	none
	$N\bar{K} \to \Lambda\pi$	N
	$N\bar{K} \to \Xi K$	Σ, Y^*, Λ
	$\Lambda\pi \to \Lambda\pi$	Σ, Y^*
	$\Lambda\pi \to \Xi K$	Ξ, Ξ^*
	$\Xi K \to \Xi K$	Ω
Ξ, Ξ^*	$\Xi\pi \to \Xi\pi$	Ξ, Ξ^*
	$\Xi\pi \to \Xi\eta$	Ξ, Ξ^*
	$\Xi\pi \to \Sigma\bar{K}$	Σ, Y^*, Λ
	$\Xi\pi \to \Lambda\bar{K}$	Σ, Y^*
	$\Xi\eta \to \Xi\eta$	Ξ, Ξ^*
	$\Xi\eta \to \Sigma\bar{K}$	Σ, Y^*
	$\Xi\eta \to \Lambda\bar{K}$	Λ
	$\Sigma\bar{K} \to \Sigma\bar{K}$	N, N^*
	$\Sigma\bar{K} \to \Lambda\bar{K}$	N
	$\Lambda\bar{K} \to \Lambda\bar{K}$	N
Ω	$\Xi\bar{K} \to \Xi\bar{K}$	Σ, Y^*, Λ

Table 2 (continued)

Bound State	Channel	Exchanged Particles
Λ	$\Sigma\pi \to \Sigma\pi$	Σ, Y^*, Λ
	$\Sigma\pi \to \Lambda\eta$	Σ, Y^*
	$\Sigma\pi \to N\bar{K}$	N, N^*
	$\Sigma\pi \to \Xi K$	Ξ, Ξ^*
	$\Lambda\eta \to \Lambda\eta$	Λ
	$\Lambda\eta \to N\bar{K}$	N
	$\Lambda\eta \to \Xi K$	Ξ, Ξ^*
	$N\bar{K} \to N\bar{K}$	none
	$N\bar{K} \to \Xi K$	Σ, Y^*, Λ
	$\Xi K \to \Xi K$	Ω^-

TABLE 3

CLOSED SETS OF COUPLING SHIFT EQUATIONS,

EIGENVALUES, AND ENHANCED EIGENVECTORS

I)

$$\delta R^{N^*}_{N\pi,N\pi} = \frac{4}{9} \ \delta R^{N}_{N\pi,N\pi} + \frac{1}{9} \ \delta R^{N^*}_{N\pi,N\pi} + X(N^*|N\pi,N\pi)$$

$$\delta R^{N}_{N\pi,N\pi} = \frac{1}{9} \ \delta R^{N}_{N\pi,N\pi} + \frac{16}{9} \ \delta R^{N^*}_{N\pi,N\pi} + X(N|N\pi,N\pi)$$

$$\lambda = 1, \ -7/9$$

for $\lambda = 1$, $\delta R^{N}_{N\pi,N\pi} = 2\delta R^{N^*}_{N\pi,N\pi}$

II)

$$\delta R^{N^*}_{N\pi,\Sigma K} = \frac{1}{6} \delta R^{Y^*}_{N\bar{K},\Sigma\pi} + \frac{1}{3} \ \delta R^{\Sigma}_{N\bar{K},\Sigma\pi} + \frac{2}{3\sqrt{6}} \ \delta R^{\Lambda}_{N\bar{K},\Sigma\pi} + X(N^*|N\pi,\Sigma K)$$

$$\delta R^{Y^*}_{N\bar{K},\Sigma\pi} = \frac{2}{9} \delta R^{N^*}_{\Sigma K,N\pi} - \frac{4}{9} \ \delta R^{N}_{\Sigma K,N\pi} + X(Y^*|N\bar{K},\Sigma\pi)$$

$$\delta R^{N}_{N\pi,\Sigma K} = \frac{1}{3} \delta R^{\Sigma}_{N\bar{K},\Sigma\pi} - \frac{4}{3} \ \delta R^{Y^*}_{N\bar{K},\Sigma\pi} - \frac{1}{3\sqrt{6}} \delta R^{\Lambda}_{N\bar{K},\Sigma\pi} + X(N|N\pi,\Sigma K)$$

$$\delta R^{\Sigma}_{\Sigma\pi,N\bar{K}} = \frac{8}{9} \delta R^{N^*}_{N\pi,\Sigma K} + \frac{2}{9} \delta R^{N}_{N\pi,\Sigma K} + X(\Sigma|\Sigma\pi,N\bar{K})$$

$$\delta R^{\Lambda}_{\Sigma\pi,N\bar{K}} = -\sqrt{6}/9 \ \delta R^{N}_{N\pi,\Sigma K} + 8\sqrt{6}/9 \ \delta R^{N^*}_{N\pi,\Sigma K} + X(\Lambda|\Sigma\pi,N\bar{K})$$

$$\lambda = 1, \ -1, \ \pm i\sqrt{\frac{2}{27}} \ , \ 0$$

for $\lambda = 1$,

$$\delta R^{N}_{N\pi,\Sigma K} = - \ \delta R^{N^*}_{N\pi,\Sigma K}$$

$$\delta R^{\Sigma}_{N\bar{K},\Sigma\pi} = \frac{2}{3} \ \delta R^{N^*}_{N\pi,\Sigma K}$$

$$\delta R^{Y^*}_{\Sigma\pi,N\bar{K}} = \frac{2}{3} \ \delta R^{N^*}_{N\pi,\Sigma K}$$

$$\delta R^{\Lambda}_{\Sigma\pi,N\bar{K}} = \sqrt{6} \ \delta R^{N^*}_{N\pi,\Sigma K}$$

Table 3 (continued)

III)

$$\delta R^{N*}_{\Sigma K, \Sigma K} = \frac{4}{9} \; R^{\overline{\Xi}}_{\Sigma \overline{K}, \Sigma \overline{K}} + \frac{2}{9} \, \delta R^{\overline{\Xi}*}_{\Sigma \overline{K}, \Sigma \overline{K}} + X(N* | \Sigma K, \Sigma K)$$

$$\delta R^{\overline{\Xi}*}_{\Sigma \overline{K}, \Sigma \overline{K}} = \frac{4}{9} \, \delta R^{N*}_{\Sigma K, \Sigma K} - \frac{2}{9} \, \delta R^{N}_{\Sigma K, \Sigma K} + X(\overline{\Xi}* | \Sigma \overline{K}, \Sigma \overline{K})$$

$$\delta R^{N}_{\Sigma K, \Sigma K} = \frac{1}{9} \, \delta R^{\overline{\Xi}}_{\Sigma \overline{K}, \Sigma \overline{K}} - \frac{4}{9} \, \delta R^{\overline{\Xi}*}_{\Sigma \overline{K}, \Sigma \overline{K}} + X(N | \Sigma K, \Sigma K)$$

$$\delta R^{\overline{\Xi}}_{\Sigma \overline{K}, \Sigma \overline{K}} = \frac{16}{9} \, \delta R^{N*}_{\Sigma K, \Sigma K} + \frac{1}{9} \, \delta R^{N}_{\Sigma K, \Sigma K} + X(\overline{\Xi} | \Sigma \overline{K}, \Sigma \overline{K})$$

$$\lambda = \frac{2\sqrt{2}}{3} \, , \quad -\frac{2\sqrt{2}}{3} \, , \; \frac{1}{3} \, , \; -\frac{1}{3}$$

for $\lambda = \dfrac{2\sqrt{3}}{3} \approx .945, \qquad \delta R^{N}_{\Sigma K, \Sigma K} = 0$

$$\delta R^{N*}_{\Sigma K, \Sigma K} = \frac{3}{\sqrt{2}} \, \delta R^{\overline{\Xi}*}_{\Sigma \overline{K}, \Sigma \overline{K}}$$

$$\delta R^{\overline{\Xi}}_{\Sigma \overline{K}, \Sigma \overline{K}} = 4 \quad \delta R^{\overline{\Xi}*}_{\Sigma \overline{K}, \Sigma \overline{K}}$$

IV)

$$\delta R^{\overline{\Xi}}_{\Xi \pi, \Xi \pi} = \frac{1}{9} \, \delta R^{\overline{\Xi}}_{\Xi \pi, \Xi \pi} - \frac{4}{9} \, \delta R^{\overline{\Xi}*}_{\Xi \pi, \Xi \pi} + X(\Xi | \Xi \pi, \Xi \pi)$$

$$\delta R^{\overline{\Xi}*}_{\Xi \pi, \Xi \pi} = -\frac{2}{9} \, \delta R^{\overline{\Xi}}_{\Xi \pi, \Xi \pi} - \frac{1}{9} \, \delta R^{\overline{\Xi}*}_{\Xi \pi, \Xi \pi} + X(\Xi* | \Xi \pi, \Xi \pi)$$

$$\lambda = \pm 1/3$$

Table 3 (continued)

V)

$$\delta R^{Y*}_{\Sigma\pi,\Sigma\pi} = \frac{1}{3}\,\delta R^{\Sigma}_{\Sigma\pi,\Sigma\pi} + \frac{1}{6}\,\delta R^{Y*}_{\Sigma\pi,\Sigma\pi} - \frac{2}{9}\,\delta R^{\Lambda}_{\Sigma\pi,\Sigma\pi} + X(Y^*|\Sigma\pi,\Sigma\pi)$$

$$\delta R^{\Sigma}_{\Sigma\pi,\Sigma\pi} = -\frac{1}{6}\,\delta R^{\Sigma}_{\Sigma\pi,\Sigma\pi} + \frac{2}{3}\,\delta R^{Y*}_{\Sigma\pi,\Sigma\pi} + \frac{1}{9}\,\delta R^{\Lambda}_{\Sigma\pi,\Sigma\pi} + (\Sigma|\Sigma\pi,\Sigma\pi)$$

$$\delta R^{\Lambda}_{\Sigma\pi,\Sigma\pi} = \frac{1}{3}\,\delta R^{\Sigma}_{\Sigma\pi,\Sigma\pi} - \frac{4}{3}\,\delta R^{Y*}_{\Sigma\pi,\Sigma\pi} - \frac{1}{9}\,\delta R^{\Lambda}_{\Sigma\pi,\Sigma\pi} + X(\Lambda|\Sigma\pi,\Sigma\pi)$$

$$\lambda \approx .69,\ .06,\ -.84$$

for $\lambda \approx .69$,

$$\delta R^{\Sigma}_{\Sigma\pi,\Sigma\pi} = -.45\ \delta R^{\Lambda}_{\Sigma\pi,\Sigma\pi}$$

$$\delta R^{Y*}_{\Sigma\pi,\Sigma\pi} = -.73\ \delta R^{\Lambda}_{\Sigma\pi,\Sigma\pi}$$

VI)

$$\delta R^{\Lambda}_{\Lambda\eta,\Lambda\eta} = -\frac{1}{3}\,\delta R^{\Lambda}_{\Lambda\eta,\Lambda\eta} + X(\Lambda|\Lambda\eta,\Lambda\eta)$$

$$\lambda = -1/3$$

VII)

$$\delta R^{\Sigma}_{\Sigma\eta,\Lambda\pi} = \frac{1}{3\sqrt{3}}\,\delta R^{\Lambda}_{\Sigma\pi,\Lambda\eta} + X(\Sigma|\Sigma\eta,\Lambda\pi)$$

$$\delta R^{Y*}_{\Sigma\eta,\Lambda\pi} = -\frac{2}{3\sqrt{3}}\,\delta R^{\Lambda}_{\Sigma\pi,\Lambda\eta} + X(Y^*|\Sigma\eta,\Lambda\pi)$$

$$\delta R^{\Lambda}_{\Sigma\pi,\Lambda\eta} = \frac{1}{3}\sqrt{3}\,\delta R^{\Sigma}_{\Lambda\pi,\Sigma\eta} - \frac{4\sqrt{3}}{3}\,\delta R^{Y*}_{\Lambda\pi,\Sigma\eta} + X(\Lambda|\Sigma\pi,\Lambda\eta)$$

$$\lambda = 1,\ -1,\ 0$$

for $\lambda = 1$,

$$\delta R^{\Sigma}_{\Sigma\eta,\Lambda\pi} = \frac{1}{3\sqrt{3}}\,\delta R^{\Lambda}_{\Sigma\pi,\Lambda\eta}$$

$$\delta R^{Y*}_{\Sigma\eta,\Lambda\pi} = -\frac{2}{3\sqrt{3}}\,\delta R^{\Lambda}_{\Sigma\pi,\Lambda\eta}$$

Table 3 (continued)

VIII)

$$\delta R^{Y*}_{\Sigma\pi,\Sigma\eta} = \frac{2}{3} \delta R^{\Sigma}_{\Sigma\eta,\Sigma\pi} + \frac{1}{3} \delta R^{Y*}_{\Sigma\eta,\Sigma\pi} + X(Y*|\Sigma\pi,\Sigma\eta)$$

$$\delta R^{\Sigma}_{\Sigma\pi,\Sigma\eta} = -\frac{1}{3} \delta R^{\Sigma}_{\Sigma\eta,\Sigma\pi} + \frac{4}{3} \delta R^{Y*}_{\Sigma\eta,\Sigma\pi} + X(\Sigma|\Sigma\pi,\Sigma\eta)$$

$$\lambda = \pm 1$$

for $\lambda = 1$, $\qquad \delta R^{Y*}_{\Sigma\pi,\Sigma\eta} = \delta R^{\Sigma}_{\Sigma\pi,\Sigma\eta}$

IX)

$$\delta R^{Y*}_{\Sigma\pi,\Lambda\pi} = -\frac{2}{3} \delta R^{\Sigma}_{\Sigma\pi,\Lambda\pi} - \frac{1}{3} \delta R^{Y*}_{\Sigma\pi,\Lambda\pi} + X(Y*|\Sigma\pi,\Lambda\pi)$$

$$\delta R^{\Sigma}_{\Sigma\pi,\Lambda\pi} = \frac{1}{3} \delta R^{\Sigma}_{\Sigma\pi,\Lambda\pi} - \frac{4}{3} \delta R^{Y*}_{\Sigma\pi,\Lambda\pi} + X(\Sigma|\Sigma\pi,\Lambda\pi)$$

$$\lambda = \pm 1$$

for $\lambda = 1$, $\qquad \delta R^{Y*}_{\Sigma\pi,\Lambda\pi} = -\frac{1}{2} \delta R^{\Sigma}_{\Sigma\pi,\Lambda\pi}$

X)

$$\delta R^{Y*}_{\Xi K,\Sigma\pi} = \frac{4}{9} \delta R^{\Xi}_{\Xi\pi,\Sigma\bar{K}} + \frac{2}{9} \delta R^{\Xi*}_{\Xi\pi,\Sigma\bar{K}} + X(Y*|\Xi K,\Sigma\pi)$$

$$\delta R^{\Sigma}_{\Xi K,\Sigma\pi} = -\frac{2}{9} \delta R^{\Xi}_{\Xi\pi,\Sigma\bar{K}} + \frac{8}{9} \delta R^{\Xi*}_{\Xi\pi,\Sigma\bar{K}} + X(\Sigma|\Xi K,\Sigma\pi)$$

$$\delta R^{\Xi}_{\Xi\pi,\Sigma\bar{K}} = -\frac{1}{3} \delta R^{\Sigma}_{\Xi K,\Sigma\pi} + \frac{4}{3} \delta R^{Y*}_{\Xi K,\Sigma\pi} + \frac{1}{3\sqrt{6}} \delta R^{\Lambda}_{\Xi K,\Sigma\pi} + X(\Xi|\Xi\pi,\Sigma\bar{K})$$

$$\delta R^{\Xi*}_{\Xi\pi,\Sigma\bar{K}} = \frac{2}{3} \delta R^{\Sigma}_{\Xi K,\Sigma\pi} + \frac{1}{3} \delta R^{Y*}_{\Sigma\pi,\Xi K} - \frac{2}{3\sqrt{6}} \delta R^{\Lambda}_{\Xi K,\Sigma\pi} + X(\Xi*|\Xi\pi,\Sigma\bar{K})$$

$$\delta R^{\Lambda}_{\Xi K,\Sigma\pi} = \frac{\sqrt{6}}{9} \delta R^{\Xi}_{\Xi\pi,\Sigma\bar{K}} - \frac{4\sqrt{6}}{9} \delta R^{\Xi*}_{\Xi\pi,\Sigma\bar{K}} + X(\Lambda|\Xi K,\Sigma\pi)$$

Table 3 (continued)

$$\lambda = 1, \ -1, \ \pm\sqrt{\frac{2}{3}}, \ 0$$

for $\lambda = 1$,
$$\delta R^{\Xi^*}_{\Xi\pi,\Sigma\bar{K}} = -2 \ \delta R^{\Xi}_{\Xi\pi,\Sigma\bar{K}}$$

$$\delta R^{\Sigma}_{\Xi K,\Sigma\pi} = -2 \ \delta R^{\Xi}_{\Xi\pi,\Sigma K}$$

$$\delta R^{Y^*}_{\Xi K,\Sigma\pi} = 0$$

$$\delta R^{\Lambda}_{\Xi K,\Sigma\pi} = \sqrt{6} \ \ \delta R^{\Xi}_{\Xi\pi,\Sigma\bar{K}}$$

XI)

$$\delta R^{Y^*}_{\Sigma\eta,\Sigma\eta} = \frac{2}{3} \ \delta R^{\Sigma}_{\Sigma\eta,\Sigma\eta} + \frac{1}{3} \ \delta R^{Y^*}_{\Sigma\eta,\Sigma\eta} + X(Y^*|\Sigma\eta,\Sigma\eta)$$

$$\delta R^{\Sigma}_{\Sigma\eta,\Sigma\eta} = -\frac{1}{3} \ \delta R^{\Sigma}_{\Sigma\eta,\Sigma\eta} + \frac{4}{3} \ \delta R^{Y^*}_{\Sigma\eta,\Sigma\eta} + X(\Sigma|\Sigma\eta,\Sigma\eta)$$

$$\lambda = \pm 1$$

for $\lambda = 1$,
$$\delta R^{Y^*}_{\Sigma\eta,\Sigma\eta} = \delta R^{\Sigma}_{\Sigma\eta,\Sigma\eta}$$

XII)

$$\delta R^{Y^*}_{\Sigma\eta,\Xi K} = -\frac{2}{3}\sqrt{\frac{2}{3}} \ \delta R^{\Xi}_{\Xi\eta,\Sigma\bar{K}} - \frac{1}{3}\sqrt{\frac{2}{3}} \ \delta R^{\Xi^*}_{\Xi\eta,\Sigma\bar{K}} + X(Y^*|\Sigma\eta,\Xi K)$$

$$\delta R^{\Sigma}_{\Sigma\eta,\Xi K} = \frac{1}{3}\sqrt{\frac{2}{3}} \ \delta R^{\Xi}_{\Xi\eta,\Sigma\bar{K}} - \frac{4}{3}\sqrt{\frac{2}{3}} \ \delta R^{\Xi^*}_{\Xi\eta,\Sigma\bar{K}} + X(\Sigma|\Sigma\eta,\Xi K)$$

$$\delta R^{\Xi}_{\Xi\eta,\Sigma\bar{K}} = \frac{1}{3}\sqrt{\frac{3}{2}} \ \delta R^{\Sigma}_{\Xi K,\Sigma\eta} - \frac{4}{3}\sqrt{\frac{3}{2}} \ \delta R^{Y^*}_{\Xi K,\Sigma\eta} + X(\Xi|\Xi\eta,\Sigma\bar{K})$$

$$\delta R^{\Xi^*}_{\Xi\eta,\Sigma\bar{K}} = -\frac{2}{3}\sqrt{\frac{3}{2}} \ \delta R^{\Sigma}_{\Sigma\eta,\Xi K} - \frac{1}{3}\sqrt{\frac{3}{2}} \ \delta R^{Y^*}_{\Sigma\eta,\Xi K} + X(\Xi^*|\Xi\eta,\Sigma\bar{K})$$

$$\lambda = \pm 1, \ \pm 1$$

for $\lambda = 1$,
$$\delta R^{Y^*}_{\Sigma\eta,\Xi K} = -\frac{2}{3}\sqrt{\frac{2}{3}} \ \delta R^{\Xi}_{\Xi\eta,\Sigma\bar{K}} - \frac{1}{3}\sqrt{\frac{2}{3}} \ \delta R^{\Xi^*}_{\Xi\eta,\Sigma\bar{K}}$$

$$\delta R^{\Sigma}_{\Sigma\eta,\Xi K} = \frac{1}{3}\sqrt{\frac{2}{3}} \ \delta R^{\Xi}_{\Xi\eta,\Sigma\bar{K}} - \frac{4}{3}\sqrt{\frac{2}{3}} \ \delta R^{\Xi^*}_{\Xi\eta,\Sigma\bar{K}}$$

Table 3 (continued)

XIII)

$$\delta R^{Y*}_{\Sigma\eta,N\bar{K}} = \frac{2}{3}\sqrt{\frac{2}{3}}\, \delta R^{N}_{\Sigma K,N\eta} + X(Y*|\Sigma\eta,N\bar{K})$$

$$\delta R^{N}_{N\eta,\Sigma K} = -\frac{1}{3}\sqrt{\frac{3}{2}}\, \delta R^{\Sigma}_{N\bar{K},\Sigma\eta} + \frac{4}{3}\sqrt{\frac{3}{2}}\, \delta R^{Y*}_{N\bar{K},\Sigma\eta} + X(N|N\eta,\Sigma K)$$

$$\delta R^{\Sigma}_{\Sigma\eta,N\bar{K}} = -\frac{1}{3}\sqrt{\frac{2}{3}}\, \delta R^{N}_{N\eta,\Sigma K} + X(\Sigma|\Sigma\eta,N\bar{K})$$

$\lambda = \pm 1,0$

for $\lambda = 1$,
$$\delta R^{Y*}_{\Sigma\eta,N\bar{K}} = \frac{2}{3}\sqrt{\frac{2}{3}}\, \delta R^{N}_{\Sigma K,N\eta}$$

$$\delta R^{\Sigma}_{\Sigma\eta,N\bar{K}} = -\frac{1}{3}\sqrt{\frac{2}{3}}\, \delta R^{N}_{N\eta,\Sigma K}$$

XIV)

$$\delta R^{Y*}_{\Lambda\pi,\Lambda\pi} = \frac{2}{3}\, \delta R^{\Sigma}_{\Lambda\pi,\Lambda\pi} + \frac{1}{3}\, \delta R^{Y*}_{\Lambda\pi,\Lambda\pi} + X(Y*|\Lambda\pi,\Lambda\pi)$$

$$\delta R^{\Sigma}_{\Lambda\pi,\Lambda\pi} = -\frac{1}{3}\, \delta R^{\Sigma}_{\Lambda\pi,\Lambda\pi} + \frac{4}{3}\, \delta R^{Y*}_{\Lambda\pi,\Lambda\pi} + X(\Sigma|\Lambda\pi,\Lambda\pi)$$

$\lambda = \pm 1$

for $\lambda = 1$, $\delta R^{\Sigma}_{\Lambda\pi,\Lambda\pi} = \delta R^{Y*}_{\Lambda\pi,\Lambda\pi}$

XV)

$$\delta R^{Y*}_{\Xi K,\Lambda\pi} = -\frac{2}{3}\sqrt{\frac{2}{3}}\, \delta R^{\Xi}_{\Xi\pi,\Lambda\bar{K}} - \frac{1}{3}\sqrt{\frac{2}{3}}\, \delta R^{\Xi*}_{\Xi\pi,\Lambda\bar{K}} + X(Y*|\Xi K,\Lambda\pi)$$

$$\delta R^{\Xi*}_{\Xi\pi,\Lambda\bar{K}} = -\frac{2}{3}\sqrt{\frac{3}{2}}\, \delta R^{\Sigma}_{\Xi K,\Lambda\pi} - \frac{1}{3}\sqrt{\frac{3}{2}}\, \delta R^{Y*}_{\Xi K,\Lambda\pi} + X(\Xi*|\Xi\pi,\Lambda\bar{K})$$

$$\delta R^{\Sigma}_{\Xi K,\Lambda\pi} = \frac{1}{3}\sqrt{\frac{2}{3}}\, \delta R^{\Xi}_{\Xi\pi,\Lambda\bar{K}} - \frac{4}{3}\sqrt{\frac{2}{3}}\, \delta R^{\Xi*}_{\Xi\pi,\Lambda\bar{K}} + X(\Sigma|\Xi K,\Lambda\pi)$$

$$\delta R^{\Xi}_{\Xi\pi,\Lambda\bar{K}} = \frac{1}{3}\sqrt{\frac{3}{2}}\, \delta R^{\Sigma}_{\Xi K,\Lambda\pi} - \frac{4}{3}\sqrt{\frac{3}{2}}\, \delta R^{Y*}_{\Xi K,\Lambda\pi} + X(\Xi|\Xi\pi,\Lambda\bar{K})$$

$\lambda = 1, 1, -1, -1$

for $\lambda = 1$,
$$\delta R^{Y*}_{\Xi K,\Lambda\pi} = -\frac{2}{3}\sqrt{\frac{2}{3}}\, \delta R^{\Xi}_{\Xi\pi,\Lambda\bar{K}} - \frac{1}{3}\sqrt{\frac{2}{3}}\, \delta R^{\Xi*}_{\Xi\pi,\Lambda\bar{K}}$$

$$\delta R^{\Sigma}_{\Xi K,\Lambda\pi} = \frac{1}{3}\sqrt{\frac{2}{3}}\, \delta R^{\Xi}_{\Xi\pi,\Lambda\bar{K}} - \frac{4}{3}\sqrt{\frac{2}{3}}\, \delta R^{\Xi*}_{\Xi\pi,\Lambda\bar{K}}$$

Table 3 (continued)

XVI)

$$\delta R^{Y*}_{N\bar{k},\Lambda\pi} = \frac{2}{3}\sqrt{\frac{2}{3}}\ \delta R^{N}_{N\pi,\Lambda K} + X(Y*|N\bar{K},\Lambda\pi)$$

$$\delta R^{N}_{N\pi,\Lambda K} = -\frac{1}{3}\sqrt{\frac{3}{2}}\ \delta R^{\Sigma}_{N\bar{K},\Lambda\pi} + \frac{4}{3}\sqrt{\frac{3}{2}}\ \delta R^{Y*}_{N\bar{K},\Lambda\pi}$$

$$\delta R^{\Sigma}_{N\bar{K},\Lambda\pi} = -\frac{1}{3}\sqrt{\frac{2}{3}}\ \delta R^{N}_{N\pi,\Lambda K}$$

$\lambda = 1,\ -1,\ 0,\ 0$

for $\lambda = 1$,
$$\delta R^{Y*}_{N\bar{K},\Lambda\pi} = \frac{2}{3}\sqrt{\frac{2}{3}}\ \delta R^{N}_{N\pi,\Lambda K}$$

$$\delta R^{\Sigma}_{N\bar{K},\Lambda\pi} = -\frac{1}{3}\sqrt{\frac{2}{3}}\ \delta R^{N}_{N\pi,\Lambda K}$$

XVII)

$$\delta R^{Y*}_{\Xi K,\Xi K} = \frac{1}{6}\ \delta R^{\Omega}_{\Xi\bar{K},\Xi\bar{K}} + X(Y*|\Xi K,\Xi K)$$

$$\delta R^{\Omega}_{\Xi\bar{K},\Xi\bar{K}} = -\frac{1}{3}\ \delta R^{\Lambda}_{\Xi K,\Xi K} + \delta R^{\Sigma}_{\Xi K,\Xi K} + \frac{1}{2}\ \delta R^{Y*}_{\Xi K,\Xi K} + X(\Omega|\Xi\bar{K},\Xi\bar{K})$$

$$\delta R^{\Sigma}_{\Xi K,\Xi k} = \frac{2}{3}\ \delta R^{\Omega}_{\Xi\bar{K},\Xi\bar{K}} + X(\Sigma|\Xi K,\Xi K)$$

$$\delta R^{\Lambda}_{\Xi K,\Xi K} = -\frac{2}{3}\ \delta R^{\Omega}_{\Xi\bar{K},\Xi\bar{K}} + X(\Lambda|\Xi K,\Xi K)$$

$\lambda = \sqrt{\frac{35}{36}},\ -\sqrt{\frac{35}{36}},\ 0,\ 0$

for $\lambda = \sqrt{\frac{35}{36}} \approx .985$,

$$\delta R^{\Sigma}_{\Xi K,\Xi K} = \frac{2}{3}\sqrt{\frac{36}{35}}\ \delta R^{\Omega}_{\Xi\bar{K},\Xi\bar{K}}$$

$$\delta R^{\Lambda}_{\Xi K,\Xi K} = -\frac{2}{3}\sqrt{\frac{36}{35}}\ \delta R^{\Omega}_{\Xi\bar{K},\Xi\bar{K}}$$

$$\delta R^{Y*}_{\Xi K,\Xi K} = \frac{1}{6}\sqrt{\frac{36}{35}}\ \delta R^{\Omega}_{\Xi\bar{K},\Xi\bar{K}}$$

Table 3 (continued)

XVIII)

$$\delta R^{Y*}_{\Xi K, N\bar{K}} = -\frac{1}{3} \delta R^{\Sigma}_{\Xi K, N\bar{K}} - \frac{1}{6} \delta R^{Y*}_{\Xi K, N\bar{K}} - \frac{1}{3} \delta R^{\Lambda}_{\Xi K, N\bar{K}} + X(Y* | \Xi K, N\bar{K})$$

$$\delta R^{\Sigma}_{\Xi K, N\bar{K}} = \frac{1}{6} \delta R^{\Sigma}_{\Xi K, N\bar{K}} - \frac{2}{3} \delta R^{Y*}_{\Xi K, N\bar{K}} + \frac{1}{6} \delta R^{\Lambda}_{\Xi K, N\bar{K}} + X(\Sigma | \Xi K, N\bar{K})$$

$$\delta R^{\Lambda}_{\Xi K, N\bar{K}} = \frac{1}{2} \delta R^{\Sigma}_{\Xi K, N\bar{K}} - 2\delta R^{Y*}_{\Xi K, N\bar{K}} - \frac{1}{6} \delta R^{\Lambda}_{\Xi K, N\bar{K}} + X(\Lambda | \Xi K, N\bar{K})$$

$\lambda = 1, -1, -1/6$

for $\lambda = 1$,
$$\delta R^{\Sigma}_{\Xi K, N\bar{K}} = \frac{5}{9} \delta R^{\Lambda}_{\Xi K, N\bar{K}}$$

$$\delta R^{Y*}_{\Xi K, N\bar{K}} = -\frac{4}{9} \delta R^{\Lambda}_{\Xi K, N\bar{K}}$$

XIX)

$$\delta R^{\Xi*}_{\Xi \pi, \Xi \eta} = \frac{2}{3} \delta R^{\Xi}_{\Xi \pi, \Xi \eta} + \frac{1}{3} \delta R^{\Xi*}_{\Xi \pi, \Xi \eta} + X(\Xi* | \Xi \pi, \Xi \eta)$$

$$\delta R^{\Xi}_{\Xi \pi, \Xi \eta} = -\frac{1}{3} \delta R^{\Xi}_{\Xi \pi, \Xi \eta} + \frac{4}{3} \delta R^{\Xi*}_{\Xi \pi, \Xi \eta} + X(\Xi | \Xi \pi, \Xi \eta)$$

$\lambda = 1, -1$

for $\lambda = 1$,
$$\delta R^{\Xi}_{\Xi \pi, \Xi \eta} = \delta R^{\Xi*}_{\Xi \pi, \Xi \eta}$$

XX)

$$\delta R^{\Xi*}_{\Xi \eta, \Xi \eta} = \frac{2}{3} \delta R^{\Xi}_{\Xi \eta, \Xi \eta} + \frac{1}{3} \delta R^{\Xi*}_{\Xi \eta, \Xi \eta} + X(\Xi* | \Xi \eta, \Xi \eta)$$

$$\delta R^{\Xi}_{\Xi \eta, \Xi \eta} = -\frac{1}{3} \delta R^{\Xi}_{\Xi \eta, \Xi \eta} + \frac{4}{3} \delta R^{\Xi*}_{\Xi \eta, \Xi \eta} + X(\Xi | \Xi \eta, \Xi \eta)$$

$\lambda = \pm 1$

for $\lambda = 1$,
$$\delta R^{\Xi}_{\Xi \eta, \Xi \eta} = \delta R^{\Xi*}_{\Xi \eta, \Xi \eta}$$

Table 3 (continued)

XXI)

$$\delta R^{\Xi}_{\Xi\eta,\Lambda\bar{K}} = - - \frac{1}{3\sqrt{2}} \delta R^{\Lambda}_{\Xi K,\Lambda\eta} + X(\Xi|\Xi\eta,\Lambda\bar{K})$$

$$\delta R^{\Xi*}_{\Xi\eta,\Lambda\bar{K}} = \frac{2}{3\sqrt{2}} \delta R^{\Lambda}_{\Xi K,\Lambda\eta} + X(\Xi*|\Xi\eta,\Lambda\bar{K})$$

$$\delta R^{\Lambda}_{\Xi K,\Lambda\eta} = - \frac{\sqrt{2}}{3} \delta R^{\Xi}_{\Xi\eta,\Lambda\bar{K}} + \frac{4\sqrt{2}}{3} \delta R^{\Xi*}_{\Xi\eta,\Lambda\bar{K}} + X(\Lambda|\Xi K,\Lambda\eta)$$

$\lambda = 1, -1, 0$

for $\lambda = 1$, $\qquad \delta R^{\Xi}_{\Xi\eta,\Lambda\bar{K}} = - \frac{1}{3\sqrt{2}} \delta R^{\Lambda}_{\Xi K,\Lambda\eta}$

$$\delta R^{\Xi*}_{\Xi\eta,\Lambda\bar{K}} = \frac{2}{3\sqrt{2}} \delta R^{\Lambda}_{\Xi K,\Lambda\eta}$$

XXII)

$$\delta R^{\Xi*}_{\Lambda\bar{K},\Sigma\bar{K}} = - \frac{2}{3} \delta R^{N}_{\Lambda K,\Sigma K} + X(\Xi*|\Lambda\bar{K},\Sigma\bar{K})$$

$$\delta R^{N}_{\Lambda K,\Sigma K} = \frac{1}{3} \delta R^{\Xi}_{\Lambda\bar{K},\Sigma\bar{K}} - \frac{4}{3} \delta R^{\Xi*}_{\Lambda\bar{K},\Sigma\bar{K}} + X(N|\Lambda K,\Sigma K)$$

$$\delta R^{\Xi}_{\Lambda\bar{K},\Sigma\bar{K}} = \frac{1}{3} \delta R^{N}_{\Lambda K,\Sigma K} + X(\Xi|\Lambda\bar{K},\Sigma\bar{K})$$

$\lambda = 1, -1, 0$

for $\lambda = 1$, $\qquad \delta R^{\Xi}_{\Lambda\bar{K},\Sigma\bar{K}} = \frac{1}{3} \delta R^{N}_{\Lambda K,\Sigma K}$

$$\delta R^{\Xi*}_{\Lambda\bar{K},\Sigma\bar{K}} = - \frac{2}{3} \delta R^{N}_{\Lambda K,\Sigma K}$$

XXIII)

$$\delta R^{\Xi*}_{\Lambda\bar{K},\Lambda\bar{K}} = \frac{2}{3} \delta R^{N}_{\Lambda K,\Lambda K} + X(\Xi*|\Lambda\bar{K},\Lambda\bar{K})$$

$$\delta R^{N}_{\Lambda K,\Lambda K} = - \frac{1}{3} \delta R^{\Xi}_{\Lambda\bar{K},\Lambda\bar{K}} + \frac{4}{3} \delta R^{\Xi*}_{\Lambda\bar{K},\Lambda\bar{K}} + X(N|\Lambda K,\Lambda K)$$

$$\delta R^{\Xi}_{\Lambda\bar{K},\Lambda\bar{K}} = - \frac{1}{3} \delta R^{N}_{\Lambda K,\Lambda K} + X(\Xi|\Lambda\bar{K},\Lambda\bar{K})$$

$\lambda = 1, -1, 0$

Table 3 (continued)

for $\lambda = 1$,
$$\delta R^{\overline{\Xi}*}_{\Lambda\overline{K},\Lambda\overline{K}} = \frac{2}{3}\, \delta R^N_{\Lambda K,\Lambda K}$$

$$\delta R^{\overline{\Xi}}_{\Lambda\overline{K},\Lambda\overline{K}} = -\frac{1}{3}\, \delta R^N_{\Lambda K,\Lambda K}$$

XXIV)

$$\delta R^N_{N\eta,N\eta} = -\frac{1}{3}\; R^N_{N\eta,N\eta} + X(N\,|\,N\eta,N\eta)$$

$\lambda = -1/3$

XXV)

$$\delta R^N_{N\pi,N\eta} = -\frac{1}{3}\, \delta R^N_{N\pi,N\eta} + X(N\,|\,N\pi,N\eta)$$

$\lambda = -1/3$

XVI)

$$\delta R^N_{N\eta,\Lambda K} = \frac{1}{3}\sqrt{\frac{1}{2}}\; \delta R^{\Lambda}_{N\overline{K},\Lambda\eta} + X(N\,|\,N\eta,\Lambda K)$$

$$\delta R^{\Lambda}_{N\overline{K},\Lambda\eta} = \frac{\sqrt{2}}{3}\; \delta R^N_{N\eta,\Lambda K} + X(\Lambda\,|\,N\overline{K},\Lambda\eta)$$

$\lambda = \pm 1/3$

TABLE 4

PREFERRED EQUATIONS

$$\delta R^{N}_{N\pi, N\pi} = 2\delta R^{N*}_{N\pi, N\pi}$$

$$\delta R^{N}_{N\pi, \Sigma K} = - \delta R^{N*}_{N\pi, \Sigma K}$$

$$\delta R^{\Sigma}_{N\bar{K}, \Sigma\pi} = \frac{2}{3} \delta R^{N*}_{N\pi, \Sigma K}$$

$$\delta R^{\Lambda}_{\Sigma\pi, N\bar{K}} = \sqrt{6} \ \delta R^{N*}_{N\pi, \Sigma K}$$

$$\delta R^{\Xi}_{\Sigma\bar{K}, \Sigma\bar{K}} = 4 \ \delta R^{\Xi*}_{\Sigma\bar{K}, \Sigma\bar{K}}$$

$$\delta R^{\Sigma}_{\Sigma\pi, \Sigma\pi} = - .45 \ \delta R^{\Lambda}_{\Sigma\pi, \Sigma\pi}$$

$$\delta R^{Y*}_{\Sigma\pi, \Sigma\pi} = - .73 \ \delta R^{\Lambda}_{\Sigma\pi, \Sigma\pi}$$

$$\delta R^{\Sigma}_{\Sigma\eta, \Lambda\pi} = \frac{1}{3\sqrt{3}} \ \delta R^{\Lambda}_{\Sigma\pi, \Lambda\eta}$$

$$\delta R^{Y*}_{\Sigma\eta, \Lambda\pi} = - \frac{2}{3\sqrt{3}} \ \delta R^{\Lambda}_{\Sigma\pi, \Lambda\eta}$$

$$\delta R^{Y*}_{\Sigma\pi, \Sigma\eta} = \delta R^{\Sigma}_{\Sigma\pi, \Sigma\eta}$$

$$\delta R^{Y*}_{\Sigma\pi, \Lambda\pi} = - \frac{1}{2} \ \delta R^{\Sigma}_{\Sigma\pi, \Lambda\pi}$$

$$\delta R^{\Xi*}_{\Xi\pi, \Sigma\bar{K}} = - 2 \ \delta R^{\Xi}_{\Xi\pi, \Sigma\bar{K}}$$

$$\delta R^{\Sigma}_{\Xi K, \Sigma\pi} = - 2 \ \delta R^{\Xi}_{\Xi\pi, \Sigma K}$$

$$\delta R^{\Lambda}_{\Xi K, \Sigma\pi} = \sqrt{6} \ \delta R^{\Xi}_{\Xi\pi, \Sigma\bar{K}}$$

$$\delta R^{Y*}_{\Sigma\eta, \Sigma\eta} = \delta R^{\Sigma}_{\Sigma\eta, \Sigma\eta}$$

$$\delta R^{Y*}_{\Sigma\eta, \Xi\bar{K}} = - \frac{2}{3}\sqrt{\frac{2}{3}} \ \delta R^{\Xi}_{\Xi\eta, \Sigma\bar{K}} - \frac{1}{3}\sqrt{\frac{2}{3}} \ \delta R^{\Xi*}_{\Xi\eta, \Sigma\bar{K}}$$

$$\delta R^{\Sigma}_{\Sigma\eta, \Xi K} = \frac{1}{3}\sqrt{\frac{2}{3}} \ \delta R^{\Xi}_{\Xi\eta, \Sigma\bar{K}} - \frac{4}{3}\sqrt{\frac{2}{3}} \ \delta R^{\Xi*}_{\Xi\eta, \Sigma\bar{K}}$$

Table 4 (continued)

$$\delta R^{Y*}_{\Sigma\eta,N\bar{K}} = \frac{2}{3}\sqrt{\frac{2}{3}}\ \delta R^{N}_{\Sigma K,N\eta}$$

$$\delta R^{\Sigma}_{\Sigma\eta,N\bar{K}} = -\frac{1}{3}\sqrt{\frac{2}{3}}\ \delta R^{N}_{N\eta,\Sigma K}$$

$$\delta R^{\Sigma}_{\Lambda\pi,\Lambda\pi} = \delta R^{Y*}_{\Lambda\pi,\Lambda\pi}$$

$$\delta R^{Y*}_{\Xi K,\Lambda\pi} = -\frac{2}{3}\sqrt{\frac{2}{3}}\ \delta R^{\Xi}_{\Xi\pi,\Lambda\bar{K}} - \frac{1}{3}\sqrt{\frac{2}{3}}\ \delta R^{\Xi*}_{\Xi\pi,\Lambda\bar{K}}$$

$$\delta R^{\Sigma}_{\Xi K,\Lambda\pi} = \frac{1}{3}\sqrt{\frac{2}{3}}\ \delta R^{\Xi}_{\Xi\pi,\Lambda\bar{K}} - \frac{4}{3}\sqrt{\frac{2}{3}}\ \delta R^{\Xi*}_{\Xi\pi,\Lambda\bar{K}}$$

$$\delta R^{Y*}_{N\bar{K},\Lambda\pi} = \frac{2}{3}\sqrt{\frac{2}{3}}\ \delta R^{N}_{N\pi,\Lambda K}$$

$$\delta R^{\Sigma}_{N\bar{K},\Lambda\pi} = -\frac{1}{3}\sqrt{\frac{2}{3}}\ \delta R^{N}_{N\pi,\Lambda K}$$

$$\delta R^{\Sigma}_{\Xi K,\Xi K} = \frac{2}{3}\sqrt{\frac{36}{35}}\ \delta R^{\Omega}_{\Xi\bar{K},\Xi\bar{K}}$$

$$\delta R^{\Lambda}_{\Xi K,\Xi K} = -\frac{2}{3}\sqrt{\frac{36}{35}}\ \delta R^{\Omega}_{\Xi\bar{K},\Xi\bar{K}}$$

$$\delta R^{Y*}_{\Xi K,\Xi K} = \frac{1}{6}\sqrt{\frac{36}{35}}\ \delta R^{\Omega}_{\Xi\bar{K},\Xi\bar{K}}$$

$$\delta R^{\Sigma}_{\Xi K,N\bar{K}} = \frac{5}{9}\ \delta R^{\Lambda}_{\Xi K,N\bar{K}}$$

$$\delta R^{Y*}_{\Xi K,N\bar{K}} = -\frac{4}{9}\ \delta R^{\Lambda}_{\Xi K,N\bar{K}}$$

$$\delta R^{\Xi}_{\Xi\pi,\Xi\eta} = \delta R^{\Xi*}_{\Xi\pi,\Xi\eta}$$

$$\delta R^{\Xi}_{\Xi\eta,\Xi\eta} = \delta R^{\Xi*}_{\Xi\eta,\Xi\eta}$$

$$\delta R^{\Xi}_{\Xi\eta,\Lambda\bar{K}} = -\frac{1}{3\sqrt{2}}\ \delta R^{\Lambda}_{\Xi K,\Lambda\eta}$$

$$\delta R^{\Xi*}_{\Xi\eta,\Lambda\bar{K}} = \frac{2}{3\sqrt{2}}\ \delta R^{\Lambda}_{\Xi K,\Lambda\eta}$$

$$\delta R^{\Xi}_{\Lambda\bar{K},\Sigma\bar{K}} = \frac{1}{3}\ \delta R^{N}_{\Lambda K,\Sigma K}$$

$$\delta R^{\Xi*}_{\Lambda\bar{K},\Sigma\bar{K}} = -\frac{2}{3}\ \delta R^{N}_{\Lambda K,\Sigma K}$$

$$\delta R^{\Xi*}_{\Lambda\bar{K},\Lambda\bar{K}} = \frac{2}{3}\delta R^{N}_{\Lambda K,\Lambda K}$$

$$\delta R^{\Xi}_{\Lambda\bar{K},\Lambda\bar{K}} = -\frac{1}{3}\ \delta R^{N}_{\Lambda K,\Lambda K}$$

Note concerning Table 4

In order to simplify computation, some of the preferred equations were excluded in the preparation of Table 4. These equations related decuplet couplings to themselves or baryon couplings to themselves. Since the problem is overdetermined, one would expect a valid solution to be insensitive to the exclusion of a small number of constraints. Of course, at the expense of greater complication in computation, these equations could have been included, but it is felt that the results would have been substantially the same. We have tabulated below a test of the consistency of the excluded equations using the couplings obtained in our calculation.

Equation	LHS	RHS
$\delta R^{Y*}_{\Sigma\pi, N\overline{K}} = \frac{2}{3} \, \delta R^{N*}_{N\pi, \Sigma K}$	$-.021$	$-.020$
$\delta R^{N}_{\Sigma K, \Sigma K} = 0$	$-.36$	$-.28$
$\delta R^{N*}_{\Sigma K, \Sigma K} = \frac{3}{\sqrt{2}} \, \delta R^{\Xi*}_{\Sigma\overline{K}, \Sigma\overline{K}}$	$-.127$	$-.106$
$\delta R^{Y*}_{\Xi\overline{K}, \Sigma\pi} = 0$	$.050$	$.083$
$\delta R^{Y*}_{\Xi K, \Xi K} = \frac{1}{6}\sqrt{\frac{36}{36}} \, \delta R^{\Omega}_{\Xi\overline{K}, \Xi\overline{K}}$	$-.040$	$-.023$

TABLE 5

RESIDUES BEFORE AND AFTER IMPOSITION OF FACTORIZATION ON
THE RESIDUE MATRICES OBTAINED IN THIS CALCULATION

I) N Residue Matrix

Eigenvalues: 1.81, .053, .0025, -4×10^{-5}.

Before Imposition of Factorization

	$N\pi$	ΣK	$N\eta$	ΛK
$N\pi$	1.487	.3280	-.08628	.5945
ΣK	.3280	.1282	-.02069	.1328
$N\eta$	-.08628	-.02069	.005015	-.03457
ΛK	.5945	.1328	-.03457	.2406

After Imposition of Factorization

	$N\pi$	ΣK	$N\eta$	ΛK
$N\pi$	1.484	.3385	-.08647	.5948
ΣK	.3385	.07722	-.01972	.1357
$N\eta$	-.08647	-.01972	.005037	-.03465
ΛK	.5948	.1357	-.03465	.2383

Table 5 (continued)

II) Λ Residue Matrix

Eigenvalues: 1.15, .093, .0002, -.0018

Before Imposition of Factorization

	N$\bar{\text{K}}$	$\Sigma\pi$	ΞK	$\Lambda\eta$
N$\bar{\text{K}}$	.4875	-.4950	.04925	-.2730
$\Sigma\pi$	-.4950	.5020	-.05435	.2781
ΞK	.04925	-.05435	.09780	-.02004
$\Lambda\eta$	-.2730	.2781	-.02004	.1529

After Imposition of Factorization

	N$\bar{\text{K}}$	$\Sigma\pi$	ΞK	$\Lambda\eta$
N$\bar{\text{K}}$	.4872	-.4949	.05364	-.2729
$\Sigma\pi$	-.4949	.5027	-.05448	.2772
ΞK	.05364	-.05448	.005905	-.03004
$\Lambda\eta$	-.2729	.2772	-.03004	.1529

Table 5 (continued)

III) Σ Residue Matrix

Eigenvalues: 1.006, .036, .005, -.005, -.03

Before Imposition of Factorization

	N$\bar{\text{K}}$	$\Sigma\pi$	$\Sigma\eta$	ΞK	$\Lambda\pi$
N$\bar{\text{K}}$	.1203	-.1327	-.1133	.2094	-.1797
$\Sigma\pi$	-.1327	.1318	.1085	-.2435	.2041
$\Sigma\eta$	-.1133	.1085	.09024	-.1933	.1575
ΞK	.2094	-.2435	-.1933	.3606	-.3047
$\Lambda\pi$	-.1797	.2041	.1575	-.3047	.3088

After Imposition of Factorization

	N$\bar{\text{K}}$	$\Sigma\pi$	$\Sigma\eta$	ΞK	$\Lambda\pi$
N$\bar{\text{K}}$	.1203	-.1327	-.1064	.2083	-.1849
$\Sigma\pi$	-.1327	.1463	.1173	-.2298	.2040
$\Sigma\eta$	-.1064	.1173	.09410	-.1842	.1636
ΞK	.2083	-.2298	-.1842	.3607	-.3203
$\Lambda\pi$	-.1849	.2040	.1636	-.3203	.2844

Table 5 (continued)

IV) Ξ Residue Matrix

Eigenvalues: .79, +.03, -9 x 10^{-6}, -.02

Before Imposition of Factorization

	$\Sigma\bar{K}$	$\Xi\pi$	$\Xi\eta$	$\Lambda\bar{K}$
$\Sigma\bar{K}$	.4907	.2884	-.2462	.02339
$\Xi\pi$	.2884	.1716	-.1533	.01438
$\Xi\eta$	-.2462	-.1533	.1583	-.01614
$\Lambda\bar{K}$	.02339	.01438	-.01614	-.01663

After Imposition of Factorization

	$\Sigma\bar{K}$	$\Xi\pi$	$\Xi\eta$	$\Lambda\bar{K}$
$\Sigma\bar{K}$	.4846	.2884	-.2576	.02422
$\Xi\pi$	.2884	.1717	-.1533	.01441
$\Xi\eta$	-.2576	-.1533	.1370	-.01288
$\Lambda\bar{K}$	.02422	.01441	-0.01288	.001210

TABLE 6

COUPLING CONSTANTS

Coupling	SU_3 Limit	DDFS Calculation	This Calculation
$N \rightarrow N\pi$	-.83	-1.28	-1.22
$N \rightarrow \Sigma K$	-.36	-.36	-.28
$N \rightarrow N\eta$	.037	.025	.071
$N \rightarrow \Lambda K$	-.43	-.47	-.49
$\Lambda \rightarrow N\bar{K}$	.61	.66	.70
$\Lambda \rightarrow \Sigma\pi$	-.69	-.86	-.71
$\Lambda \rightarrow \Xi K$	.052	.071	.077
$\Lambda \rightarrow \Lambda\eta$	-.40	-.34	-.39
$\Xi \rightarrow \Sigma\bar{K}$	.83	.60	.70
$\Xi \rightarrow \Xi\pi$	.36	.36	.41
$\Xi \rightarrow \Xi\eta$	-.43	-.26	-.37
$\Xi \rightarrow \Lambda\bar{K}$	.037	.050	.035
$N^* \rightarrow N\pi$	.50	.88	.80
$N^* \rightarrow \Sigma K$	-.50	-.28	-.35
$Y^* \rightarrow \Sigma\pi$	-.29	-.28	-.24
$Y^* \rightarrow \Lambda\pi$	.35	.53 (input)	.53 (input)
$Y^* \rightarrow \Sigma\eta$	-.35	-.18	-.24
$Y^* \rightarrow N\bar{K}$	.29	.43	.44
$Y^* \rightarrow \Xi K$	-.29	-.16	-.21
$\Sigma \rightarrow \Sigma\pi$	.38	.42	.38
$\Sigma \rightarrow \Lambda\pi$	.40	.50	.53
$\Sigma \rightarrow \Sigma\eta$	.40	.25	.31
$\Sigma \rightarrow N\bar{K}$	-.29	-.29	-.35
$\Sigma \rightarrow \Xi K$	-.68	-.49	-.60

Table 6 (continued)

Coupling	SU_3 Limit	DDFS Calculation	This Calculation
$\Xi^* \to \Xi\pi$	.35	.34 (input)	.40
$\Xi^* \to \Sigma\bar{K}$	-.35	-.24	-.27
$\Xi^* \to \Lambda\bar{K}$	.35	.43	.40
$\Xi^* \to \Xi\eta$	-.35	-.18	-.31
$\Omega \to \Xi\bar{K}$	-.71	-.49	-.60

TABLE 7

A COMPARISON OF THE THEORETICAL CHARGE CONJUGATION BEHAVIOR
OF COUPLINGS WITH THE BEHAVIOR OBTAINED IN THIS CALCULATION

Ratio	Theory	This Calculation
$g_{N\Sigma K}/g_{\Sigma N\bar{K}}$	1.23	$(-.28\ )/(-.35\ ) = \ .80$
$g_{N\Lambda K}/g_{\Lambda N\bar{K}}$	-.709	$(-.49\ )/(\ .70)) = -.70$
$g_{\Sigma\Lambda\pi}/g_{\Lambda\Sigma\pi}$	-.576	$(\ .53\ )/(-.71\ ) = -.75$
$g_{\Lambda\Xi K}/g_{\Xi\Lambda\bar{K}}$	1.41	$(\ .077)/(\ .035) = 2.2$
$g_{\Sigma\Xi K}/g_{\Xi\Sigma\bar{K}}$	-.817	$(-.60\ )/(\ .70\ ) = -.86$

TABLE 8

THE CONSISTENCY OF THE MASS EQUATIONS, USING THE COUPLINGS OBTAINED IN OUR CALCULATION

Particle	Input Mass (MeV)	Output Mass (MeV)	Output Mass, Using Modified Crossing Matrix (MeV)
N	939	811	808
Σ	1193	1213	1204
Ξ	1320	1414	1348
N^*	1238	1193	1171
Y^*	1385	1421	1411
Ξ^*	1530	1648	1597
Ω	1685	1799	1755
Λ	1115	1184	1147

Figure 1a: COMPLETELY ELASTIC RESONANCE
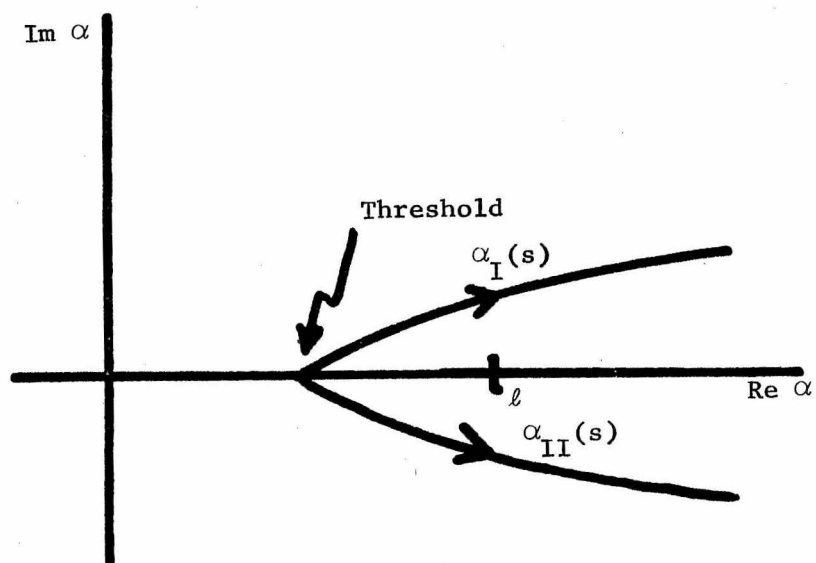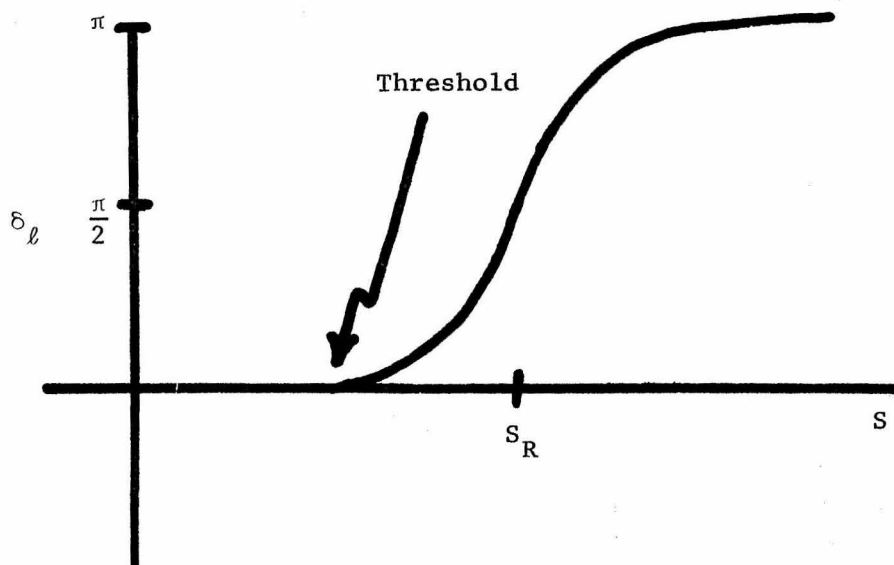
Pole and Zero trajectories in the complex plane.

Phase shift as a function of energy for the given pole

and zero trajectories. Re $\alpha_I (S_R)$ = Re $\alpha_{II} (S_R)$ = ℓ

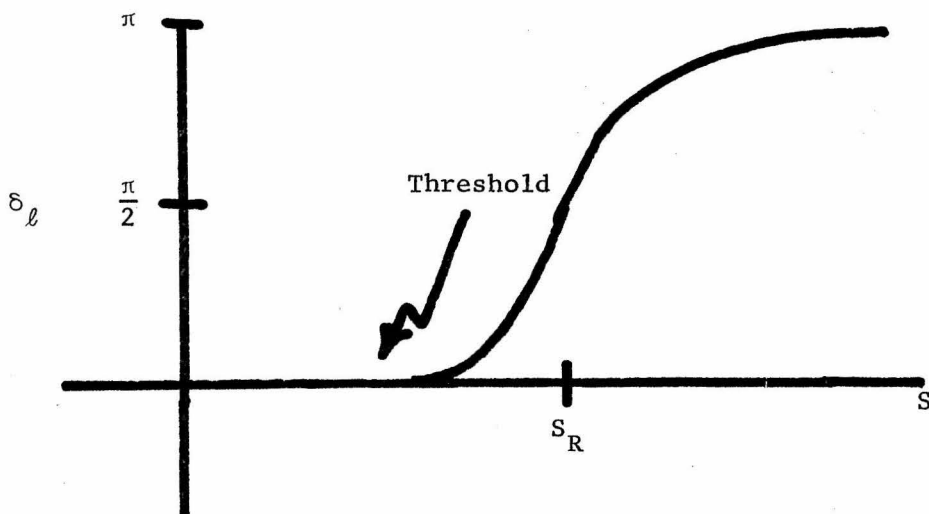Figure 1a (continued)
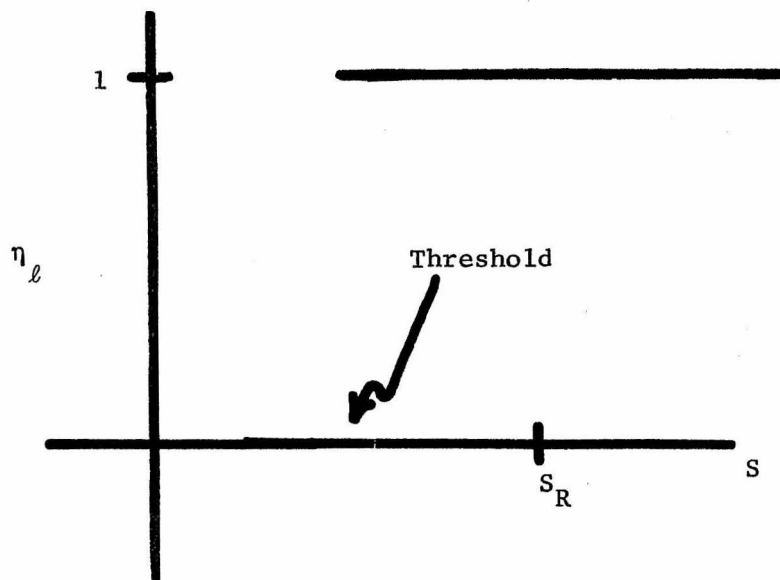
Elasticity as a function of energy for the given pole and zero trajectories.

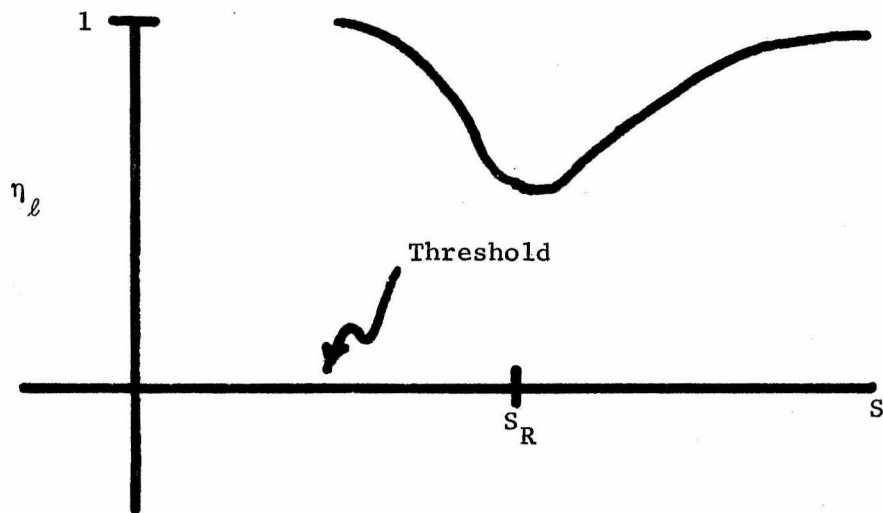<u>Figure 1b:</u>   SLIGHTLY INELASTIC RESONANCE
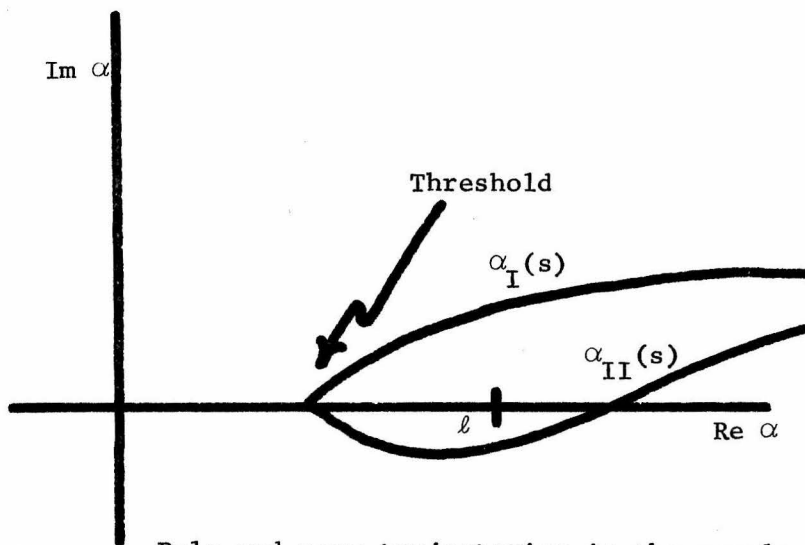
Pole and zero trajectories in the complex plane.

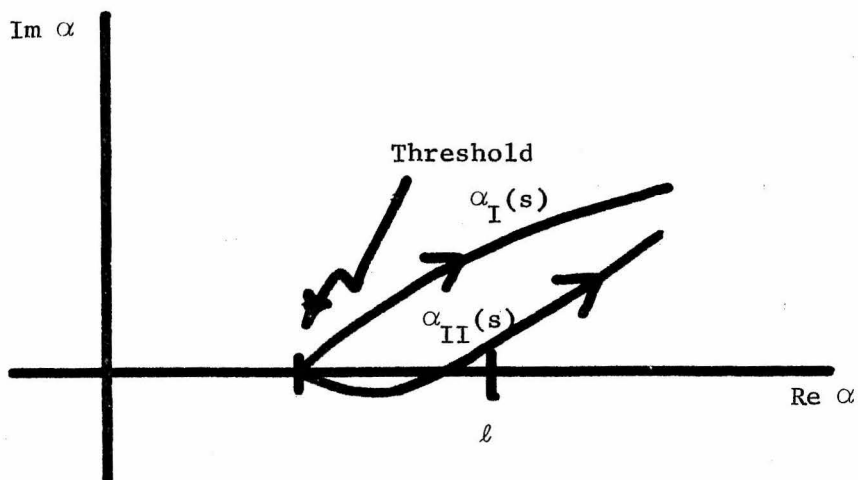Phase shift as a function of energy for the given

and zero trajectories. $Re \, \alpha_I(S_R) = Re \, \alpha_{II}(S_R) = \ell$
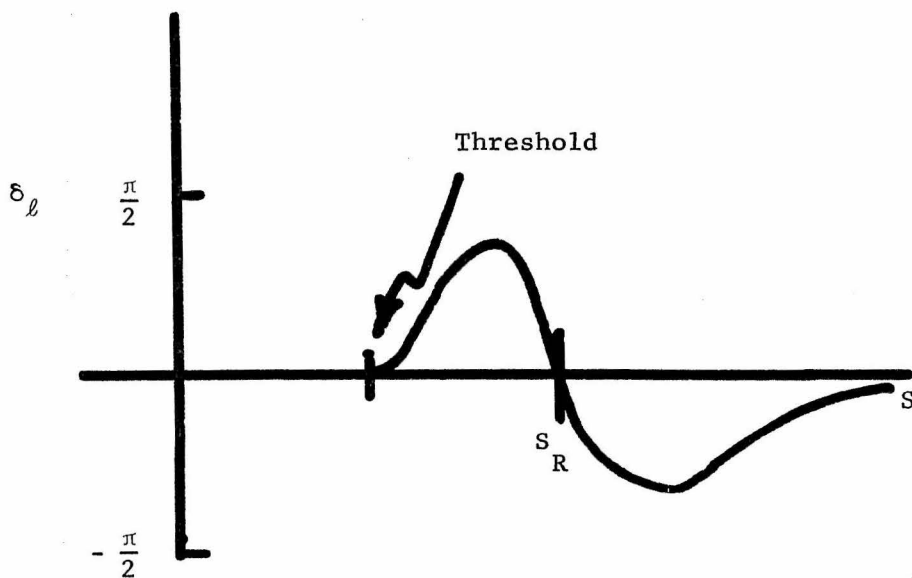
Figure 1b (continued)

Elasticity as a function of energy for the given pole

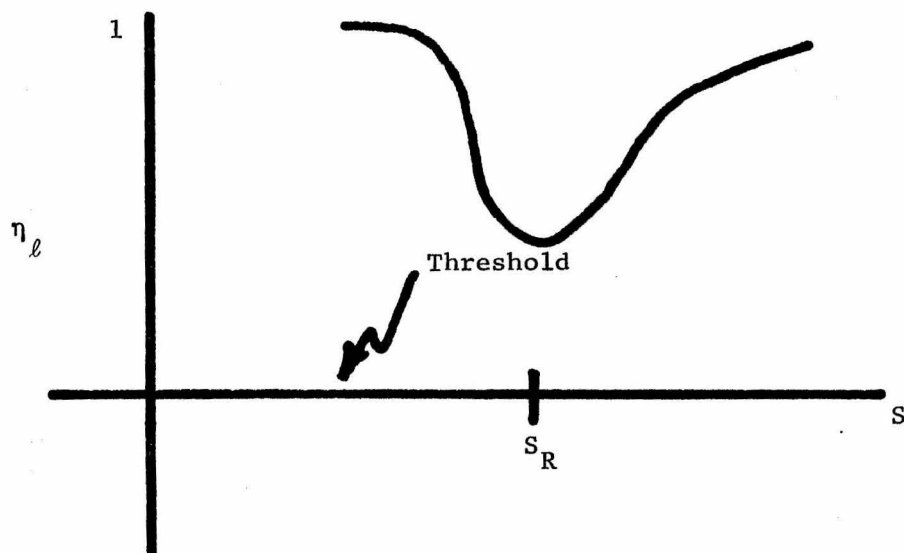and zero trajectories.

Figure 1c: VERY INELASTIC RESONANCE

Pole and zero trajectories in the complex plane.

Phase shift as a function of energy for the given pole and zero trajectories. $\mathrm{Re}\,\alpha_I(S_R) = \mathrm{Re}\,\alpha_{II}(S_R) = \ell$.

Figure 1c: (continued)

Elasticity as a function of energy for the given pole and zero trajectories.

Figure 2: SCHEMATIC REGGE TRAJECTORIES WHICH ACCOUNT FOR
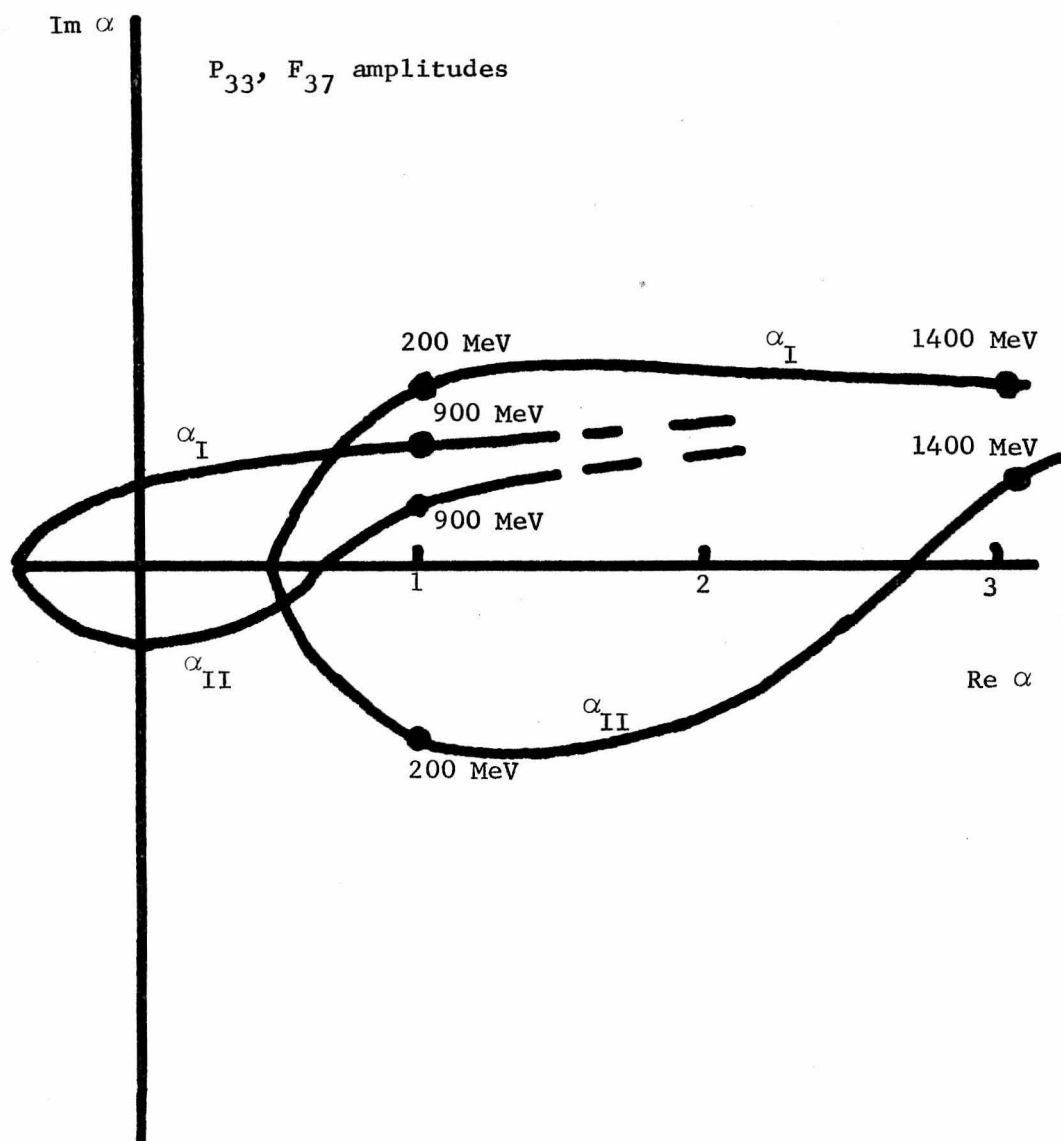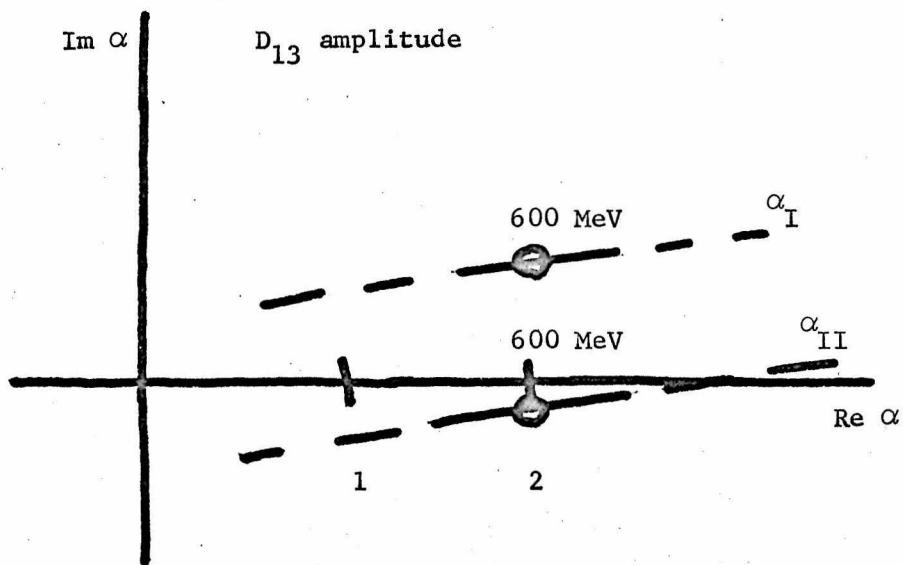SOME OF THE LOW ENERGY Nπ PHASE SHIFT RESULTS

Figure 2 (Continued)

Figure 3: $y = \text{Log} \dfrac{a_\ell(s)}{a_0(s)}$ versus $x = \ell \sqrt{2a}$ where $a_\ell(s)$ is the ℓth partial wave amplitude for $s^{\alpha(0)} + t\alpha'(0)$ and $a = 2\, q_s^2\, \alpha'(0)\, \text{Log}\,(s)$. $(S \gg 0.)$

$y \sim \text{const.}\ x^2$

$y \sim -1-2(x-1)$
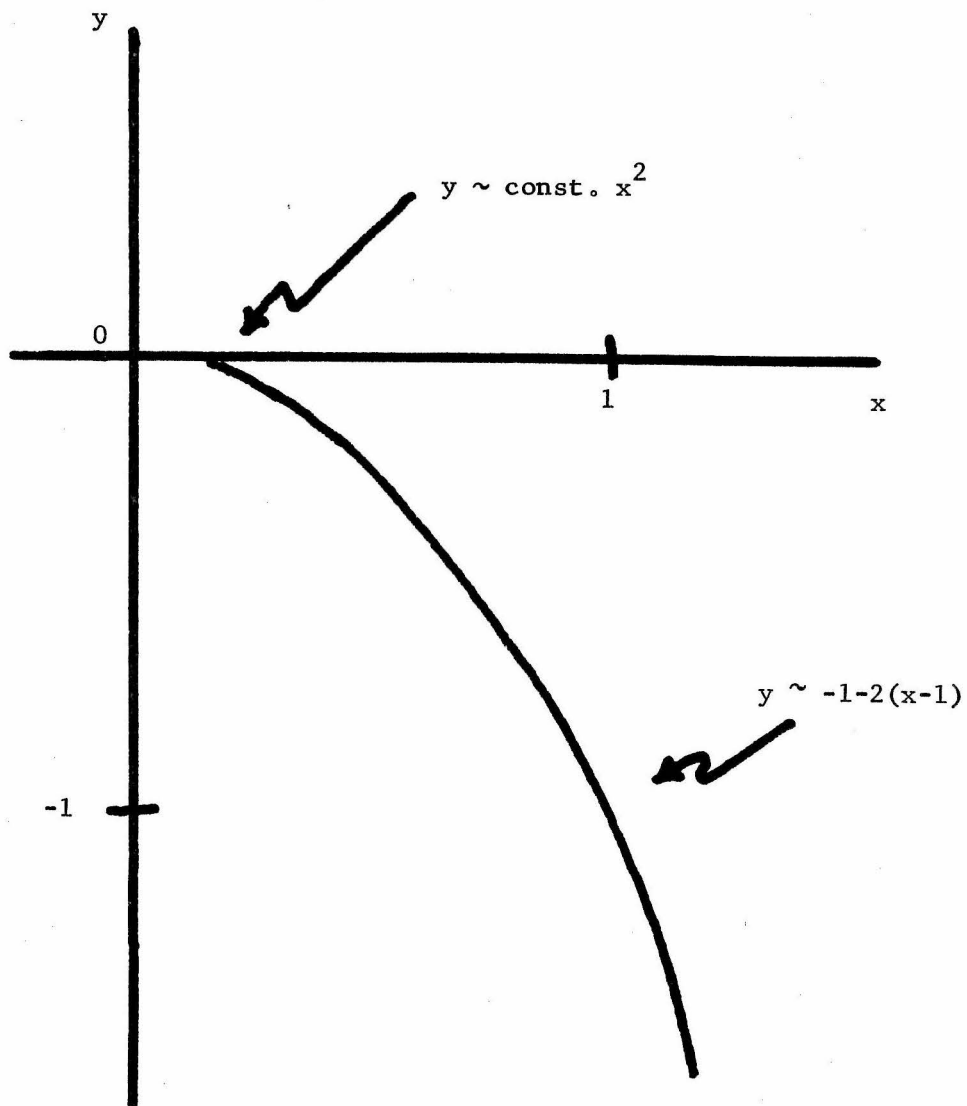
Figure 4: The complex ℓ-plane for an idealized Reggeized

amplitude

Im ℓ

Regge poles and cuts (Regge zeros not shown)

There can be Regge poles out here, but they will be very decoupled.

L( )

Re ℓ

Highly inelastic scattering: $a_\ell \cong -\dfrac{1}{2_i K(s)}$

Elastic scattering: behavior of a_ℓ dictated by cut structure in the crossed channel.

$$a_\ell(s) \sim O(e^{-\ell \xi}/\sqrt{\ell})$$

$$\ell \to \infty$$
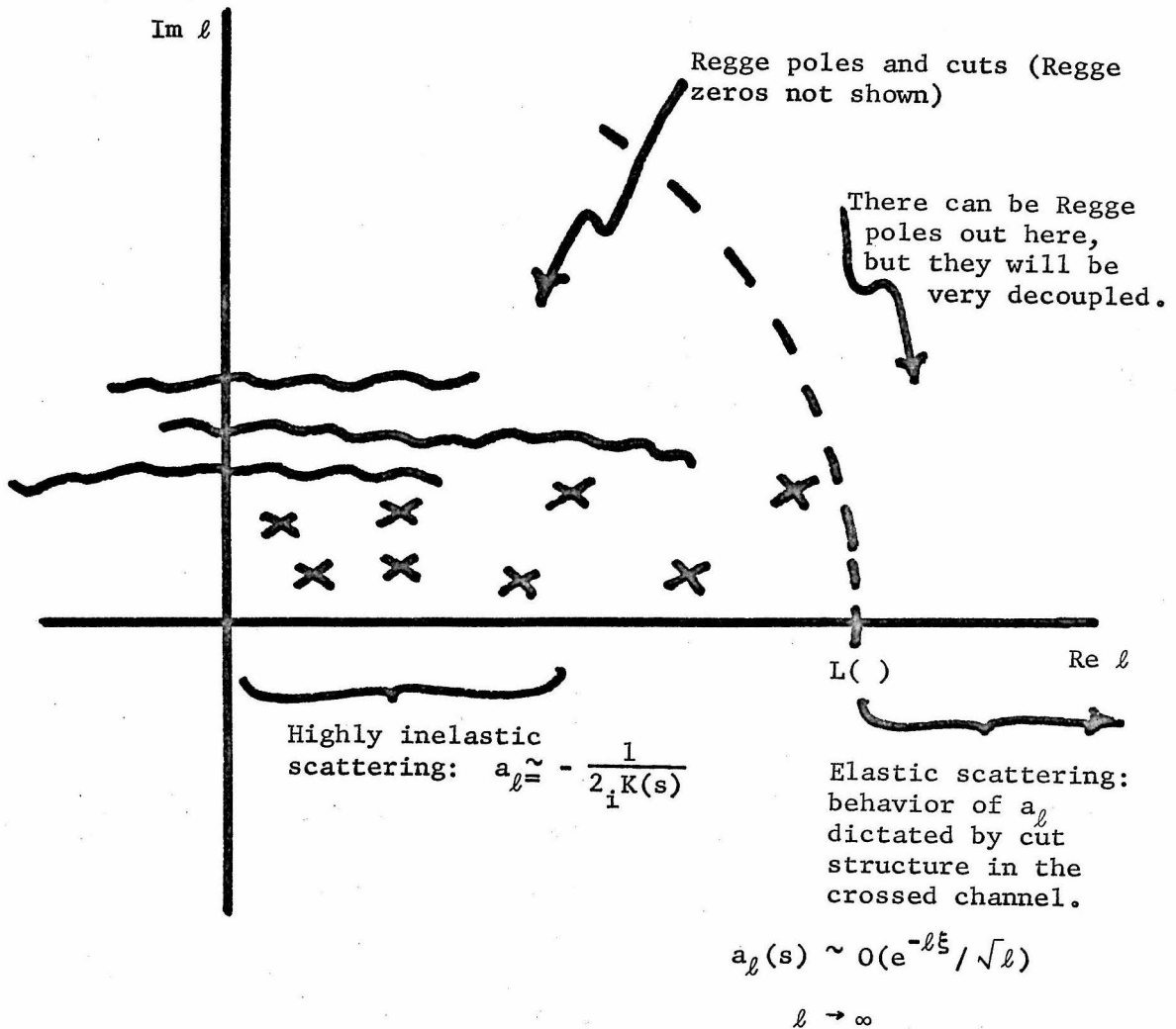
$$\text{Log} \ \frac{L(s)}{\sqrt{s}} \underset{s \to \infty}{\sim} 1$$

<u>Figure 5</u>:   (Following Page)

Using the Cheng representation, a typical scattering cross

section, computed using an infinite number of evenly spaced

Regge trajectories, is compared with cross sections computing

using various finite numbers of Regge trajectories, evenly

spaced below the same leading trajectory.

DIFFERENTIAL CROSS SECTION (arbitrary units)

Cos θ

———— : Infinite number of Regge poles.

O : One Regge pole.

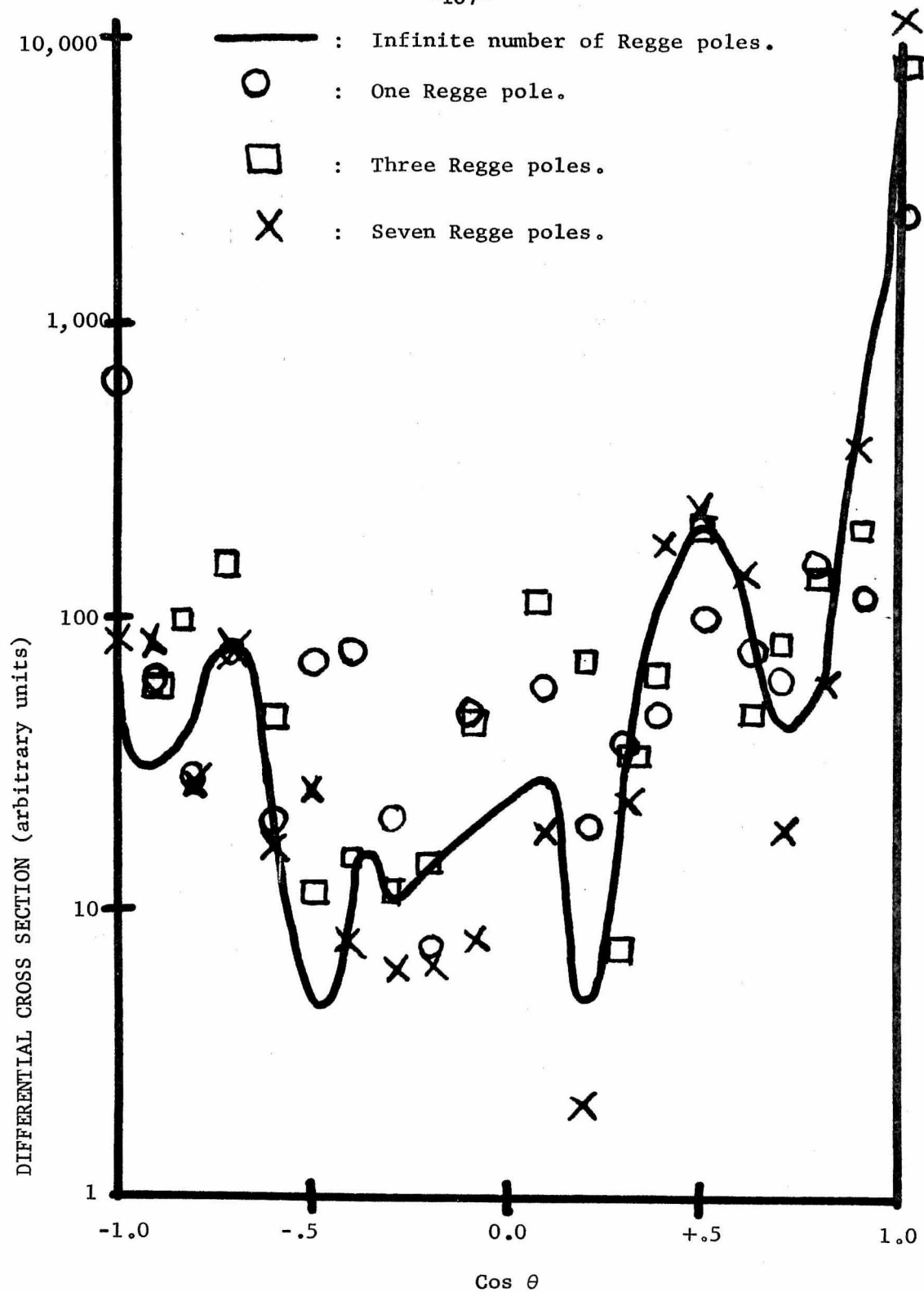☐ : Three Regge poles.

✕ : Seven Regge poles.

Figure 6:   (Following Page)

Expanded view of forward peak for a typical infinite
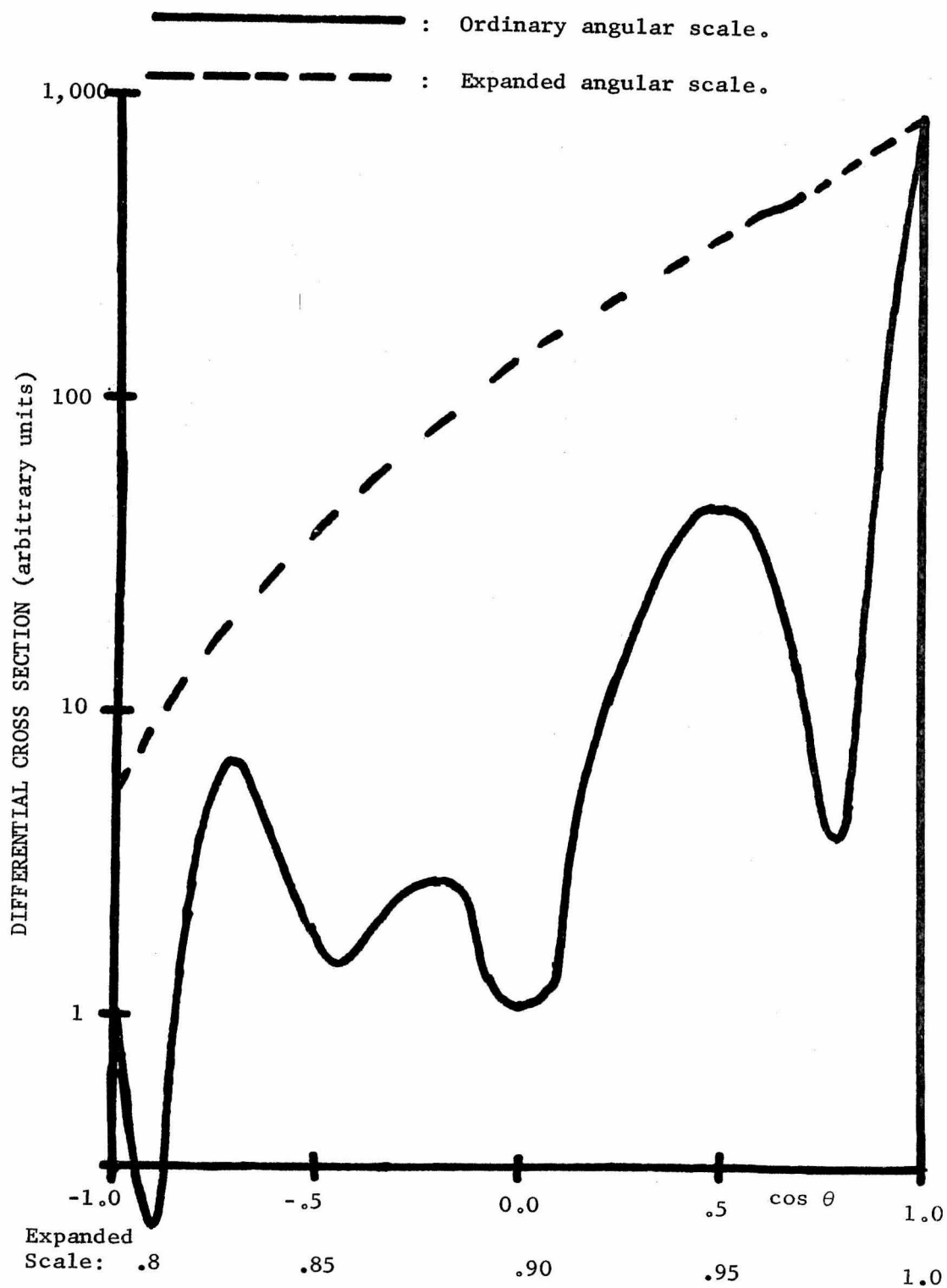
trajectory cross section.

Figure 7: Perspective sketch of the complex s-plane, showing where a Regge pole trajectory and its corresponding zero trajectory, are evaluated, for rising energies, when there are inelastic thresholds.

$\alpha_I(s) = \alpha(s_I)$

$\alpha_{II}(s) = \alpha(s_{II})$

Im S

S_I

S_{II}

Re S

Elastic Threshold

First inelastic threshold
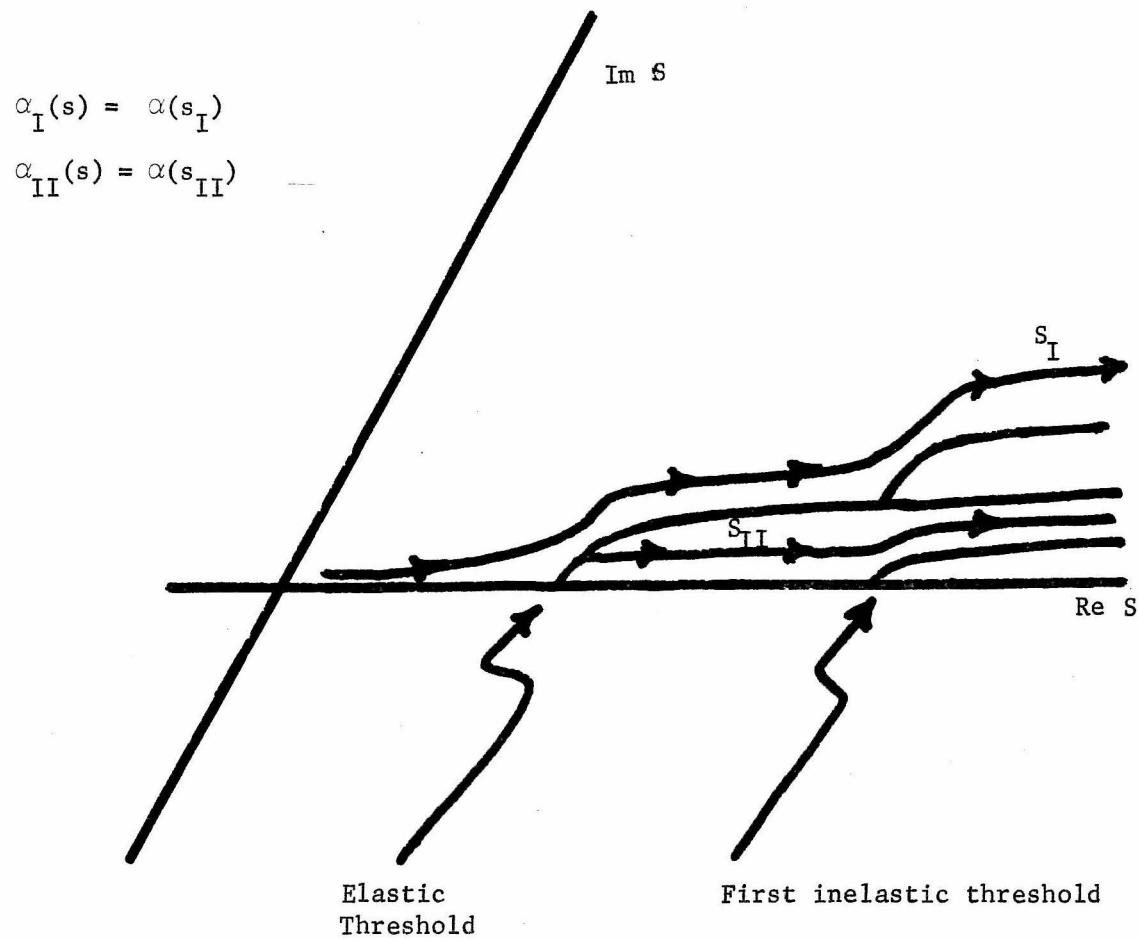
Figure 7 (continued): Path of integration in a Cheng-like representation for elastic scattering.

$$\text{Log } S_\ell = \int_{\alpha_I(s)}^{\alpha_{II}(s)} G_\ell(\lambda) = \int_{S_{II}}^{S_I} F_\ell(s) \, ds$$

Around elastic branch point.

Figure 7 (continued):   Path of integration in a Cheng-like representation for energies above inelastic threshold.

$$\text{Log } S_\ell = \int_{S_I}^{S_{II}} F_\ell(s)\,ds = \int_{S_I}^{S_{III}} F_\ell(s)\,ds + \int_{S_{III}}^{S_{II}} F_\ell(s)\,ds = \int_{\alpha_I}^{\alpha_{III}} \overset{\text{inel.}}{G_\ell(\lambda)d\lambda} + \int_{\alpha_{III}}^{\alpha_{II}} \overset{\text{el.}}{G_\ell(\lambda)d\lambda}$$
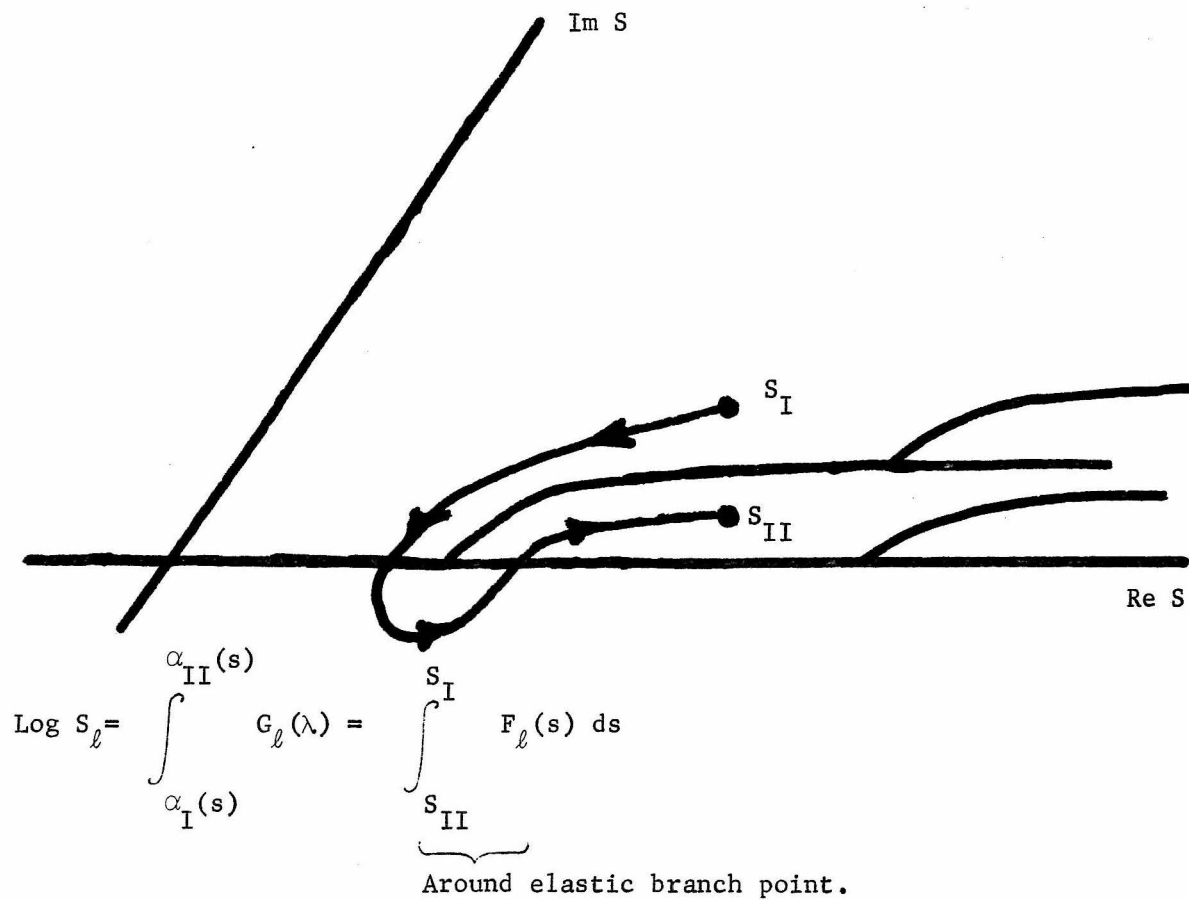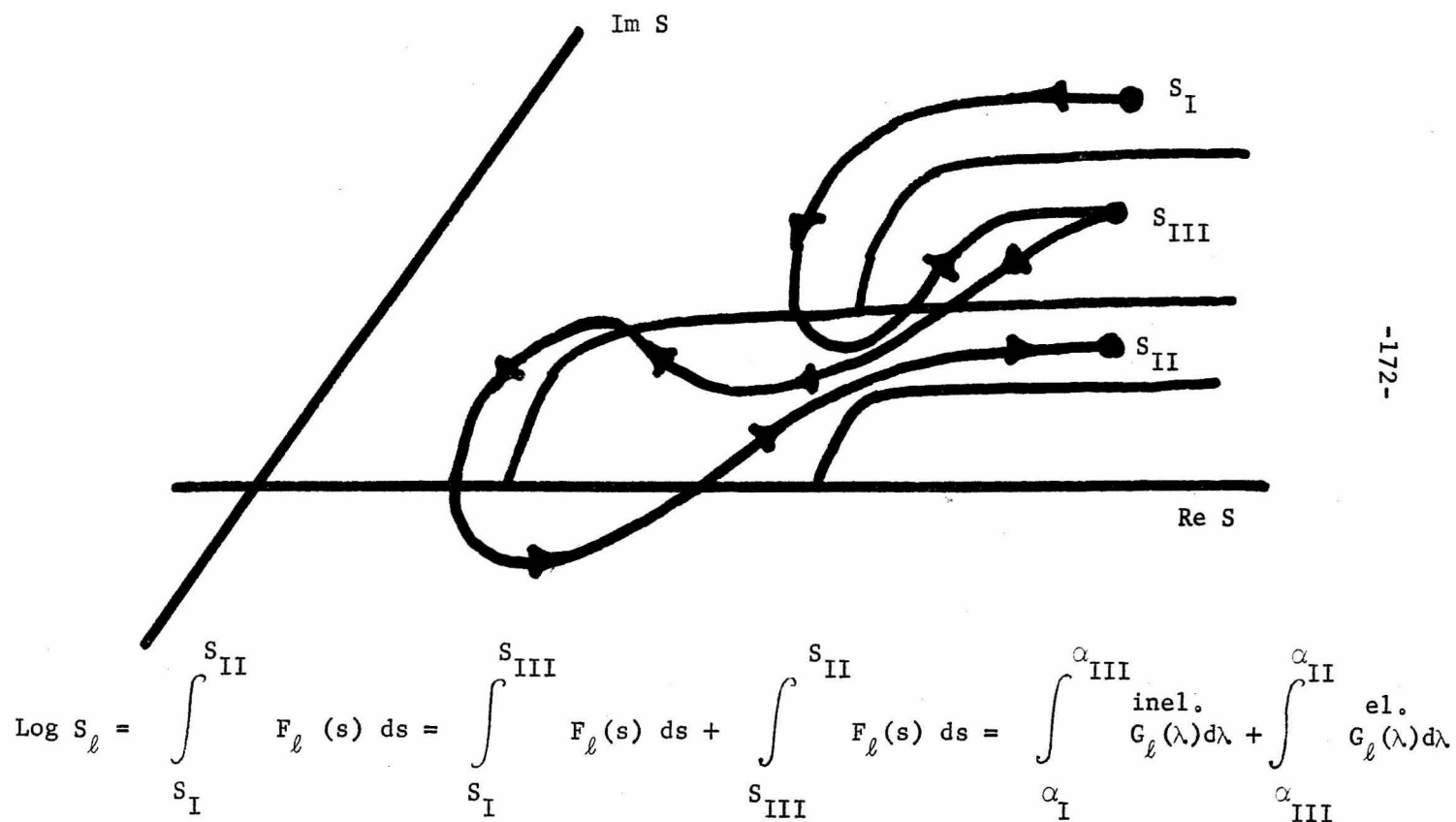
REFERENCES

1. R.F. Dashen, Y. Dothan, S.C. Frautschi, and D. Sharp, Phys. Rev. 143, 1185 (1966) and Phys. Rev. 151, 1127 (1966). These two papers will henceforth be referred to as DDFS.

2. R.F. Dashen et al., Phys. Rev. 151, 1127 (1966) contains a discussion of such a model, as well as references to other papers.

3. The following discussion is patterned after R.F. Dashen and S.C. Frautschi, Phys. Rev. 135, B1190 (1964), and Phys. Rev. 137, B1318 (1965). We extend the discussion of Dashen and Frautschi to include effects in all orders of the perturbation.

4. We neglect any distinctions between bound states and resonances. In a more precise calculation, our formulation would have to be modified at this point.

5. DDFS investigated this question in more detail than we will consider here.

6. J.K. Kim (Phys. Rev. Letters 19, 1074 (1967)) has argued that experimental results are consistent within present statistics with baryon-baryon-pseudoscalar couplings obtained in the SU_3 limit. This conclusion is based on a determination of $g^2_{p\Lambda K}$ and $g^2_{p\Sigma^o K}$, wherein the value of $g^2_{p\Lambda K}$ is found to be larger than previous estimates. Our results (see Table 6) are consistent with Kim's values for $g^2_{N\Sigma K}$ but not with his value of $g^2_{N\Lambda K}$, where we find $g^2_{N\Lambda K}$ lower by a factor of 7 ± 1, approximately. Since our calculation began with an SU_3-symmetric solution having a different $F/(F + D)$ ratio ($f = .28$ vs. Kim's $f = 0.41 \pm .07$);

it might be argued that strict comparison is difficult, since
the broken-symmetry solution is a function of the underlying
symmetric solution.

7. R. Slansky, Phys. Rev. <u>162</u>, 1627 (1967), for example, found that
    the right-hand cut made a significant contribution to mass-
    shifts in an orthodox N/D calculation.

8. P.G. Federbush, M.T. Grisaru, and M. Tausner, Annals of Physics,
    <u>18</u>, 40 (1962).

9. In some cases (see Table 3) a matrix had two unit eigenvalues.
    The "enhanced" vector was then taken to be a linear combination
    of the two eigenvectors. In a few other cases, a matrix had
    one eigenvalue exactly equal to one, and another eigenvalue
    nearly equal to one. In these cases, we used only the eigen-
    vector corresponding to the unit eigenvalue. It might be ar-
    gued that X contains unknown terms in δR which might change
    the eigenvalues slightly; in this case, we could have construc-
    ted a linear combination of the two eigenvectors and determined
    the relative mixing by our optimization procedure, just as we
    did for the exactly degenerate case.

10. For a discussion of the applications of this technique to prob-
    lems of classical physics, see Arnold Sommerfeld, <u>Partial Dif-
    ferential Equations in Physics</u> (Academic Press, New York 1964),
    page 282.

11. For a discussion of this problem , as well as reference to other
    works, see R.G. Newton, <u>The Complex j-Plane</u> (W.A. Benjamin,
    Inc., New York, 1964), pp. 114-120.

12. Amplitudes with both t-channel and u-channel cuts can be represented by separately Reggeizing the two sets of partial wave states of different signature.

13. E.W. Hobson, Spherical and Ellipsoidal Harmonics (Chelsea, New York, 1965), page 305.

14. N.N. Khuri, Phys. Rev. 130, 429 (1963).

15. Hung Cheng and Tai Tsun, Phys. Rev. 144, 1232 (1966).

16. N.N. Khuri, op. cit.

17. This fact was noted by Hung Cheng and Tai Tsun, op. cit., and S. Mandelstam, Annals of Physics 19, 254 (1962).

18. Earlier investigations of product representations were made by B.P. Desai and R.G. Newton, Phys. Rev. 129, 1445 (1963), by Hung Cheng, Phys. Rev. 144, 1237 (1966), and by W.J. Abbe, P. Kaus, P. Nath, and Y.N. Srivastava, Phys. Rev. 140, B1595 (1965).

19. E.W. Hobson, op. cit., page 364.

20. Ibid., page 37.

21. Blankenbecler, Goldberger, Khuri and Treiman, Annals of Physics 10, 69 (1960).

22. E.W. Hobson, op. cit., pagr 60.

22a. G.H. Hardy, Divergent Series (University Press, Oxford 1949).

23. Daniel Shanks, J. Math. and Physics 34, 1 (1955).

24. A. Erdelyi, ed. Higher Transcendental Functions, Vol. 1 (McGraw-Hill, New York, 1953), page 167.

25. P. Wynn, Mathematical Tables and Other Aids to Computation 10, 91 (1956). Note that Wynn's notation differs slightly from Shank's.

26. Dr. Peter Kaus has informed the author that he has also noticed this interpretation of phase shift behavior in terms of Regge-pole trajectories.

27. C. Lovelace, Rapporteur's Talk at the 1967 Heidelberg Conference, CERN Preprint TH. 837 (1967).

27a. γ is the Euler-Mascheroni constant and A is some small positive number.

28. M. Abramowitz and I.A. Stegun, eds., <u>Handbook of Mathematical Functions</u> (Dover, New York, 1965), eq. 10.2.36, page 445.

29. G.N. Watson, <u>A Treatise on the Theory of Bessel Functions</u> (Cambridge University Press, 1966), page 181.

30. M. Abramowitz and I.A. Stegun, <u>op. cit</u>., pp. 295-329.

31. A. Erdelyi, <u>op. cit</u>., page 156.

32. M. Abramowitz and I.A. Stegun, <u>op. cit</u>., eq. 9.7.1, page 377.

33. <u>Ibid</u>., eq. 9.7.7., page 378.

34. For example, by considering the uniform asymptotic expansion for large orders, making the replacement $a = \nu z$, holding a fixed and allowing ν to increase.

35. E.W. Hobson, <u>op. cit</u>., page 407.

36. If one attributes the forward peak in t to exponential behavior in the Reggeized couplings (as is sometimes believed to be the case in exchanges involving the Pomeranchon, which some people believe to have flat trajectory) then our argument is modified in a nonessential way: $\alpha'(0)$ log s is replaced by the coefficient of t in the exponential.

37. See, for example, V. Barger, Review paper presented at the CERN

Topical Conference on High-Energy Collisions of Hadrons, January, 1968, Figure 17. Our discussion would seem to indicate that pp scattering has trajectories not associated with easily identified resonances. In our original product representation, we allowed explicit poles in ℓ associated with multiplicative factors $\exp(\varphi_n(\ell,s))$, as well as an over-all multiplicative factor $\exp(G(\ell,s))$. This latter factor could be used to account for some of the behavior of the amplitude above inelastic threshold, and would contain terms due to Regge cuts, Regge poles not explicitly included, and background effects not properly taken care of by the factors $\varphi_n(\ell,s)$. In a practical calculation one might use as a first approximation a few leading Regge trajectories whose behavior could be determined roughly from experiment, absorbing the rest of the amplitude into the factor $\exp(G(\ell,s))$, with some reasonable parametrization.

38. Hung Cheng and Tai Tsun Wu, op. cit.

39. Hung Cheng, op. cit.

40. M. Abramowitz and I.A. Stegun, op. cit., pp. 228-254.

41. E.W. Hobson, op. cit., Eq. 10, page 15.

42. This formula can be obtained from E.W. Hobson, op. cit., Eq. 122, page 262.

43. See, for example, D.Z. Freedman and J.M. Wang, Phys. Rev. Letters 18, 863 (1967).

44. M. Abramowitz and I.A. Stegun, op. cit., Eq. 5.1.11, page 229.

45. Ibid., Eq. 6.1.3, page 255.

46. These formulas simplify for real, integer spacing of daughter
    trajectories. In fact, one obtains a recursion relation
    relating the S-matrix for a single trajectory (S_ℓ^1) to the
    S-matrix for an infinite number of integer spaced daughters
    (S_ℓ^∞) lying below a leading trajectory identical to the
    single trajectory of S_ℓ^1:

$$S_{\ell+1}^\infty = S_\ell^\infty \cdot S_\ell^{1*}$$

This relation is also valid for a slightly larger class of
product representations. Transforming back to $\cos\theta$ space, one
obtains for $A^\infty(\cos\theta)$ an integral equation involving a kernel
given in terms of $A^1(\cos\theta)$.

47. These amplitudes have only t-channel singularities. In order to
    obtain more realistic amplitudes, we would use the signature
    device and two sets of direct-channel trajectories correspond-
    ing to the two signatures. For our purposes, however, the
    present case will suffice.

48. W.J. Abbe, P. Kaus, P. Nath, and Y.N. Srivastava, Phys. Rev. 140,
    B1595 (1965). This work will henceforth be referred to as
    AKNS.

49. E.W. Hobson, op. cit., Eq. 82, page 239.

50. E. Hille, Arkiv för Matematik, Astronomi och Fysik 13, No. 17
    (1918-1919), Eq. 26, Page 18.

51. E.W. Hobson, op. cit., Eq. 24, page 306.

52. E. Hille, op. cit., and E. Hille, Arkiv för Matematik, Astronomi
    och Fysik 17, Nr. 22, 1 (1922-1923).

53. E.W. Hobson, op. cit., Eq. 41, page 210.

54. Ibid., Eq. 22, page 305.

55. Readers accustomed to solving mathematical problems by physical

reasoning may notice the similarity between the Legendre

series for $R(\xi, z, \lambda)$ and the surface Green's function for the

electrostatic problem in prolate spheroidal coordinates

(E.W. Hobson, op. cit., page 417). One might search for an

alternative method for solving the potential problem in these

coordinates and perform the required sum using the physical

analogy. In fact, however, there does not seem to be a

straightforward way to carry out this task. Accordingly, the

summation is presented here as a mathematical exercise. The

function

$$f(x,y) = \sum \frac{(2\ell + 1)}{P_\ell(y)} P_\ell(x)$$

has interesting properties in itself; for example, it has a

set of poles dense on the line $- 1 \leq y \leq 1$, and therefore

possesses a natural boundary in y. Consequently, the limit

$y \to 1$ or, in our case, $\xi \to 0$ or equivalently $s \to \infty$, must be

approached with some care.

56. In the two works previously cited, E. Hille considered the dis-

tributions of zeros of the Legendre functions. The function

$P_\alpha(x)$ was treated in somewhat greater detail than the function

$Q_\alpha(x)$, although Hille did prove that in the cut plane there

were no zeros of $Q_\alpha(x)$ for Re $\alpha > - 1/2$, and that in the case

of α real, $\alpha < - 1/2$ and $- n < \alpha < - n - 1/2$, there are no

zeros on the real interval $1 < x < \infty$, while if

$- n - 1/2 < \alpha < - n$ there is one zero on that interval. He

demonstrated that as $\alpha \uparrow - n$, the zero approaches the value

$x = 1$, while as $\alpha \downarrow - n - 1/2$, the zero approaches the value

$x = \infty$, and that the variation is monotonic. Using the re-

presentation

$$Q_\alpha(\cosh x) = \sum_{\ell=0}^{\infty} \frac{e^{-(\ell + \alpha + 1)x}}{(\ell + \alpha + 1)} P_\ell(\cosh x)$$

it is trivial to show that there are no zeros for x real,

$x > 0$ and $\text{Im } \alpha \neq 0$, which completes the extension of Hille's

results to our special case, where the argument of the

Legendre function $Q_\alpha(z)$ is held fixed at $z = \cosh x$ (x real)

and the zeros computed as a function of the complex index, α.

57. This value was taken from R.J. Eden, <u>High-Energy Collisions of</u>

<u>Elementary Particles</u> (Cambridge University Press, 1967),

page 245. For the purposes of the following discussion,

the precise value of this constant is immaterial.

58. See, for example, S.-Y. Chiu, G. Epstein, P. Kaus, R.C. Slansky,

and F. Zachariasen, Phys. Rev. <u>175</u>, 2098 (1968).

59. This idea is widespread, that the opening of new thresholds allows

the trajectory to rise, perhaps by simulating low-energy be-

havior in some sense. R. Slansky, for example, calls this

the "Boost Im Alpha" model, while P. Kaus refers to it as "Its

Always Christmas." This author is therefore not presenting

it here as an idea that is very new, but is only indicating

how it arises naturally out of this new Reggeized representation.